THE EFFECTS OF TITANIUM-COATED MICROMACHINED GROOVED SUBSTRATA ON OSTEOGENESIS *IN VITRO*

by

Alireza Khakbaznejad

B.Sc., University of British Columbia, Vancouver, Canada, 1995

A THESIS SUBMITTED IN PARTIAL FULFILMENT OF

THE REQUIREMENTS FOR THE DEGREE OF

MASTER OF SCIENCE IN DENTAL SCIENCE

in

THE FACULTY OF GRADUATE STUDIES

(Department of Oral Biological and Medical Sciences, Dentistry)

We accept this thesis as conforming

to the required standard

THE UNIVERSITY OF BRITISH COLUMBIA

September, 2000

In presenting this thesis in partial fulfilment of the requirements for an advanced degree at the University of British Columbia, I agree that the Library shall make it freely available for reference and study. I further agree that permission for extensive copying of this thesis for scholarly purposes may be granted by the head of my department or by his or her representatives. It is understood that copying or publication of this thesis for financial gain shall not be allowed without my written permission.

Department of Oral Biological and Medical Sciences (OBMS).

The University of British Columbia
Vancouver, Canada

Date Oct. 11/2000.

Abstract

Although previous studies have indicated that titanium-coated micromachined grooved substrata increase osteogenesis both *in vitro* and *in vivo*, the underlying cell behaviours have not been given much attention. One suggestion is that osteogenesis may be induced by appropriate cell orientation. It has also been suggested that the increased production of bone-like tissue on micromachined grooves results from the formation of a favourable microenvironment between the walls of the grooves. A third possibility is based on the hypothesis that extracellular matrix, mainly collagen, orientation plays an important role in increasing bone-like tissue formation. It was hypothesized that grooved surfaces, through orienting osteoblast-like cells, promoted osteogenesis *in vitro*. This study investigated cell and collagen orientation and the formation of bone-like nodules in response to surface topographies.

Osteogenic cells (OGC) from newborn rat calvariae were plated (2×10^5 cells/cm^2) on smooth surface controls and test substrata in which smooth surfaces (gaps) were flanked by groups of parallel grooves of 47μm pitch and 3μm, 10μm, or 30μm depth. The medium used was α-MEM with 15% fetal calf serum (v/v). The medium was supplemented with β-glycerophosphate (10mM) and ascorbic acid (50μg/ml) after the eighth day and changed three times weekly thereafter. Von Kossa staining technique, propidium iodide staining of nuclei, and picro-sirius staining of collagen fibers were used to study bone-like tissue formation, cell orientation, and collagen orientation respectively. Histological sectioning and scanning electron microscopy (SEM) of the cultures were carried out to further examine cell orientation on the micromachined grooved surfaces.

The results of the study indicated that both micromachined grooves and the smooth gaps within them produced more bone-like nodules than the smooth surface controls. It was found that the cells within the grooves generally aligned themselves with the direction of the grooves whereas the cells above the ridge of the grooves formed cell layers of parallel orientation at an angle to the grooves. The orientation angle (OA) of the cell layers above the ridge level increased with distance from the grooves. In the smooth gaps, the cell layer closest to the titanium surface had the best alignment with the direction of the flanking grooves, but the OA of the cell layers above it increased with distance from the titanium surface. The cells on the smooth surface controls showed no preferred orientation. Collagen fibers in the grooves were generally oriented with the grooves whereas collagen fibers in the smooth gaps had several distinguishable orientations including parallel to the grooves, perpendicular to the grooves, and diagonal to the grooves. Collagen fibers on the smooth surfaces were in arrays of parallel fibers in a criss-cross pattern.

The current study provides further evidence that micromachined grooved substrata promote bone-like tissue formation of osteogenic cells in culture. Moreover, bone-like nodule formation is associated with an interplay of several factors including cell orientation, number of cell layers, and collagen fiber organization.

Table of contents

List of tables

Page

List of figures

Page

List of movies (Attached CD)

Movie 1. Osteoblast-like cells spreading on a 50μm-wide gap of a surface with 10μm-deep grooves.

Movie 2. Osteoblast-like cells spreading on a 50μm-wide gap of a surface with 10μm-deep grooves.

Movie 3. Osteogenic cells shortly after spreading on a 50μm-wide gap of a surface with 10μm-deep grooves.

Movie 4. Osteogenic cells on a 50μm-wide gap of a surface with 10μm-deep grooves on day 3.

Movie 5. Osteogenic cells on a 50μm-wide gap of a surface with 10μm-deep grooves on day 4.

Movie 6. A calcifying nodule situated on the border of a 100μm-wide gap and 10μm-deep grooves on day 14.

Movie 7. Possible developing nodule on 10μm-deep grooves next to a 50μm-wide gap on day 16.

Movie 8. An oriented nodule on 10μm-deep grooves on day 21.

Movie 9. An oriented nodule on 10μm-deep grooves on day 21.

Movie 10. Two round nodules on 3μm-deep grooves on day 44.

Acknowledgements

First and foremost, I would like to thank Dr. Brunette for supervising my research and allowing me to use the facilities in his laboratory. I would also like to thank him for his guidance, encouragement, and patience during the course of the experiments. I am very grateful to the members of my committee, Drs. Waterfield, Uitto, and Diewert for their advice and guidance. I am very thankful to Dr. Chehroudi for his constructive criticism. Dr. Chehroudi, with his experience in the field of biomaterials and implantology, was a great asset to my research. I would like to thank Mrs. Lesley Weston for her technical advice on cell culture techniques. Without Mrs. Weston's assistance, none of the experiments in my research would have been possible. I am also very thankful to Mr. Andre Wong for his advice on SEM and confocal microscopy. Special thanks are extended to Drs. Jaeger and Kulpa and Mr. Kato of the Electrical Engineering at UBC for their help in preparing the micromachined grooved substrata used in my experiments.

At last, but not least, I would like to thank my family and my girlfriend, Yasamin, for their emotional support and encouragement throughout the course of my research. Without you people this goal would not have been accomplished. Thanks a million!

The funding for this research was provided by the Medical Research Council (MRC) of Canada.

I. Introduction

A. Overview

Although implants have been in use for a long time, little has been learned about their characteristics, in particular surface properties in detail, until recently. Implants are used today in ophthalmic, coronary, orthopaedic, and dental applications. Implant technique in dentistry was first studied systematically in the 1950's, but implants were not in frequent use until thirty years later, and since then the demand for dental implants has been steadily increasing (Stedman, 1995).

A successful implant must be one that is non-toxic, causes minimal or no foreign-body reaction and integrates well into the surrounding tissue (Martin *et al*, 1995). Long-term stability of a dental implant depends on the integration of the artificial material into the surrounding bone tissue (Groessner-Schreiber and Tuan, 1992). The integration of an implant into alveolar bone involves apposition of mineralized tissue adjacent to the implant surface, a phenomenon called osseointegration. The mechanisms leading to osseointegration are not known in detail, but there has been a number of suggestions in the literature of a possible role for cell orientation (Hasegawa *et al*, 1985; Chehroudi *et al*, 1992), collagen bundle organization (Gebhardt, 1905, cited in Boyde and Riggs, 1990; Boyde *et al*, 1984; Ascenzi and Benvenuti, 1986; Gerstenfeld *et al*, 1988; Davies and Matsuda, 1988; Weiner *et al*, 1997), and possibly an osseoinductive microenvironment (Selye *et al*, 1960, cited in Ratkay, 1995; Tenenbaum and Heersche, 1982; Nakahara *et al*, 1991; Critchlow *et al*, 1994). The purpose of this thesis is to investigate the organization of collagen and osteoblast-like cells in a topographically controlled system where experimental parameters can be controlled and the experiments can be repeated in short periods of time.

1. Osteogenesis and osseointegration

Osteogenesis or bone formation *in vivo* results from a complex chain of events that involves proliferation of primitive mesenchymal cells, differentiation into osteoblast precursor cells (osteoprogenitors or pre-osteoblasts), maturation of osteoblasts, formation of matrix, and finally mineralization (Hill *et al*, 1998). In osseointegration there are three distinct phases. The first, osteoconduction, relies on the migration of differentiating osteogenic cells onto the implant surface. The second, *de novo* bone formation, results in a mineralized interfacial matrix, equivalent to that observed in cement lines in natural bone tissue, being laid down on the implant surface (Davies and Baldan, 1997; Davies, 1998) or near it (Clokie and Warshawsky, 1995). The third tissue response, bone remodelling, will also at discrete sites, develop a bone-implant interface comprising *de novo* bone (Davies, 1998).

Osborn and Newesely have classified osteogenesis involving titanium implants into two kinds: distance and contact osteogenesis (Furlong and Osborn, 1991). In distance osteogenesis, new bone is formed on the old peri-implant bone and the existing bone surfaces provide the osteogenic cells that lay down the new matrix. In contact osteogenesis, new bone forms on the implant surface or, in this case, titanium-coated silicon wafers.

Briefly, the pre-requisite to contact osteogenesis is the attachment and spreading of osteoblasts on the implant surface. The attachment of these cells to the surface was found to be mediated by serum proteins, particularly fibronectin (Doillon *et al*, 1987), and for osteoblast attachment osteopontin and bone sialoprotein are also instrumental (Davies, 1996). These proteins promote cell attachment and spreading by interacting with glycosaminoglycans and the cytoskeleton (Doillon *et al*, 1987; Schwartz and Boyan, 1994).

Schwartz and Boyan (1994) have suggested that the binding of serum proteins in turn depends on surface adsorption of metal ions. Osteopontin and bone sialoprotein are secreted by osteoblasts and are the major components of the organic matrix laid down before the start of osteogenesis (Davies, 1996). Mineralization of this matrix starts by seeding of crystalline calcium phosphate, which is then followed by the assembling of collagen fibres (Davies, 1996). *In vivo*, differentiating osteogenic cells are derived from undifferentiated peri-vascular connective tissue stromal cells and once these differentiating cells start secreting bone matrix, they stop migrating (Davies, 1998).

After the osteogenic cells have attached and spread on the implant surface, *de novo* bone formation follows. According to Albrektsson *et al* (1981 and 1983) and Davies (1998), the osteogenic population secretes a matrix, made up of osteopontin and bone sialoprotein, which constitutes the interface between the implant surface and the new bone and serves as a nucleation site for calcium phosphate mineralization. In contrast, Clokie and Warshawsky (1995) argue that the above matrix is formed after *de novo* bone formation is completed to close the gap between the new bone and the implant surface. It has been suggested that immediately after implantation the bone adjacent to the implant surface dies (Clokie and Warshawsky, 1995) and new bone formation starts at the surface of the old bone and moves towards the implant surface (Clokie and Warshawsky, 1995; Schwartz *et al*, 1997). Once at the implant surface, osteoblasts secrete the afibrilar layer (Clokie and Warshawsky, 1995). The thickness of the afibrilar layer was found to be between 200Å and 1μm (Albrektsson *et al*, 1981; Davies and Baldan, 1997) and according to Johansson *et al* (1989) the thickness varies with implant material. It is worth noting that metallic surfaces, such as titanium surfaces, instantaneously form an oxide layer (TiO, TiO_2, Ti_2O_3, and Ti_3O_4) which is about

100Å thick (Albrektsson *et al*, 1981). Therefore, the calcified non-collagenous layer which Davies and his team likened to the cement line in living bone, will not be in direct contact with metal in titanium implants. In contrast, Chehroudi *et al* (1992), using transmission electron microscopy on titanium-coated implants, demonstrated that collagen fibers in the matrix come in direct contact with implant surface.

Bone can remodel in response to mechanical stresses (Duyck and Naert, 1997) caused by physical exercise (skeletal) and mechanical loading during tooth or implant movement (Hill, 1998). Bone is very dynamic in that it constantly undergoes remodelling even after the growth and modelling of the skeleton have been completed. In remodelling old bone is resorbed by osteoclasts and new bone is laid down by osteoblasts and this whole process is thought to be under autocrine and paracrine regulation (Hill, 1998). Sensing mechanical stress (as a result of physical exercise), osteocytes release paracrine factors such as insulin-like growth factor (IGF)-I to trigger osteoclastic activities, hence bone resorption (Hill, 1998). During resorption, the osteoclasts release local factors from the bone, which according to Hill could have two effects: inhibition of osteoclast function and stimulation of osteoblast activity. Osteoclasts, when finished resorption, also secrete proteins that enhance osteoblast attachment (McKee *et al*, 1993). Among the factors that osteoclasts release is TGF-β which inhibits bone resorption by osteoclasts and can induce apoptosis (autocrine) (Hill, 1998). TGF-β also has paracrine effects on osteoblasts (Pfeilschifter *et al*, 1990a,b) as it chemotactically attracts osteoblasts to the resorption site and induces osteogenesis. It has been suggested by Mundy *et al* (1984) that collagen type I may have a similar role in osteogenesis, but it is generally agreed that collagen's main role is structural.

Different scientists have differing viewpoints on osseointegration and different biomaterials. Collins (1954) claimed that implanted objects never become fully integrated into the bone. More than a decade later (1970) Southam *et al* maintained that a layer of fibrous tissue will always develop around an implant and will prevent it from becoming stable in bone tissue. Several scientists (Jacobs 1976, 1977; Muster and Champy, 1978, cited in Albrektsson *et al*, 1981) believed that a direct bone-implant contact was only possible if the implant was made of ceramic. Later, it was established that osseointegration was achievable when other materials were used such as stainless steel (Linder and Lundskog, 1975), vitallium (Klawitter and Weinstein, 1974; Linder and Lundskog, 1975; Weiss, 1977), tantalum (Grundschober *et al*, 1980, cited in Albrektsson *et al*, 1981), and titanium (Branemark *et al*, 1969 and 1977; Linder and Lundskog, 1975; Karagianes *et al*, 1976; Schroeder *et al*, 1976, cited in Albrektsson *et al*, 1981; Juillerat and Kuffer, 1977, cited in Albrektsson *et al*, 1981).

2. Implant properties

Apart from the kind of materials used in an implant, other factors or characteristics of implants have been reported to play crucial roles in the promotion of osteogenesis at the implant surface. The most discussed properties of implant surfaces in the literature are surface chemistry, surface energy, and surface topography (Ratner, 1987). These properties seem to collectively contribute to osteogenesis and most importantly influence the cellular responses, therefore, influencing the rate and quality of tissue formation and the regeneration process (Schwartz and Boyan, 1994; Schwartz *et al*, 1997).

a. Surface chemistry

Schwartz *et al* (1997) observed that surface chemistry could affect cell proliferation and differentiation. In their studies costocondral chondrocytes were cultured on polystyrene dishes sputter-coated with different materials including titanium, aluminum oxide, zirconium, and calcium phosphate. Titanium coatings in their studies were of two kinds: one that was formed in the presence of oxygen and another in the absence of oxygen. In the latter one, the coating had an amorphous TiO_2 layer whereas in the former one the TiO_2 was crystalline. The cellular responses to the two different titanium coatings were intriguing as the chondrocytes on the film with amorphous TiO_2 showed higher alkaline phosphatase specific activity than the chondrocytes grown on the crystalline titanium oxide or the tissue culture polystyrene controls. The surfaces did not differ in their ability to support cell proliferation, but changes in cellular matrix production, particularly in the amount of collagen synthesized, have already been confirmed by the studies of Hambleton *et al* (1994). It has been suggested that as the chemical composition of the surface determines its surface energy, it can influence the adsorption of serum constituents to the surface which in turn can alter the way cells attach and spread on implant material (Schwartz *et al*, 1997). These studies, thus, suggest that changes in attachment and spreading of cells due to altered adsorption pattern of serum proteins to the surface can change the phenotypic expressions of cells.

b. Surface energy

Surface energy has been defined as a measure of the extent to which bonds are unsatisfied at the surface of a material (Hench *et al*, 1982). It has been suggested that a high surface energy is preferable to a low surface energy because the former results in enhanced

wettability (Kilpadi *et al*, 1998), higher cellular attachment (Carlsson and Berman, 1989), as well as increased cellularity and cellular activity at the implant surface (Meenaghan *et al*, 1979; Baier *et al*, 1984). The adhesion and subsequent spreading of cells on a surface are dependent on adhesion of matrix and serum proteins whose conformation and bioactivity are, in turn, affected by both topography and energy of that surface (Jensen *et al*, 1991; Stanford *et al*, 1994; Kieswetter *et al*, 1996).

The surface energy level of an implant surface to a certain extent depends on the pre-implantation sterilization and handling techniques as different methods yield different levels of bond saturation at the surface. Cellular response is affected also by adsorbed surface species (contaminants) that are a function of the surface composition and charge (Ratner and McElroy, 1986; Kasemo and Lausmaa, 1988; Baier and Meyer, 1988). High surface energies (30-50 dynes/cm) have been achieved by plasma cleaning of the surfaces whereas the more traditional autoclaving results in the contamination of the surface by organic and ionic residues (Meenaghan *et al*, 1979; Baier *et al*, 1982 and 1984; Doundoulakis, 1987). To avoid autoclave-induced contamination, other alternatives such as, UV radiation (Doundoulakis, 1987; Hartman *et al*, 1989) and dry heat (Doundoulakis, 1987) have been suggested, but neither have proven as effective as plasma cleaning in increasing surface energy when assessed by contact angle measurements (Doundoulakis, 1987; Baier and Meyer, 1988).

In the radio-frequency glow discharge (RFGD) procedure the surface of the implant is bombarded by energetic ions formed in the plasma, removing atoms and molecules on the surface and as a result creating unsaturated chemical bonds (Kasemo and Lausmaa, 1988; Carlsson *et al*, 1989). These unsaturated bonds created in the process are ready to interact with any charged ions, atoms, or molecules and therefore facilitate cell adhesion and

spreading. The RFGD cleaning technique results in little or no contamination, is very quick, and most importantly elevates the surface energy of implant surfaces. Thus RFGD was chosen for the experiments explained in this thesis.

c. Surface topography

Over the years implant materials have been designed with different surface topographies to make them more biocompatible, or as Ratner said (1993), "to exploit the proteins and the cells of the body to achieve specific results". A good example would be the use of horizontal grooves on the implant surface to prevent epithelial downgrowth (Chehroudi *et al*, 1990), as cells are extremely sensitive to microstructures of biomaterials and their behaviour and function can be modified by different patterns (Chehroudi and Brunette, 1995).

The effects of surface topography on cell adhesion and spreading depend on cell type. Osteoblast-like cells preferentially attach to roughened surfaces (Bowers *et al*, 1992), whereas gingival fibroblasts have a preference for smooth polished surfaces (Kononen *et al*, 1992), and epithelial cells have an affinity for micromachined grooved substrata (Chehroudi *et al*, 1988 and 1989). Such results have led to the concept that implant surfaces can be designed to select for specific cell populations. For example, where osseointegration is the desired outcome, roughened surfaces can be used to encourage the attachment of osteoblast-like cells. However, as Rich and Harris (1981) observed, macrophages also preferred rough surfaces, a concept described as "rugophilia" or rough-loving. Abe (1983) has also reported that osteoclasts too, preferentially attach to rough surfaces. This rugophilia of resorptive cells could be problematic if the rough surface of an implant selected for bone-resorptive or inflammatory cells.

Generally rough surfaces have performed well where osseointegration is the desired response. Thomas and Cook (1985) investigated the variables affecting implant fixation by direct bone apposition using polymethylmethacrylate (PMMA), carbon, titanium, and aluminum oxide (Al_2O_3) implants and found that implants roughened by grit blasting exhibited direct bone apposition, whereas smooth implants promoted fibrous tissue formation. In a similar study, Pilliar (1986) reported that porous titanium alloy implants promoted bone ingrowth but only when pore sizes exceeded 100μm. Chehroudi *et al* (1992) studied the role of surface topography of implants with tapered pits and V-shaped grooves on mineralization *in vitro* and *in vivo*. In both studies, they noticed greater amounts of mineralized matrix adjacent to micromachined surfaces compared to the smooth control surfaces. Qu *et al* (1996) found that not only will micromachined grooved surfaces (*in vitro*) produce more bone-like nodules when compared to smooth surfaces, but also the mineralized accretions get oriented in the direction of the grooves. They also demonstrated that osteogenic cells could be influenced in terms of their shape, cytoskeletal patterns, and attachment by surface topography.

Micromachined grooved substrata have been very effective in orienting fibroblasts, epithelial cells (Brunette, 1983, 1986a,b) and osteoblasts (Qu *et al*, 1996) and have been demonstrated to inhibit epithelial downgrowth on percutaneous implants (Chehroudi *et al*, 1989 and 1990). Grooved surfaces also encouraged mineralized tissue formation both *in vitro* and *in vivo* (Chehroudi *et al*, 1992). Over the years, grooved substrata have received some attention because of their ability to modify cell behaviour and achieve osteogenesis, and also because of the affinity that osteoblast-like cells have for rough surfaces (Bowers *et al*, 1992). However, little has been done to investigate the underlying mechanism(s) on the

basis of which the grooved surfaces produce such results. The micromachining technique (Camporese *et al*, 1981) is used to make grooves with desired dimensions (depth and pitch), therefore making it possible to study the effects of well-defined topographies on osteogenic mechanism(s).

3. Proposed mechanisms leading to osteogenesis on implant surfaces

Many commercially available bone-contacting implants have been designed with different surface topographies including porous, rough, and machined surfaces (Brunette, 1988). So far, studies have been done to characterize these surfaces, but unfortunately the underlying mechanisms responsible for promoting osteogenic responses on these surfaces are not known. Among some suggested possibilities (Chehroudi *et al*, 1992) that are of particular interest to micromachined surfaces are the following:

a. Bone-inductive microenvironment

Selye *et al* (1960, cited in Ratkey, 1995) tested the effect of microenvironment produced by an implant by implanting glass cylinders of various sizes and shapes into rats. The results were interesting in that bone and cartilage ingrowth occurred but only in some sizes and shapes of cylinders. One possible explanation was that the glass cylinders formed a microenvironment that favoured mineralized tissue formation.

According to Evans and Potten (1991), regulation of stem cell activity *in vivo* depends on restriction of the distribution of regulatory factors (i.e. growth factors and cytokines). Supporting evidence for bone formation comes from the *in vitro* studies of Nijweide (1975) and Tenenbaum and Heersche (1982) where periosteal sheets had to be folded in order to

produce an osteogenic microenvironment. A direct role for growth factors was demonstrated by Critchlow *et al* (1994) who injected TGF-β into the periosteum of calvariae or long bones and they noted an increase in bone and cartilage production in the area. Nakahara *et al* (1991) demonstrated that periosteal cells enzymatically derived from chick tibia produced bone and cartilage only when cells were plated at high density. With respect to micromachined grooved substrata, it is possible that the walls of the grooves act to restrict osteoprogenitor cells into a confined microenvironment in which regulatory factors reach concentrations that are permissive for calcified tissue formation (Chehroudi *et al*, 1992).

b. Orientation of collagen bundles

It is generally agreed that a prerequisite for mineralization is the synthesis and assembly of a collagenous extracellular matrix (ECM) that lays the foundation upon which crystals of mineral can be formed (Gerstenfeld *et al*, 1988). In lamellar bone, collagen fibers are orthogonally arranged in longitudinal and transverse arrays (Gebhardt, 1905, cited in Boyde and Riggs, 1990; Boyde *et al* 1984; Ascenzi and Benvenuti, 1986; Weiner *et al*, 1997) and this orthogonal arrangement serves a functional purpose (Schenk and Buser, 1998). Gebhardt was one of the first to study the relationship between the microstructure of bone and function. Using structural models, he demonstrated that longitudinal fibers might be expected to endow tensile strength whereas transverse fibers would endow compressive strength (cited in Boyde and Riggs, 1990). Evans and Vincentelli's study of human cortical bone of tibiae (1971) demonstrated a significant relationship between tensile stress and strain and collagen fiber orientation. *In vitro*, Gerstenfeld (1988) observed that embryonic chicken calvariae osteoblast cultures, when three to four layers thick, formed a matrix and each cell

layer was associated with a layer of collagen fibrils orthogonally arranged with respect to neighbouring layers.

Collagen fibers in the matrix, through their orthogonal arrangement, may also influence osteoblast-like cells' metabolism. It has been suggested that the extracellular matrix can make cells more responsive to soluble signals, perhaps by allowing them to assume a particular spatial organization (Watt, 1991). Epithelial cells, for example, stop producing mRNA and protein when removed from substratum and cultured in suspension, but can resume making both when allowed to reattach (Benecke *et al*, 1978).

Davies and Matsuda (1988) found out that the orientation and spatial arrangement of collagen fibrils appeared to be different on smooth and rough surfaces. Collagen fibrils were morphologically more organized on some substrata and there was an association between collagen organization and enhanced mineralization (Davies and Matsuda, 1988). It has been suggested that, perhaps, micromachined substrata may produce an arrangement of collagen fibrils that promotes mineralization (Chehroudi *et al*, 1992), but it is yet to be determined whether the collagen orientation produced by grooved substrata bears any resemblance to the collagen arrangement found in situ.

The presence of collagen type I can be detected by several techniques. Immunohistology (use of monoclonal antibodies) is the most specific method, but unfortunately antibodies that are specific for collagen type I can also react with intracellular procollagen. Also, monoclonal antibodies are very expensive and wastage can be very costly. In a pilot project, monoclonal antibodies were used and the results were less than satisfactory as the intracellular procollagen was also stained and as a result the extracellular or ECM collagen and intracellular procollagen were not distinguishable. Trichrome procedure (Kiernan,

1990), van Gieson's method (Lillie, 1964), and Periodic acid-Schiff (PAS) (Kiernan, 1990) make use of anionic dyes to stain collagen. The three stains listed above are somewhat specific, but there is still some cross-reaction of the dyes with other proteins and sometimes there is too much background staining associated with them.

One histochemical technique that seemed very appealing with little background staining and cross-reaction, is picro-sirius red staining of collagen. This method takes advantage of the birefringent nature of the collagen fibers and the use of polarized light microscopy to beautifully demonstrate the presence of both tightly and loosely packed collagen bundles.

Constantine and Mowry (1968) first developed the picro-sirius staining technique. Sirius Red is a strong anionic dye that stains collagen by reacting, via its sulphonic acid groups, with the basic amino groups in the collagen molecule (Junqueira *et al*, 1979). The collagen molecule is birefringent. The birefringence is due to different optical densities along different planes of the collagen molecule, and as a result, light is refracted and retarded at different rates (Wolman, 1970). Sirius Red dye molecule has an elongated shape and attaches to the collagen molecule in such a way that its long axis is parallel to the collagen fiber. Sirius Red has been found to enhance the birefringency of collagen (Junqueira *et al*, 1979; Dziedzic-Goclawska *et al*, 1982). According to Junqueira *et al*, the picro-sirius staining results in an increase of at least 700% in light intensity when compared with samples stained only in saturated picric acid. Junqueira also made the observation that Sirius Red stains pure collagen strongly and does not stain proteoglycans, a problem observed with most anionic dyes (Junqueira *et al*, 1979). However, some staining of basic proteins may occur and if Sirius Red is used without picric acid non-basic proteins may also get stained (Junqueira *et al*, 1979). Another disadvantage is that the picric acid may interfere with the

study of collagen fibers in calcified nodule-like structures, as the picric acid tends to decalcify them.

Junqueira *et al* (1979) at first proposed that different types of collagen produce different polarization colours, but subsequently it was determined that birefringency colour changes with increasing thickness of collagen fibers (Junqueira *et al*, 1982; Dayan *et al*, 1989; Trau et al, 1991). A shift to longer wavelength (form greenish yellow to orange or red) occurs with better-aligned and tightly packed collagen molecules.

c. Cell shape and orientation

Numerous studies have demonstrated the profound effect that cell shape and orientation have on differentiation and, and therefore on protein expression of cells. Changes in cell shape that follow alterations in cell-cell and/or cell-ECM contacts are associated with changes in the differentiated phenotype of cells (Ben-Ze'ev, 1991). Alterations in cell shape can produce changes in cytoskeletal elements, which may affect the position and function of much of a cell's metabolism (Ingber, 1987). Changing cell shape by mechanical stretching of epithelial cells (Brunette, 1984) or osteoblasts (Hasegawa *et al*, 1985) increased the number of cells synthesizing DNA in culture and altered their pattern of collagen and non-collagenous protein synthesis. Examples of the effects of cell shape on cell metabolism are abundant.

In the study of Hong and Brunette (1987) on the effect of cell shape on neutral proteinase secretion by epithelial cells from porcine periodontal ligament, cells that were more round in shape secreted more porteinase. Solursh reported in 1989 that a rounded cell shape promoted differentiation of mesenchymal cells into chondrocytes whereas a flattened cell shape

promoted differentiation into fibroblasts. Mammary epithelial cells, when cultured in collagen gel, assumed their native shape and secreted a basal lamina, achieving a configuration much more tissue-like than in a culture spread out on plastic (Emerman and Pitelka, 1977). Emerman found from the contraction of the gel medium, on which the cells were grown, that a correlation existed between cell shape and the degree of differentiation (Emerman *et al*, 1977). Another good example is Watt's study of mammary epithelial cells when grown on floating collagen gel (Watt, 1986). She found that the cells assumed a cuboidal morphology and secreted some of milk proteins, including caseins.

Thus, diverse studies on diverse cell populations using diverse methods of altering cell shape all indicate a relationship between cell shape and metabolism. As osteogenic cells *in vivo* polarize to differentiate into osteoblasts, bone production could be enhanced *in vitro* by, perhaps, producing a cell orientation that is instrumental in the development of a functional cell polarity (Chehroudi *et al*, 1992). Micromachined grooved substrata, through orienting osteoprogenitor cells, are a possible means of achieving such functional polarity.

One could measure the effect of cell orientation on mineralization by studying micromachined grooved substrata. Many studies have been done to show that micromachined grooves are very effective in orienting cells, but the relationship between cell orientation and mineralization is still unclear.

In culture, fibroblasts form multilayers of cells where the long axes of the cells in one layer are parallel (Elsdale and Foley, 1969). Osteoblast-like cells extracted from chicken embryos behaved similarly as Gerstenfeld *et al* (1988) noted and every layer was associated with well-developed collagen fibrils orthogonally arranged with respect to adjacent layers. According to Jones *et al* (1975 and 1976), cell orientation governs collagen orientation when

they studied mammalian bones and they reported (1975) that 80% of the osteoblasts they studied were aligned within 30° of the collagen fibers underneath the cells. The reverse relationship between collagen fibers and osteoblast-like cells has been demonstrated by the study of Elsdale and Bard (1972) in which fibroblasts aligned themselves parallel to an oriented collagen substratum as they did to most grooved surfaces (Rovensky *et al*, 1971). However, on surfaces that lack such orienting effects, the orthogonal arrangement of collagen fibers should parallel the cell orientation and vice versa.

Cell orientation has been quantified in different ways (Brunette, 1988a; Dunn and Brown, 1986; Clark *et al*, 1990). One method uses the orientation index (OI). Orientation index is the ratio of the longest axis of the cell parallel to the grooves to the width of the cell at the widest point perpendicular to the grooves (Brunette, 1986b). An OI value of 1.0 indicates no preferred orientation whereas an OI value of greater than 1.0 indicates that the cell is favouring the direction of the grooves (Brunette, 1986b). Brunette (1986b) found that tightly spaced grooves were most effective in orienting epithelial cells.

One elegant method, though complex, is the method developed and used by Dunn and Brown (1986). Their method involves a highly sophisticated mathematical equation by which measures of cell shape and alignment are derived from the moments of cell shapes (Dunn and Brown, 1986). The method, however, is complex and has not been employed frequently.

Another way of measuring orientation is by way of orientation angle (OA). This is a simple method that uses the angle of the largest axis of the cell parallel to the direction of the grooves, or an arbitrary, randomly selected axis in the case of a smooth surface (Brunette, 1986a). Clark *et al* (1990) defined cells as being aligned when their OA was less than 10°.

This means of characterizing of orientation on surface has been widely used due to its simplicity (Brunette, 1988a; Oakley, 1995; den Braber *et al*, 1996, 1998; Qu *et al*, 1996). However, it is somewhat an insensitive measure since only two categories ($< 10^{o}$ and $\geq 10^{o}$) are used.

One way to measure cell orientation is to measure the orientation angle of cells with respect to a chosen axis, but in crowded cultures where cells form multilayers, such as osteoblast-like cell cultures, measuring the OA of individual cells is difficult because the cell outlines are not distinct. It has been shown that fibroblast elongation on cylindrical substrata is accompanied by nuclear elongation in the same direction (Margolis *et al*, 1975; Dunn and Heath, 1976; Weinreb *et al*, 1997). Therefore, orientation of the nuclei can be used rather than the whole cell outline to measure their orientation angle.

More than twenty methods have been developed to stain the nuclei of cells by fluorescent dyes. Propidium iodide is a fluorescent stain that is widely used for staining nuclear materials. The method was developed by Hudson *et al* (1969). Propidium iodide has several advantages. 1) Its maximum excitation is at about 530nm and maximum fluorescence at 615nm and therefore it can be used as a fluorescent marker with confocal microscopes that do not have UV excitation source (Orsulic and Peifer, 1994; Matsuzaki *et al*, 1997). 2) Propidium iodide can be used in conjunction with other fluorescent dyes for multicolour staining (Orsulic and Peifer, 1994). 3) Propidium iodide bleaches very slowly (months) compared to other commonly used stains, such as DAPI (4,6-diamidino-2-phenylindole), Hoechst, and ethidium bromide (Orsulic and Peifer, 1994; Matsuzaki *et al*, 1997). The only significant disadvantage of propidium iodide is that it also stains RNA and samples should be RNase-treated before staining if specific staining of DNA is desired (Matsuzaki *et al*, 1997).

B. Extracellular matrix (ECM) of bone-like tissue produced *in vitro*

As mentioned previously, for dental implants to be successful, they have to become osseointegrated. Mineralized tissue has to form around the implant to secure it in place. This mineralized tissue may resemble real bone, but it may lack some characteristics such as osteons and trabecular and Haversian systems. The ECM formed in the mineralized tissue comprises organic and inorganic components, which will be discussed below.

1. Organic matrix

Collagen and mucopolysaccharides make up the major portion of the organic material (Basset, 1962). Ninety five percent of the organic matrix is collagenous protein, 4% is proteoglycans and glycosaminoglycans (chondroitin sulphate, hyaluronic acid, heparan sulphate, and dermatan sulphate), and the remaining consists of non-collagenous proteins (Sammon and Thomas, 1981; Aubin *et al*, 1992). Glycosaminoglycans (GAGs) and proteoglycans (PGs) form a highly hydrated, gel-like ground substance in which the fibrous proteins (collagens and elastin) are embedded (Birk *et al*, 1991; Reichardt and Tomaselli, 1991). Glycosaminoglycans owe their name to the fact that one of the two sugar residues in the repeating disaccharide is always an amino sugar, N-acetylglucosamine or N-acetylgalactosamine (Jackson *et al*, 1991). Proteoglycans are GAGs that are covalently attached to a protein (Hardingham and Fosang, 1992). In bone, PGs are of two classes; byglycan or PG I and decorin or bone PG II, which differ in the protein core and the number of attached sulphated chains (Fisher and Termine, 1985; Stanford and Keller, 1991).

The major constituent of the organic matrix, collagen, is a structural protein which comes in at least fifteen types (Uitto and Larjava, 1991). Most have three polypeptide chains which

are rich in proline and hydroxyproline. These chains form a three-dimensional triple helix and upon maturation inter- and intramolecular linkages form. Collagen is first formed in the form of procollagen intracellularly and its transformation into collagen is a membrane-associated event. Collagen network gives the extracellular matrix its integrity and it is suggested that through its association with osteoblast-secreted phosphoproteins it may serve as nucleation site for hydroxyapatite crystals (Sodek *et al*, 1991; Veis, 1993). The two collagen types mostly found in the ECM of bone are type I and III. Type III collagen is present at low levels (<5%) in cultures of osteoblast-like cells (Aubin *et al*, 1982; Scott *et al*, 1980; Wiestner *et al*, 1981).

Non-collagenous proteins in bone are mostly polyanions which bind Ca^{++} ions strongly and are most likely associated with the mineralization process, but their exact functions are not clear (Glimcher, 1989). Perhaps the most studied non-collagenous protein is osteonectin, a phosophoprotein with great affinity for collagen and hydroxyapatite that is thought to be involved in mineralization of collagen type I (Termine *et al*, 1981a,b). There is a difference of opinion on the tissue specificity of osteonectin in the literature. Some authors believe that osteonectin is bone-specific (Termine *et al*, 1981a,b), but it has been found that osteonectin can also be produced by fibroblasts (Young *et al*, 1986).

Sialoproteins make up another family of non-collagenous proteins that are distinguished by their sialic acid content. Osteopontin or secreted phosphoprotein I (SPP I) and bone sialoprotein (BSP) are members of this family (Triffitt, 1987; Linde, 1989, Mikuni-Takagaki *et al*, 1995). Osteopontin acts as a ligand between osteocytic cells and hydroxyapatite and it is rendered bone specific only through post-translational sulphation (Sodek *et al*, 1991). BSP is bone-specific and is possibly involved in mineralization (Glimcher, 1989).

Osteocalcin, another non-collagenous protein, has been considered as the most specific marker of mature osteoblasts and calcified bone matrix (Gundberg *et al*, 1984; Price, 1985, Aubin 1998). Osteocalcin formation is dependent on vitamin K and the protein is found in association with bone morphogenic protein (BMP). There is evidence that osteocalcin inhibits hydroxyapatite formation and it is necessary for osteoclastic bone resorption (Price *et al*, 1983; Price and Williamson, 1985).

Enzymes and growth factors are also present in bone matrix and are thought to play important roles in bone metabolism and its maintenance. Growth factors identified in bone matrix include transforming growth factor-β (TGF-β), platelet-derived growth factor (PDGF), fibroblast growth factor (FGF), and bone morphogenic protein (BMP) (Wozney *et al*, 1988). Collagenases, proteinases, and alkaline phosphatase are the most abundant enzymes present in bone matrix (Bonewald and Mundy, 1990).

2. Inorganic matrix

About 70% of the dry weight of bone is its inorganic matrix, mostly composed of hydroxyapatite (Glimcher, 1989). During mineralization, osteoblasts secrete vesicles containing non-collagenous proteins, alkaline phosphatase, and ATPase. These vesicles are reportedly associated with calcification of the matrix as they are sometimes transported 10-20μm to the mineralization front (Boyan *et al*, 1993).

Anionic non-collagenous proteins bind to collagen and entrap calcium ions (Linde, 1989). After the alkaline phosphatase enzyme has released phosphate ions from organic sources, casein kinase II phosphorylates matrix proteins and mineralization is triggered as a result (Mikuni-Takagaki *et al*, 1995).

Davies (1991a) and Lowenberg *et al* (1991) have identified mineralized globules that appear to be attached to the substratum. Chehroudi *et al* (1992) classified these into small sizes (0.5-3 μm in diameter) and large ones (≥10μm in diameter) and found that smaller globules were primarily at the periphery of osteoblasts and osteocytes.

To detect the presence of bone or mineralized tissue, one can search for several criteria: a) cells showing osteoblastic morphology, function (Holtrop, 1990), and biochemical markers (Aubin, 1998), b) presence of collagen type I, and c) mineralization (Aubin, 1998).

Light and scanning electron microscopy can be used to look for phenotypic traits that are characteristic of active osteoblasts. Holtrop (1990) has summarized these traits as basophilic, cuboidal, rich in rough endoplasmic reticulum, mitochondria, vesicle-rich Golgi apparatus, and numerous microtubules and microfilaments. Monoclonal antibodies can be used to detect biochemical markers such as osteocalcin, osteopontin, and bone sialoprotein.

To visualize the presence and arrangement of collagen bundles, picro-sirius staining can be used which takes advantage of the birefringent nature of the collagen molecule.

To detect mineralization, several methods are widely used including Alizarin red staining, GBHA or glyoxal-*bis*-(2-hydroxyanil), and von Kossa. Alizarin red is a hydroxyanthraquinone dye which forms chelates with calcium (Kiernan, 1990). One problem with this technique is that calcium has to be released from its insoluble form to form chelates with the dye and consequently, some diffusion from the site of deposition is inevitable. Other problems with this method include non-specific pink background and sensitivity to pH of the solution (Kiernan, 1990). GBHA is a chelating agent for metals, including calcium (Kiernan, 1990). Like Alizarin red, GBHA is also sensitive for soluble calcium and insoluble calcium deposits remain largely unstained. Also, the sample to be

stained has to be freeze-dried. If the method is applied to samples that are conventionally fixed in aqueous reagents, calcium deposits will get stained but so will nuclei, cytoplasmic RNA, and proteoglycans (Kiernan, 1990).

In vitro tetracycline labelling of bone is another method of visualizing mineralized tissue. This procedure involves adding low concentrations (5μg/ml) of tetracycline to the vitamin C and phosphate supplement (Gruber, 1993). Tetracycline becomes incorporated in the newly formed mineralized tissue and fluoresces when viewed under blue or U.V. light.

The von Kossa technique is often used for staining mineralized tissue, but it is really a method for phosphate and carbonate with which calcium is associated in normal calcified tissue (Kiernan, 1990). Silver ions (from silver nitrate solution) replace calcium from calcified deposits and the use of bright light promotes the reduction to metal of silver ions in the crystals of the insoluble silver phosphate and silver carbonate (Meloan and Puchtler, 1985; Kiernan, 1990). Although it is less sensitive than the two methods described above and may result in staining artifacts, it is the most commonly used method because it provides sharp and precise localizations of calcified deposits (Kiernan, 1990).

C. Osteogenic cell cultures

In vitro studies of mineralization owe their feasibility to rapid adaptation of osteoblast-like cells to culture conditions and more importantly, these studies allow one to obtain more reliable results in shorter times than their *in vivo* counterparts; they are reproduced more easily, and allow for more control of different parameters.

Osteogenic cells may be obtained using different techniques. Jones and Boyde (1977) made use of the migratory behaviour of osteoblast-like cells in medium and were able to

collect these cells from denuded parietal bone fragments onto glass spicules. Another widely used technique is the enzymatic extraction of osteoblast-like cells from fetal or neonatal calvariae of rodents and chickens (Rao *et al*, 1977; Ecarot-Charrier *et al*, 1983). Cells isolated in this manner were quite capable of forming bone-like tissue (Tenenbaum and Heersche, 1982; Bellows *et al*, 1986). A third technique, described by Maniatopoulos *et al* (1988), uses adult rat bone marrow as the source for osteoblast-like cells. Although this procedure makes cell collection simple, a drawback is that it results in a heterogeneous population of hematopoietic cells and the cells of the reticular system, which consist of fibroblasts, chondroblasts, osteoblasts, and stem cells. Also, the culture period after extraction of almost thirty days is longer than those of the former two techniques.

For an osteogenic culture to be successful and produce mineralized tissue *in vitro*, specific culture conditions must be met. As with any other type of culture the basic requirements are a minimum essential medium, serum which provides the culture with amino acids, 37°C temperature, CO_2, and air. Antibiotics are added to prevent contamination by opportunistic microorganisms. Several labs (Tenenbaum, 1981; Nijweide *et al*, 1982; Nefussi *et al*, 1985; Bellows *et al*, 1986) reported that osteogenic cell cultures *in vitro* formed osteoid material, but the osteoid only mineralized when the culture media were supplemented with organic phosphate, particularly in the form of β-glycerophosphate. The organic phosphate is needed as a substrate for alkaline phosphatase. Tenenbaum (1981) recommended the use of 10mM concentration in completely defined media with no serum.

Another key ingredient for osteoblast-like cells to produce mineralized tissue is ascorbic acid or vitamin C (Bellows *et al*, 1986). Ascorbic acid or ascorbate is required in the synthesis of hydroxyproline in collagen (Barnes, 1975; Kivirikko and Myllyla, 1984;

Schwartz *et al*, 1987), and indeed hydroxyproline content has been generally used as an index of collagen synthesis. Ascorbate is also necessary for maintenance and stimulation of osteogenic phenotype (Spindler *et al*, 1989). According to Spindler, addition of sodium ascorbate to confluent cultures of isolated rat calvarium osteoblast-like cells caused an increase in DNA synthesis, [^{14}C] proline incorporation into collagenous and non-collagenous proteins, and alkaline phosphatase activity. The concentration widely used in osteogenic experiments is 50 μg/ml and it is replaced frequently once the culture becomes confluent.

In conventional cultures, osteogenic cells proliferate to confluence and eventually form multilayers (Peterson and Yamaguchi, 1996). Bone cells in culture go through a lag, log, and stationary phase of growth and also become growth-arrested, suggesting that DNA synthesis and proliferation are cell density dependent (Peterson and Yamaguchi, 1996). Lian and Stein found (1992), that proliferation and differentiation were related in osteogenic cell cultures and that differentiation is always preceded by a decline in proliferation. Peterson and Yamaguchi argue that for the down-regulation of proliferation to take place, a minimum critical cell density must be reached and report it to be 2 x 10^5 cells/cm^2. At this cell density, cell culture is a mixed population of quiescent and dividing cells, most undergoing differentiation or already committed osteoblasts (Peterson and Yamaguchi, 1996).

D. Cell behaviour on grooved substrata: contact guidance

Although contact guidance was first defined by Harrison in 1914 (cited by Oakley, 1995) it was Weiss who systematically studied the phenomenon by plating chick brain or spinal ganglial cells on a variety of substrata including fish scales, scratched glass, and clots (Weiss, 1959). Contact guidance is best described as the tendency of cells to be guided in their

direction of locomotion by the shape of the substratum (Brunette, 1988b). Rovensky *et al* (1971) took the studies another step further when they used the sound recording technology to create grooves of specific depths and dimensions on polyvinylchloride plates. They noted that embryonic fibroblast-like cells, when plated on grooved polyvinylchloride discs, acquired an orientation parallel to the direction of the grooves. More controlled surface conditions have been achieved through the use of microfabrication, a process used in microelectronics fabrication (Brunette, 1983, 1986a,b; Dunn and Brown, 1986; Clark *et al*, 1987). The above process allows for fabrication of surface features, such as grooves, with precise dimensions and therefore has revolutionized the study of contact guidance. The influence of surface topography is cell type dependent, as Clark *et al* (1987) learned from their experiments with fibroblasts, neutrophils, and embryonic neural cells. Several hypotheses have been suggested to explain cell orientation and locomotion on micromachined surfaces (Brunette, 1988b).

Weiss (1958) hypothesized the microexudate hypothesis and suggested that macromolecular material, such as fibrin, exuded from cells were responsible for orienting cells. Although plausible, the above hypothesis has been criticized by several authors, as cells have been able to orient themselves on substrata (glass cylinders) where orientation of any microexudate had not been expected or where little microexudate was formed (Curtis and Varde, 1964). Furthermore, it has been suggested that contamination of substrata by oriented structures is possible when preparing the surfaces (Dunn, 1982).

Dunn and Heath (1976) suggested that if a distortion of microfilament bundle geometry hindered cellular traction, cells would move in a manner to reduce the microfilament bundle impairment. Supporting evidence for the microfilament bundle hypothesis comes from the

work of Curtis and Varde (1964) who observed movement of fibroblasts along glass cylinders where the diameter of the cylinders did not exceed 100μm and that cells avoided bending with the curvature of the cylinders. The microfilament bundle hypothesis is, however, argued against by Brunette (1988b), who observed that cell alignment preceded microfilament bundle formation, and Lazarides and Revel (1979) who reported that fibroblasts could move without any microfilament bundles. Moreover, Oakley and Brunette (1993 and 1997) showed that microtubules, not the actin microfilament bundles, were the most sensitive cytoskeletal element in response to topography. Contrary to Dunn's hypothesis that cells would avoid crossing boundaries with sharp curvatures, Oakley and Brunette (1993) demonstrated that fibroblasts could spread across groove edges.

Another contact guidance hypothesis, centered on focal contacts, was first presented by Ohara and Buck (1979). Ohara and Buck showed that fibroblasts aligned themselves on grooved substrata with a pitch smaller than a cell length and that the cells aligned on the ridges more often than within the grooves. They argued that fibroblasts formed focal contacts along the ridges where limited areas of attachment were available and that focal contacts were also aligned. The difficulty with the focal contact hypothesis is that groove depth is a deciding factor in the degree of the orientation of cells (Clark *et al*, 1987) and it is unlikely that the formation of focal contacts is affected by different groove depths (Brunette, 1988a). On grooved surfaces with narrow ridges focal contacts may span several grooves and become corrugated as a result (Dunn, 1991). Brunette (1986a and 1988a) used time-lapse cinematography to demonstrate that locomotion was often associated with close contact rather than focal contact as he observed an interaction between the grooves and the cells' leading lamellae. Moreover, Oakley and Brunette (1993) found that focal contacts were

formed long after cells were aligned with the direction of the grooves and that individual focal contacts could bend around groove edges.

Stochastic models, in contrast, suggest that cells do not respond to topographical features in an "all or none" manner, but rather in a probabilistic or statistical way (Brunette 1986a,b, 1988b; Clark *et al*, 1987). Brunette reasoned that a grooved substratum does not absolutely impede cell locomotion across the grooves, but it substantially reduces the chances of that happening (Brunette, 1986a,b, 1988b; Clark *et al*, 1987). For example, cell processes at or near the edges of the grooves were less stable than those formed on flat surfaces of the edges, and therefore the average duration of adhesions of cells within the proximity of the edges is probably shorter than on a flat surface (Brunette, 1988b). Clark *et al* (1987) studied the effect of a single step on cell migration path and reported that the step aligned a cell by reducing its chances of making a process or moving in a direction that would cross the step. Briefly, this model of contact guidance suggests that cell migration and alignment in a direction other than the direction of the grooves is possible, but highly improbable.

Each one of the above hypotheses tries to explain cell alignment and locomotion, but no single hypothesis seems to be able to explain in detail the behaviour of cells on different substrata (Brunette, 1988b). It may be possible that at any given time more than one mechanism is at work. For example, it was shown that fibroblasts orient hierarchically to the grooves of different dimension (Brunette, 1986a). Fibroblasts, when plated on substrata with both major and minor grooves, aligned themselves with the major grooves, although minor grooves were able to orient cells in the absence of any other orienting effect. TEM showed that the filamentous cytoskeletal elements reflected the orientation of the cell as a whole and also it was suggested that the duration of attachment to groove edges may affect the contact

guidance (Brunette, 1986a). Despite all the uncertainties of the above hypotheses, there is little doubt that a variety of grooves of different dimensions affect cell migration and locomotion (Brunette, 1988b).

E. Objective of the thesis

The main objective of this thesis is to study and compare the responses of osteogenic cells to precisely defined substrata and investigate some of the mechanisms that have been proposed for the promotion of mineralization on micromachined grooved substrata. Given the current hypotheses on the possible mechanisms, the increased mineralization effected by micromachined grooved substrata and the orientation of cells and the organization of collagen fibers as well as creation of different microenvironments were investigated. Micromachining allows for fabrication of substrata with desired designs and dimensions, therefore making it possible, through manipulation of different variables, to create systems where each mechanism might be studied individually. This study is aimed at gaining more knowledge as to how micromachined grooved substrata work, hoping that in the future, implants may be designed with improved surface topographies, specialized to encourage osseointegration.

1. Hypothesis

Micromachined grooved substrata, through orienting osteoblast-like cells, promote mineralization *in vitro*.

2. Specific aims of this thesis

- To create an *in vitro* system, by incorporating smooth areas into the grooved substrata, whereby the effect of cell orientation on osteogenesis can be separated from that of the groove walls. The above system is aimed at understanding whether the increased mineralization on micromachined grooved substrata is due to the effect of the groove walls or due to the orientation of the osteogenic cells.

- To study the effect of groove depth on cell orientation and mineralization.

- To obtain information on the organization of collagen fibers in the extracellular matrix and its relationship with osteogenesis *in vitro*.

II. Materials and Methods

A. Substrata

1. Micromachining

The micromachining techniques used to produce surfaces for this thesis were developed at the Electrical Engineering Department of University of British Columbia by Camporese et al (1981) for the fabrication of photomasks for solar cells. The first step in micromachining is the production of a master pattern which is reduced to desired dimensions. The eventual end result is a photomask, which is a glass plate with a metallic master pattern placed on it. The pattern on the mask is then transferred onto a silicon wafer by photolithography. Photolithography involves covering the silicon wafer first with a thin layer of silicon oxide and then with a UV sensitive photoresist polymer. The wafer is then radiated with UV light through the photomask; the photoresist material is removed and the result is a negative copy of the mask design. Then the silicon oxide layer is chemically removed and this is followed by the removal of the rest of the polymer. The result is a positive copy of the photomask design made out of silicon oxide on the wafer. The positive copy is then chemically etched to desired depths using anisotropic etchants such as hydrofluoric acid. The duration of the etching process determines the depth of the grooves being produced; the longer the etching, the deeper the grooves.

2. Surface design

For the surfaces used in the experiments of this thesis one mask was produced to my design by Mr. Hiroshi Kato. The only surface variable was depth, which was controlled by the duration of etching. The pitch or the spacing of the grooves was held constant at 47μm. Pitch is defined as one groove width and one ridge (Figure 1). In order to separately

investigate the effect of cell orientation on mineralization, smooth gaps of different widths were introduced in the grooved area of the surfaces (Figure 2). The smooth gaps, despite their different widths, were designed to have equal areas (90,000 μm^2). The widths chosen for the smooth gaps were designed based on previous observations as to how far osteoblast-like cells could stretch out of grooves. Consequently, smooth gaps with widths of 50μm, 100μm, 150μm, and 200μm were designed and integrated into the grooved area of each surface at a frequency of ten each per surface (*i.e.* total of forty gaps per surface). To investigate the effect of groove depth on mineralization and cell orientation, three depths of 3μm, 10μm, and 30μm were used. The 30μm grooves were V-shaped, but because the same photomask was used to produce the 3μm and 10μm grooves, they had a truncated shape (*i.e.* with a flat bottom). The surfaces were all etched on silicon wafers and sputter-coated with 50nm of titanium.

3. Preparation of replicas

Plastic replicas of the surfaces were made for sectioning. Using Provil impression material (Haraeus Kulzer Inc., South Bend, IN) negative copies of the above surfaces were obtained. Small tombstone-like epoxy blocks (about 1 cm x 0.5 cm) were made using EPO-TECH (Epoxy Technology, Billerica, MA). The positive copies of the surfaces were made by placing a drop of fresh EPO-TECH material on the blocks and putting the negative copies face down on the blocks and fresh resin material. The blocks with the negative copies on them were allowed to dry at room temperature overnight and then baked in the 70°C oven for a period of three days. After baking, the negative copies were peeled off and the blocks were sent to the Electrical Engineering Department (UBC)

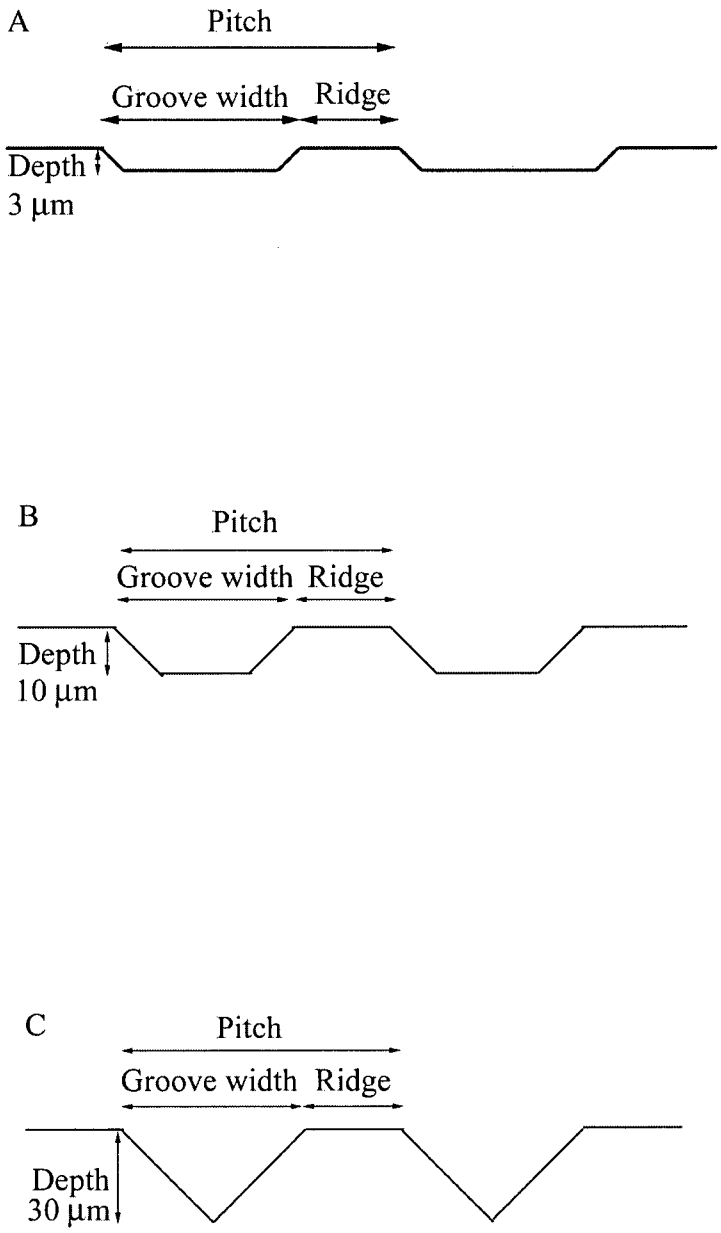

Figure 1: Cross-sectional diagram of grooves.
A. 3µm grooves. B. 10µm grooves. C. 30µm grooves.

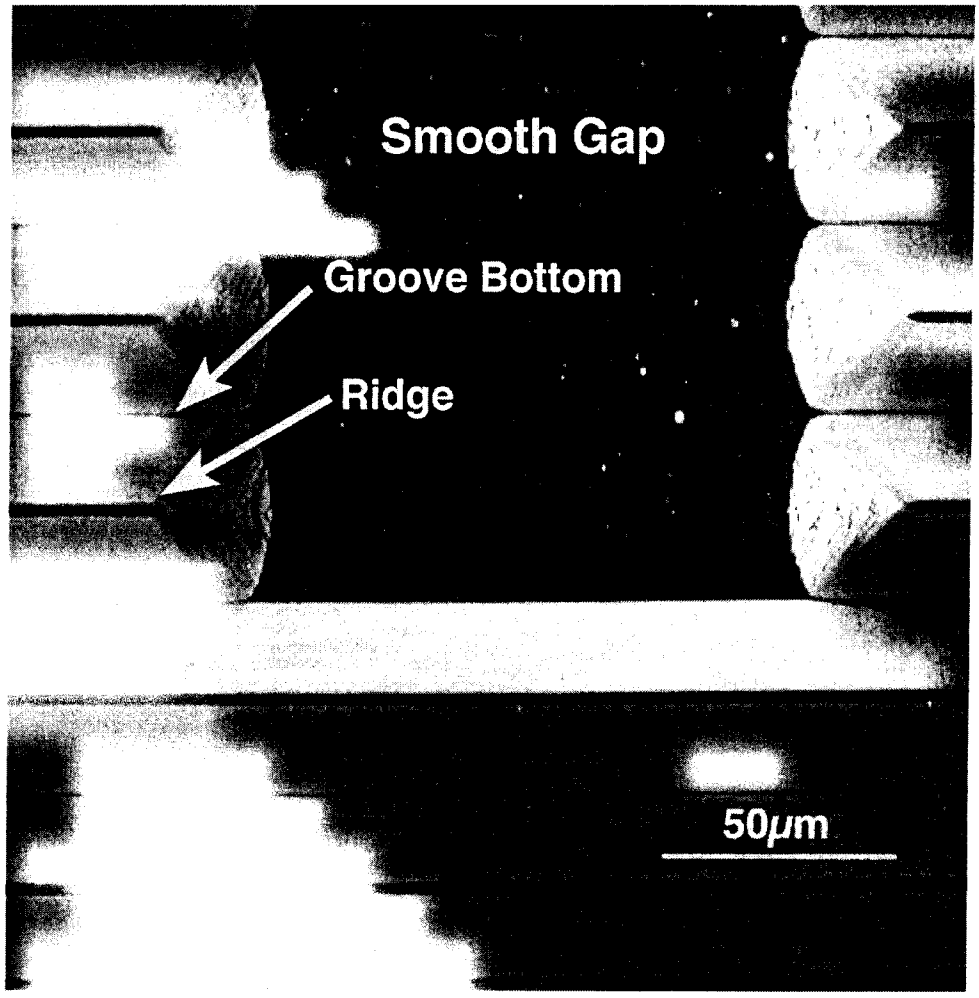

Figure 2: Scanning electron micrograph of the 30μm deep grooves. (Courtesy of David Perizzolo)

for coating with 50-80nm of titanium. The surfaces were coated using a sputter coater (Randex 3140 Sputtering System, Palo Alto, CA).

4. Cleaning and preparation of substrata for cell culture

In the studies involving biocompatible surfaces one has to take extra care that the surfaces are thoroughly cleaned before culturing. The cleaning process used here involves three steps: a) ultrasonication, b) washing, and c) glow-discharging.

a. Ultrasonication

Surfaces were placed in a 250ml plastic beaker with half water and half 7X detergent (Flow Laboratories, McLean, VA). The container was then placed in an ultrasonicator and ultrasonicated for 15 minutes. Ultrasonication helps remove any particulate and organic debris that may be present on the surfaces.

b. Washing

After ultrasonication the surfaces were meticulously washed ten times with tap water and ten times with distilled water. This helped in removing the 7x detergent used in the ultrasonication process. During washing and at all times after ultrasonication, the surfaces were handled with sterilized titanium forceps to avoid contamination with organic matter and extra care was taken to prevent scratching. The surfaces were allowed to dry overnight in a Petri dish in a tissue-culture laminar-flow fume hood.

c. Glow-discharging

After the surfaces were fully dry, they were placed in a glow-discharge apparatus (Aebi and Pollard, 1987) and glow-discharged for three minutes. Glow-discharging not only cleans the surfaces, but also achieves high surface energies on them (Meenaghan MA *et al*, 1979; Baier RE *et al*, 1982 and 1984). High surface energy, as mentioned earlier, is important in cell attachment and spreading.

B. Cell culture

Osteoblast-like cells were obtained from neonatal Sprague-Dawley rats' calvariae. The method used was similar to the method described by Hasegawa *et al* (1985). Frontal, parietal, and occipital bones of calvariae were dissected from eighteen neonatal rats. The dissected bones were rinsed in sterile phosphate buffer saline (PBS) solution and stored in tissue culture medium (α-minimum essential medium, α-MEM, StemCell Technologies Inc., Vancouver, B.C.) with 15% fetal calf serum (Cat. #CS-C10-500, Cansera, ON, Canada) and antibiotics (100 μg/ml Penicillin G, Sigma, St. Louis, MO; 50 μg/ml Gentamicin, Sigma; and 0.3 μg/ml Fungizone, Gibco, Grand Island, NY). The calvariae were then further dissected into 1-2 mm^3 pieces using a pair of sterile scissors. The pieces were placed in 5 ml of a digestion solution containing 180 units/ml of clostridial collagenase (type Ia, Sigma) and 0.5 mg/ml trypsin (Gibco) in PBS and allowed to digest for 10 minutes at 37°C in a Pierce "Reacti-Vial" (Pierce Chemical Company, Rockford, IL) with constant stirring. The supernatant was pipetted and discarded (population I). Five ml of the enzyme solution was added into the Reacti-Vial and the mixture was allowed to digest under above conditions for 15 minutes. The supernatant was pipetted and discarded (population II). Again, 5 ml of the

enzyme solution was added to the Reacti-Vial and the mixture was allowed to digest for 20 minutes. The supernatant was pipetted and using a 10ml syringe (Becton Dickinson & Co., Franklin Lakes, NJ) pushed through a 0.3mm mesh assembly (Gelman, Ann Arbor, Michigan) to remove any undigested tissue. The filtered supernatant was mixed with 5 ml of cold fetal calf serum (FCS, Flow Laboratories Inc.) to stop the enzymatic reaction. The mixture was then centrifuged at 1500 rpm for 5 minutes. The supernatant was discarded and the pellet was resuspended in 5 ml of α-MEM (StemCell). The suspension was added to a $75cm^2$ tissue culture flask (Becton Dickinson Labware, Franklin lakes, NJ) with 20 ml of α-MEM culture medium containing 15% FCS and antibiotics and incubated in a humid atmosphere of 95% air, 5% CO_2, and 37°C temperature for later subculturing.

1. Subculturing

After about a week of incubation, with medium changes twice weekly, the primary cell culture had reached confluency. At this point the medium was pipetted off and the cells were rinsed with 10 ml of a 0.25% trypsin solution made of trypsin (Gibco) in citrate saline (pH 7.8) and 0.1% glucose (Sigma). Then, 10 ml of the trypsin solution were added to the cells and the cells were incubated at 37°C for 10 minutes until the cells came off the floor of the flask. The suspension of the cells and the trypsin was transferred into a sterile test tube and centrifuged at 1500 rpm for 5 minutes. The supernatant was discarded and the pellet was resuspended in 10 ml of warm α-MEM with 15% FCS and antibiotics. The suspension was transferred into two sterile $75cm^2$ flasks (5 ml each) and 20ml of medium with 15% FCS and antibiotics were added to each flask and the flasks were incubated. These gave rise to subculture I. After about a week, the same procedure was repeated and the result was four

flasks of subculture II. Subculturing was repeated to obtain subculture III. Subcultures II or III osteoblast-like cells were used in all the experiments described in this thesis.

2. Cell population density

Cell population density refers to the cell concentration per area (cm^2) of substrata. The same cell density (2 x 10^5 cells/cm^2) was used in all the experiments. This density was selected in pilot experiments (Appendix A) in which three cell densities (2 x 10^3 cells/cm^2, 2 x 10^4 cells/ cm^2, and 2 x 10^5 cells/cm^2) were plated. It was observed that when cells were plated at 2 x 10^5 cells/cm^2, more mineralized accretions were produced by the osteoblast-like cells. Cell counts were determined using a Coulter Counter (Coulter Electronics Ltd., Beds, England).

3. Medium supplements

When the cell cultures were confluent, usually on the eighth day, the culture medium was supplemented with 50μg/ml ascorbic acid (BDH Inc., ON) and 10mM Na-β-glycerophosphate (Sigma), as vitamin C and an organic phosphate sources are required for collagen synthesis and mineralization respectively (Tenenbaum, 1981; Bellows *et al*, 1986). The supplements were added to the media of the experimental cultures, where mineralization was the desired outcome, and the cultures were fed with fresh medium and supplements three times weekly. Stock cultures were supplied with medium (α-MEM, 15% FCS, and antibiotics) twice weekly.

C. Qualitative and quantitative techniques

1. Reflected light microscopy (RLM)

Reflected light microscopy (RLM) technique was used for counting calcified accretions that were stained using the von Kossa method. Titanium-coated wafers bearing grooved surfaces with smooth gaps (Figure 2) were ultrasonicated, washed, and glow-discharge treated as described above. The grooves used were of three different depths (3μm, 10μm, and 30μm) and smooth titanium-coated silicon wafers were used as control. Osteoblast-like cells of subculture II were plated on the substrata in quadruplets in six-well culture dishes (Becton Dickinson Labware) at the cell density 2 x 10^5 cells/cm^2. The cultures were incubated in humid air (5% CO_2) at 37°C. Media were changed three times weekly and on the eighth day they were supplemented with vitamin C and β-glycerophosphate.

a. von Kossa staining

After 43 days the cultures were washed with medium that contained no FCS and fixed in 10% buffered formalin (Fisher Scientific, Fair Lawn, New Jersey) for about two hours. After being in fixative the cultures were rinsed three times with distilled water and 5% silver nitrate solution (BDH) was added to the surfaces for 20 minutes under bright light. Silver nitrate solution was washed away by rinsing with distilled water for five times and 5% sodium thiosulphate solution (BDH) was added for 2 minutes. Sodium thiosulphate solution was removed and surfaces were rinsed three times with distilled water and counter-stained with 1% methylene blue dye (BDH). The dye was rinsed off with distilled water and the surfaces were stored in phosphate buffer saline (PBS) in a refrigerator for later counting.

b. Counting of calcified nodules

Surfaces stored in PBS were rinsed with distilled water and allowed to dry. Once completely dry, the surfaces were mounted on glass slides (Fisher Scientific) and observed on an inverted microscope (IM 35, Zeiss, Oberkoken, Germany) equipped with Differential Interference Contrast (DIC) and using reflected light and a 16x objective lens. When counting calcified nodules that were stained with von Kossa, extra care was taken to only count the nodules that were similar in appearance to the ones reported in previous studies. To avoid counting stained artifacts that could easily pass for calcified nodules, it was decided to count nodules that were larger than 50 μm in diameter, as smaller entities could not be clearly resolved. Upon the review of the literature, it was noticed that there was no agreement as to what constitutes a nodule and the von Kossa staining is often used as the sole criterion for confirming calcified deposits (Bellows *et al*, 1985, 1986; Nefussi *et al*, 1985; Ecarot-Charrier *et al*, 1983,1988; Chehroudi *et al*, 1992). Mineralized accretions usually have well-delineated, three-dimensional nodular structures whereas unmineralized or mineralizing accretions have mound-like appearance and are usually smaller than the mineralized ones (Bellows *et al*, 1985, 1986). Meloan and Puchtler (1985), in their study of the von Kossa technique, reported that silver phosphate stains yellow to yellowish brown and the use of bright light causes the irreversible blackening of organic matter. Calcified nodules that met the above criteria were counted on all the surfaces (grooves, smooth gaps, and smooth controls) and their concentrations per unit area (cm^2) were calculated. Mineralization on the grooved surfaces was quantified on a total area equal to the total area covered by the smooth gaps. For example, nodules were counted a distance, equal to the width of the smooth gap, away from the gap. The NIH program was used to measure and mark the area.

Nodules were counted on forty such areas, since there were forty gaps. This measure was taken to even the sampling areas from both surfaces.

2. Transmission light microscopy (TLM)

TLM was used to investigate the physical characteristics of osteoblast-like cell cultures and mineralized accretions *in vitro*. Replicas of titanium-coated wafers (30μm grooves with smooth gaps) were produced as described in A.3 and sputter-coated with 50nm of titanium. Surfaces were cleaned by ultrasonication and glow-discharging, placed in six-well culture dishes (Becton Dickinson) and seeded with osteoblast-like cells of subculture II at 2 x 10^5 cells/cm^2. Fresh media containing FCS and antibiotics was supplied three times weekly and vitamin C and phosphate supplements were supplied on the 14^{th} day. The supplementation of the media was deliberately delayed (from the eighth day) to ensure the confluency of the cultures, since the replicas are not transparent and therefore difficult to examine on a transmission light microscope. Two weeks after supplements were added and every week thereafter one culture was subjected to fixation up to and including the sixth week.

a. Sectioning

Cultures were first fixed in 10% formalin (Fisher Scientific), stained with von Kossa method and counterstained with either 1% methylene blue (BDH) or 1% toluidine blue (BDH) and then fixed in 2% OsO_4 (JBS). Once fixed, the surfaces were dehydrated in graded ethanol solutions (30% to 100%) and embedded (Jembed 812 resin, JBS). The blocks were baked in a 70°C oven for three days, trimmed, and sectioned at 2μm intervals with a

microtome (Porter-Blum MT-2, Sorvall Inc., Newtown, Connecticut). Sections were mounted and pictures were taken using a light microscope (Photomicroscope, Zeiss) equipped with a camera and a 35mm Fuji film (Fujicolor 400, Fuji Photo Film Co., Ltd., Tokyo, Japan).

3. Confocal laser scanning microscopy (CLSM)

Titanium-coated grooved surfaces of 3μm, 10μm, and 30μm depths (six each) with smooth gaps were ultrasonicated, washed, and glow-discharge treated. Titanium-coated smooth surfaces were used as controls. Osteoblast-like cells of subculture III were plated on the surfaces at the cell density 2 x 10^5 cells/cm^2 in six-well culture dishes (Becton Dickinson Labware) and incubated in humid air (5% CO_2) and 37°C. Cultures were provided with fresh media three times weekly. Vitamin C and phosphate supplements were not added, as the formation of mineralized nodules would have obscured the cells from microscopic observations.

a. Propidium iodide staining of nuclei

The staining technique described here is a modified protocol developed by Andre Wong of the Faculty of Dentistry at UBC (personal communication). Cultures were fixed in 100% ethanol and then taken through baths of 95%, 85%, 70%, 50%, and 35% ethanol solutions at culture times of 8 hours, 24 hours, 4 days, 7 days, 14 days, and 21 days. Surfaces were submerged in each alcohol dilution for five minutes and at the end they were rinsed with distilled water three times. Propidium iodide (Sigma) was diluted in PBS and 50 μl of the 10^{-3} dilution was used to stain each surface. The staining was done in the absence

of light, as propidium iodide is light sensitive. After staining the surfaces were rinsed with distilled water (3x) and mounted on glass slides (Fisher Scientific) using immersion oil and glass cover slips (Fisher Scientific). The surfaces were wrapped in aluminum foil, and stored in a refrigerator prior to examination by confocal laser scanning microscopy.

i. Measurement of cellular angle of orientation

Cell cultures on microfabricated surfaces were optically sectioned using a confocal laser scanning microscope (MC 80, Zeiss) equipped with a helium-neon laser (λ_{max}=543nm). Scanning was done under a 40x objective and at an interval of 3μm for 30μm depth grooves and 1μm for all other surfaces. The choice of a 3μm sampling interval for the 30μm grooves was made deliberately as the computer could not store the 30 images required for a 1μm sampling protocol. The 3μm sections were sufficient to include all the cells in any of the fields. Furthermore, special care was taken to ensure that no detail was missed when the deeper grooves were examined. Three areas per surface were optically sectioned and the areas were randomly chosen. The images were stored and transferred onto a personal computer and recorded on a disc. Figure 3 shows examples of the sections. Three-dimensional composites of the sections (examples in Figure 4) were made and printed using a video printer (UP 5000, Sony, Richmond, B.C.). The optical sections were examined and orientation angle of every nucleus relative to the direction of the grooves was measured and recorded using the NIH program and a PowerTower Pro 180 computer (Power Computing Corp., Round Rock, Texas). On the smooth controls the orientation angles were measured with respect to an arbitrary horizontal axis. All nuclei that appeared at the same depth were considered to make up one cell layer. Thus, the mean orientation angle of one group of cells

reflects the overall orientation of the cell layer that they occupy. Where there was any doubt about the location of a nucleus in relation to other nuclei or layers, the 3D composites were used to locate the nucleus. To avoid measuring the orientation of the same nucleus more than once every nucleus was marked after its orientation angle was measured.

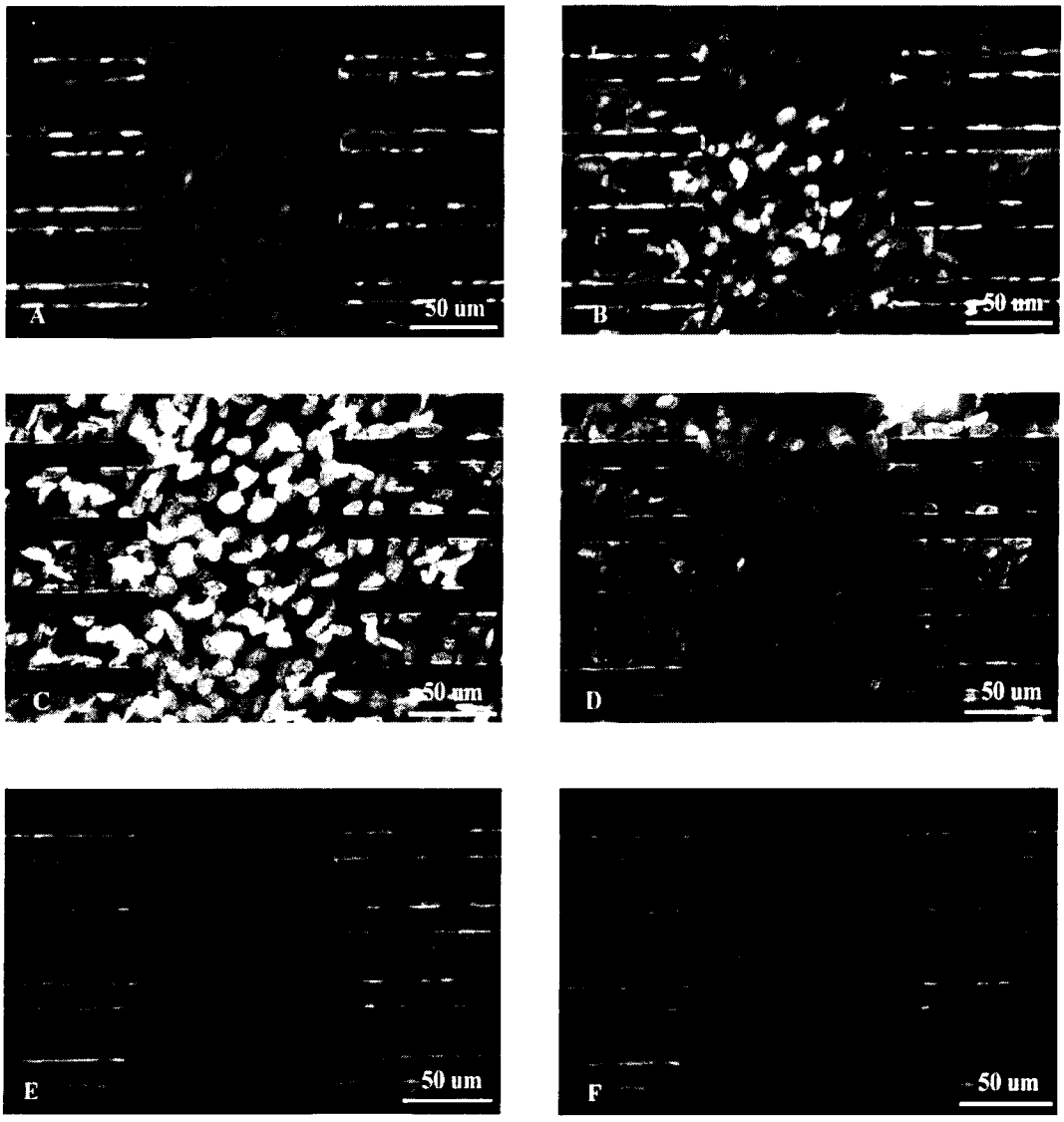

Figure 3: Propidium iodide staining of osteoblast-like cells' nuclei on a 100μm gap of a 21-day old culture. A through F show optical sections 1 through 6 from top to bottom respectively.

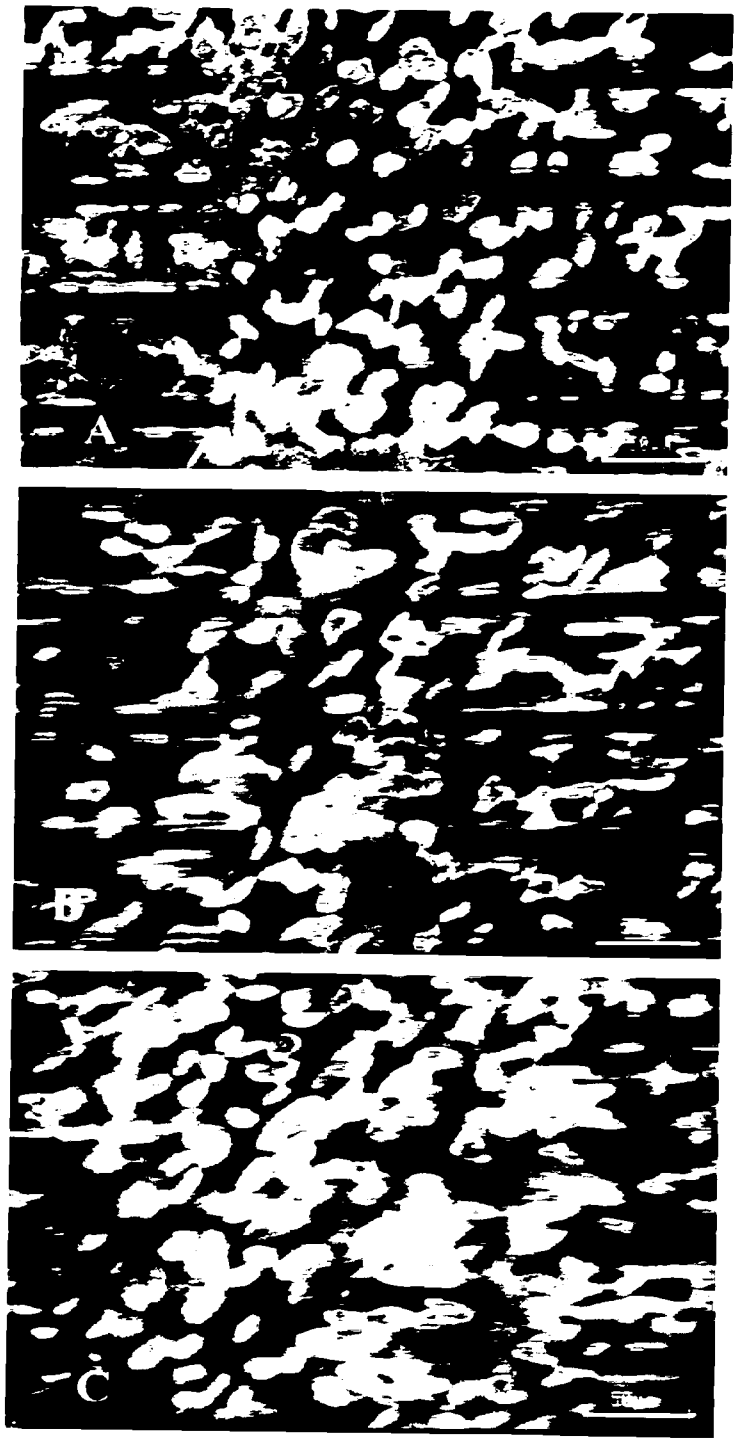

Figure 4: A. composite picture of images in Fig. 3. B. cells on a 50μm gap in a 14-day culture. C. cells on a 200μm gap in a 7-day culture.

4. Scanning electron microscopy (SEM)

Two titanium-coated surfaces (silicon wafers) with 10μm-deep grooves were cleaned and glow-discharge treated as described above. Osteoblast-like cells of subculture III were plated on the surfaces at 2 x 10^5 cells/cm^2 and the cultures were provided with fresh medium containing FCS and antibiotics three times weekly. Vitamin C and phosphate supplements were supplied on the eighth day. After two weeks and three weeks cultures were fixed in 2.5% gultaraldahyde (Fisher Scientific) for 2 hours, rinsed in 0.1 M sodium cacodylate buffer for 5 minutes three times, and stored in the buffer in a refrigerator until secondary fixation. Secondary fixation started by soaking the surfaces in freshly made 2% osmium tetroxide (OsO_4, J.B. EM Services Inc., Pointe-Claire-Dorval, Quebec) solution for one hour at room temperature. The surfaces were rinsed with distilled water three times and treated with 5% tannic acid (Fisher Scientific) for 30 minutes. Distilled water was used to rinse the acid off (three times) and the surfaces were again subjected to fixation in 2% OsO_4, but this time only for 30 minutes. The fixative was washed off three times with distilled water and the wafers were dehydrated in graded ethanol (30% to 100% ten minutes each). The wafers were critical point dried (Ladd Research Industries Inc., Burlington, VT) with liquid CO_2, sputter-coated with gold (Hummer VI Sputtering System, Technics, Alexandria, VA), and examined using a scanning electron microscope (Cambridge Stereoscan 260, Cambridge Instruments, Leica, Canada). Scanning electron micrographs were recorded on Polaroid 55 film (Polaroid, Cambridge, Mass.).

5. Polarized light microscopy (PLM)

To visualize collagen fibers in *in vitro* cultures picro-sirius red staining technique

(Constantine and Mowry, 1968) and PLM were used. The collagen molecule is birefringent and the Sirius Red stain enhances its birefringence by as much as 700% (Junqueira *et al*, 1979).

a. Collagen staining with Picro-sirius Red

Eight surfaces with 10μm-depth grooves and smooth gaps were cleaned and glow-discharge treated as described above. Osteoblast-like cells of subculture II were plated at 2×10^5 cells/cm^2 on seven of the above surfaces and one was used as a control with no cells. Fresh medium with FCS and antibiotics was supplied to the cultures three times weekly. On the eighth day vitamin C and phosphate supplement was supplied to cultures of week 2 through week 6 only. Cultures were fixed in 10% phosphate-buffered formalin (Fisher Scientific) for one hour after 24 hours and every week for a period of six weeks. Then the surfaces were soaked in PBS three times, five minutes each time, and were stored in PBS in a refrigerator until staining with Picro-sirius Red. Dr. Clive Roberts (OBMS, UBC) and Michael Iagallo of UBC Hospital (personal communications) provided the staining protocol described here. After the culture from week 6 was fixed, all surfaces were rinsed with tap water and 95% ethanol and treated for 10 minutes in alkaline ethanol (prepared by adding ammonium hydroxide (Fisher Scientific) to 95% ethanol until pH > 8) in a 60°C oven. The surfaces were rinsed with tap water and submerged in 2% F3B Picro-sirius Red stain (BDH, a gift from the histology laboratory at the UBC hospital) for one hour at room temperature. After staining the surfaces were rinsed with 1% acetic acid (BDH) until acid was clear. The surfaces were then dehydrated by submerging them twice in 75%, 100% ethanol, and xylene one minute each time. Once the surfaces were dry, they were mounted on glass slides (Fisher

Scientific), covered with cover slips (Fisher Scientific), and examined using a light microscope (Zeiss, Jenapol, Germany) equipped with polarizing filters, a 20x objective lens, and a centered rotatable stage. Images were recorded on a 35mm film (Kodak Ektachrome 160T, Eastman Kodak Company, Rochester, NY). Every field was photographed at zero degrees and forty five degrees.

6. Time-lapse video microscopy (TLVM)

A titanium-coated wafer with 10μm grooves and smooth gaps was cleaned, glow-discharge treated, and placed inside a Pentz chamber (Bachofer, Reutlingen, Germany) on a glass slide (Fisher Scientific). The substratum was seeded with osteoblast-like cells of subculture III at 2 x 10^5 cells/cm^2 using a 10ml syringe (Becton Dickinson). The Pentz chamber containing the substratum and the cell suspension was placed on a stage incubator on an upright microscope (IM 35, Zeiss) equipped with reflected Nomarski differential interference contrast (DIC) optics and an 8x objective lens (Zeiss). A television camera (Hamamatsu C2400, Hamamatsu Photonics K. K., Hamamatsu City, Japan) was used to capture images of the surface every four minutes. The digital images were stored on a hard drive and then recorded on a compact disc (CD) using a TEAC CD writer (TEAC America Inc., Taiwan). The culture medium was changed three times weekly and supplements were added on the eighth day.

E. Statistics

Numeric results are presented in mean $\pm$ standard error (SE). One way analysis of variance (ANOVA) with Tukey's honestly significant difference (HSD) or Student's t-test was used

for comparing results. Where data clearly skewed, Kruskal-Wallis non-parametric test for independent samples was used for comparisons. Significant differences in results were determined based on a level of 5%. SPSS software (1995, SPSS Inc.) was used for the above tests and the Excel program (Office 1997 version) was used to plot all graphs.

III. Results

A. Counts of bone-like nodules *in vitro*

To determine the effects of substrata on bone formation von Kossa staining method was used to visualize the nodules. The effects of surface topography were investigated using microfabricated surfaces comparing grooves of various depths, smooth gaps in the grooves, and smooth controls. Smooth gaps were used to separate the effect of cell orientation from that of the microenvironment created by the groove walls.

von Kossa stained surfaces of all depths of grooves, smooth gaps, and smooth controls were examined and nodules that could easily be distinguished (*i.e.* > 50μm in diameter) were counted per unit area (cm^2). The results of the counts are summarized in Table 1.

1. Nodule formation on grooved surfaces

The number of nodules on grooved surfaces was quantified and the results suggest that nodule number decreased as groove depth increased. The 3μm-deep grooves produced the highest number of calcified nodules per area, followed by 10μm- and 30μm-deep grooves respectively. The results of the different depths were all found to differ significantly ($P < 0.05$) from each other. Examples of calcified nodules are shown in Figure 5.

2. Nodule formation on smooth gaps

The smooth gaps, surprisingly, produced the highest number of nodules, even higher than the 3μm-deep grooves. One way analysis of variance (ANOVA) showed that the number of nodules in the smooth gaps differed significantly from that found on the grooved surfaces ($P < 0.05$). There were no significant differences among the smooth gaps of different widths on

the grooves of same or different depths and therefore, they were all placed in one group when compared with other surfaces.

3. Nodule formation on smooth surfaces

Smooth surfaces produced fewer bone-like nodules than all other surfaces ($P < 0.05$) (Table 1).

Table 1: Number of bone-like nodules on different surface topographies

Surface Topography	Nodules/cm^2 $\pm$ SE
Smooth	165.3 $\pm$ 16.5
3μm-deep grooves	545.1 $\pm$ 55.6
10μm-deep grooves	388.9 $\pm$ 27.3
30μm-deep grooves	239.6 $\pm$ 26.0
Smooth gaps	1004.6 $\pm$ 61.3

$P < 0.05$

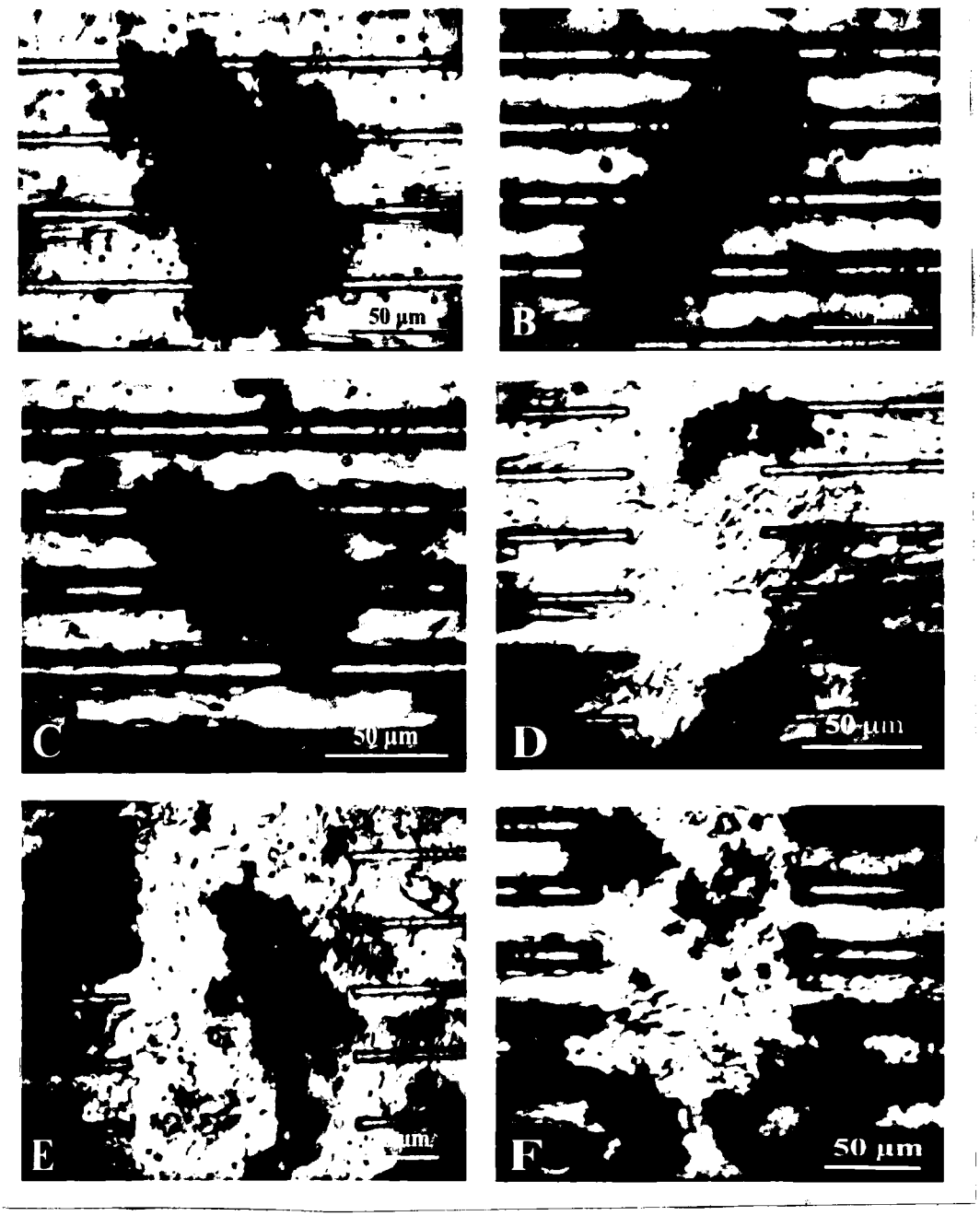

Figure 5: von Kossa staining of nodules. A. A nodule on 3µm-deep grooves. B & C. Nodules on 10µm-deep grooves. D & E. Nodules on 50µm- and 150µm-wide smooth gaps respectively (flanked by 3µm-deep grooves). F. Nodules on a 100µm-wide smooth gap flanked by 10µm-deep grooves. Cultures were all fixed and stained after 43 days.

B. Measurements of calcified nodules

1. Measurement of diameters of nodules on different surface topographies

To measure the size of a nodule, the longest axis of the nodule, regardless of the orientation of the nodule with respect to the grooves, was measured using the NIH Image software. Table 2 summarizes the results of measuring the diameters of nodules on the smooth gaps of titanium-coated micromachined grooved substrata where groove depth and smooth gap width are the variables. Two-way analysis of variance indicated that the depth of the flanking grooves had no effect on the size of the nodules formed inside the smooth gaps, but within a given depth of the flanking grooves, the gaps of different sizes differed significantly in diameter of nodules ($P < 0.05$). However, a pattern could not be established between gap width and nodule size. For example, on 3μm substrata the largest mean nodule diameter occurred on the 150μm gaps, but on 30μm substrata the largest mean nodule diameter was found on the 200μm gaps.

Table 2: Mean diameters of nodules on smooth gaps

Depth of Flanking Grooves (μm)	Gap Width (μm)	n	Mean Diameter (μm) ± SE	Mean (μm) ± SE
3	50	35	109.9 ± 6.0*	99.4 ± 3.5
	100	37	87.4 ± 6.4*	
	150	24	111.4 ± 8.2*	
	200	24	90.5 ± 6.5*	
10	50	41	84.6 ± 6.1 *	99.8 ± 3.7
	100	27	112.0 ± 8.7 *	
	150	30	102.7 ± 6.5*	
	200	25	108.0 ± 8.2*	
30	50	20	83.8 ± 5.8*	109.2 ± 4.5
	100	27	104.4 ± 5.9*	
	150	22	112.5 ± 7.5*	
	200	18	140.8 ± 13.3*	

* indicates means that are significantly ($P < 0.05$) different (one-way ANOVA and Tukey's HSD tests) when compared within a given depth of flanking grooves.

The size of nodules on micromachined grooved substrata varied with the groove depth (Table 3). It was found that the deeper the grooves the longer the diameter of nodules (i.e. the longest axis of nodule regardless of the direction of the grooves). There was no significant difference between the mean diameters of the nodules on the smooth surfaces and the 3μm-deep grooves. The diameters of nodules on the 10μm- and 30μm-deep grooves were similar and there was no statistical difference between the diameters of the accretions in both groups. However, the results of the smooth surfaces and 3μm-deep grooves were statistically ($P < 0.05$) different from those of the 10μm- and 30μm-deep grooves. The smooth gaps within the grooved areas produced the smallest calcified nodules and the difference with the nodules of all other surfaces was statistically significant ($P < 0.05$).

Table 3: Mean diameters of nodules on different surface topographies

Surface Topography	n	Mean Diameter (μm) ± SE
Smooth	160	135.8 ± 6.6
3μm-deep grooves	160	150.3 ± 6.8
10μm-deep grooves	160	174.9 ± 7.0*
30μm-deep grooves	160	187.0 ± 7.3*
Smooth gaps	330	102.1 ± 2.2

* These two means are significantly ($P < 0.05$) different from the other means (one-way ANOVA and Tukey's HSD tests).

2. Orientation of calcified nodules

The angle of orientation was measured as the angle between the longest axis of a nodule and the direction of the grooves. For the smooth surfaces, the angle between the longest axis of the nodule and an arbitrary horizontal axis was measured. Nodules on the smooth gaps of different widths showed no particular orientation with respect to the direction of the flanking grooves. Table 4 is the summary of the orientation measurements of the calcified nodules in the smooth gaps. Also, there was no statistically significant difference among the orientation angles (OA) of the nodules on the smooth gaps of different widths as they appeared to be randomly oriented. The depth of the neighbouring grooves played no apparent role in orienting the calcified nodules in the gaps, as their mean OA did not differ from the smooth gaps of surfaces with grooves of different depths. The overall mean OA for the nodules on the smooth gaps of surfaces with 3μm-, 10μm-, and 30μm-deep grooves was $40.2^{\circ} \pm 1.2$ (SE), close to the value (45°) expected if no orienting influences were present.

Table 4: Orientation of nodules on the smooth gaps of different widths

Depth of Flanking Grooves (μm)	Gap Width (μm)	n	Orientation Angle (°) ± SE	Mean (°) ± SE
3	50	59	44.3 ± 3.7	42.4 ± 1.9
	100	47	37.9 ± 3.5	
	150	32	37.2 ± 4.1	
	200	27	52.0 ± 3.3	
10	50	36	40.5 ± 4.2	38.5 ± 2.0
	100	40	38.6 ± 3.9	
	150	52	36.6 ± 3.4	
	200	25	39.4 ± 4.7	
30	50	18	51.3 ± 6.9	39.0 ± 2.7
	100	29	33.5 ± 4.2	
	150	30	37.5 ± 5.2	
	200	22	38.2 ± 5.5	

Angular orientation measurement of nodules on micromachined grooved substrata showed that nodules become more oriented with the direction of the grooves as the grooves become deeper. As a result, 30μm-deep grooves produced nodules with the lowest mean OA. The mean OA of the nodules on the 30μm-deep grooves was significantly ($P < 0.05$) different from those of the nodules on smooth gaps, smooth surfaces, and 3μm-deep grooves. Table 5 presents the results from the measurements of the OA's of calcified nodules on different surface topographies. For the smooth surfaces the angle was measured with respect to an arbitrary axis as defined by the horizontal of the image documenting the nodule.

Table 5: Orientation of nodules on different surface topographies

Surface Topography	n	Mean Angle of Orientation (°) ± SE
Smooth	160	38.6 ± 1.8
3μm-deep grooves	160	37.2 ± 2.1
10μm-deep grooves	160	33.8 ± 2.1*
30μm-deep grooves	160	29.6 ± 2.1*
Smooth gaps	417	40.1 ± 1.2

* These two means are significantly ($P < 0.05$) different from the other means (one-way ANOVA and Tukey's HSD tests).

3. Histology

von Kossa-stained nodules on the grooves and the smooth gaps were sectioned and several observations were made. Nodules on the grooved areas and the smooth gaps all consisted of multilayers of osteoblast-like cells (minimum 5 layers). Figure 6 presents examples of the overall structure of the nodules on grooves. These nodules have mound-like shapes and are about 5-6 cell layers above the ridges of the grooves. Most of the mineralization inside the nodule was located above the grooves and little inside the grooves. The cultures from which these nodules were selected for sectioning were 4-6 weeks old, but the age of a single nodule cannot be determined from the age of the culture since at any given time nodules of different sizes can be found. It was noted that the majority of mineralization occurred above the surface of the substrata and little von Kossa staining was located in immediate contact with the titanium coating of the substrata. Figure 7 presents a closer look at the cross-section of a nodule on the grooves. Where mineralized accretions were thick, the von Kossa technique only stained the surface of the accretion and the centre remained

unstained. Examples of these accretions can be seen in Figures 7 and 8. Figure 8 is the cross-section of a nodule on a 50μm-wide smooth gap.

The distribution of cells within the nodules was consistent in that most of the cells visible in the sections were located in the upper part of the nodule, fewer in the centre of the nodule, and the least at the bottom. This pattern was more pronounced in the nodules on the grooves. Figures 6 and 7 clearly show that most of the osteogenic cells were situated at the top and the centre and relatively few cells were found inside the grooves.

Another observation was that some mineralized accretions were rod shaped in cross section, as can be seen in Figures 7 and 8. It is possible that while other accretions appeared circular in cross section the long axes of the rods coincided with the direction of the grooves and hence the proportion of the rod-like accretions is underestimated.

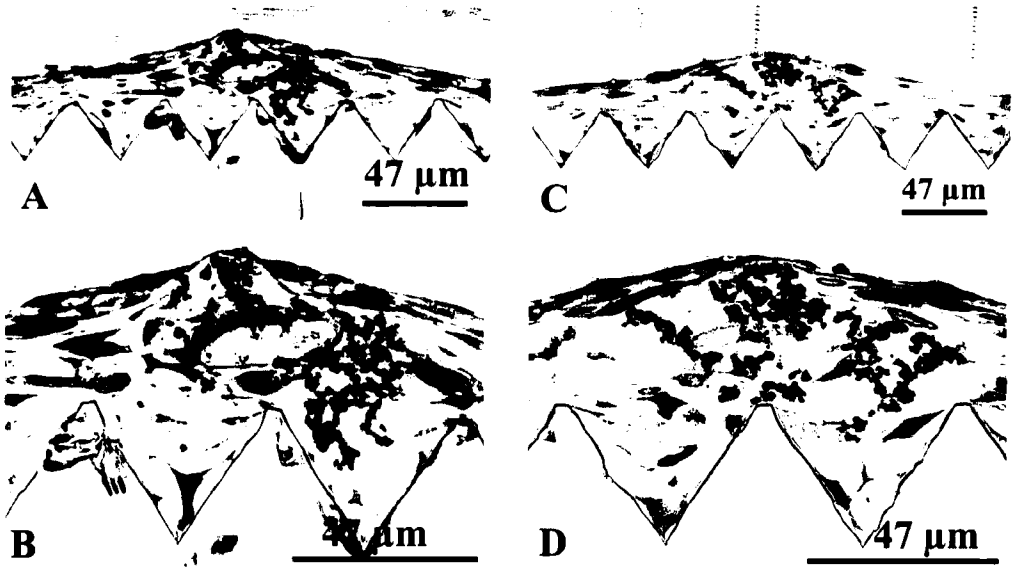

Figure 6: von Kossa and toluidine blue sections of two nodules on 30µm-deep grooves. B and D are higher magnifications (40x oil immersion) of A and C (16x objective) respectively.

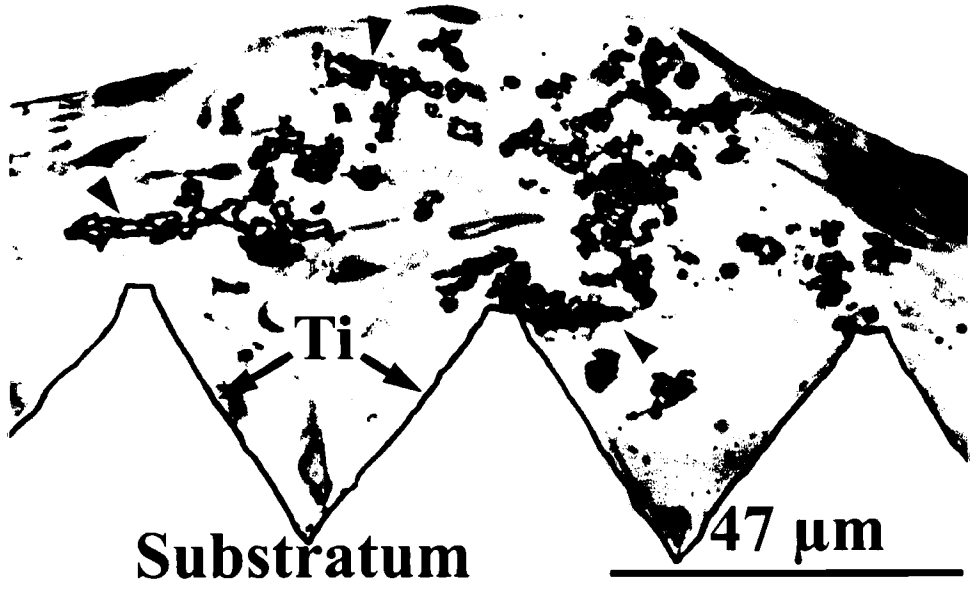

Figure 7: von Kossa and methylene blue section of a nodule on 30µm-deep grooves. Note mineralized areas in the centre of the nodule (arrowheads). On the left, one mineralized accretion is stained with von Kossa only in its periphery.

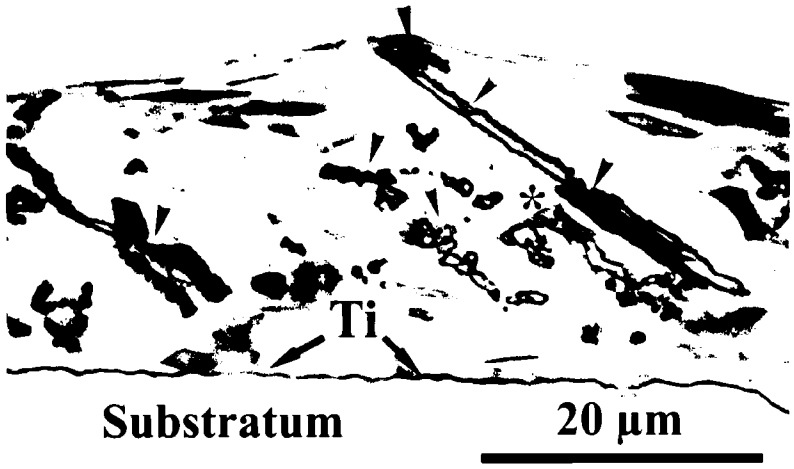

Figure 8: von Kossa and toluidine blue section of a nodule on a 50µm-wide smooth gap (40x oil immersion). The direction of the flanking grooves is coming out of the micrograph. Note the mineralized areas (arrowheads) and possibly an osteoblast (asterisk) close to the mineralization front. It is possible that some mineralized accretions appearing as rods in section, could be plate-like.

C. Effect of surface topography on cell orientation *in vitro*

1. Cell orientation on 3μm-deep grooves

Since optical sections were used to determine the orientation of the cells on the surfaces, a cell layer consisted of all the cells that appeared at the same level and a cell layer was defined as being one cell thick. The optical sections were obtained from top to bottom of the culture, and the cells that appeared in the last optical section and closest to the surface were considered to be in layer 1. Sometimes cells appeared in more than one optical section and there were instances of overlap between adjacent sections. In such instances a cell was considered to be in the cell layer where the majority of its nucleus was located. According to this definition of cell layer, for cells on smooth surfaces, and 3μm grooves, the number of the cell layers corresponds more or less directly to distance from the titanium surface. For surfaces with 10μm- and 30μm-deep grooves, however, the correspondence is not as direct, as cells growing on the groove walls would be classified as being in different layers even though each cell was in contact with titanium.

The osteoblast-like cells plated on 3μm-deep grooves reached confluency four days after plating at which time the culture consisted of one cell layer. Around the 7^{th} day a second cell layer was observed. By the 14^{th} day the culture consisted of three cell layers. Using the propidium iodide staining technique and CLSM (described in C.3), the cell layer for each cell was assigned and its orientation angle relative to the grooves was measured. The mean OA's of cell layers at different times were compared and found to be significantly different ($P < 0.05$). However, it was observed that the mean angle of orientation for a particular cell layer changes over time. For example, the mean OA of cell layer 1 at day 4

was different from the mean OA of cell layer 1 at day 21. The differences, however, between the mean OA of the equivalent cell layers at different times were not always statistically significant. It was noted that over time, cell layer 1 became less oriented with respect to the direction of the grooves whereas layers 2 and 3 became slightly more oriented. However, overall and at all times, cell layer 1 was more oriented with the direction of the grooves than cell layer 2, and cell layer 2, in turn, was more oriented than cell layer 3. Table 6 summarizes the results from the measurements of the mean OA's for all cell layers. To facilitate comparison the results for equivalent cell layers in Table 6 have been shaded alike.

Table 6: Orientation angles of cell layers over time for 3μm-deep grooves.

Time	Cell Layer	n (No. of cells)	Mean Angle of Orientation (°) ± SE
8 hrs.	1	249	14.4 ± 0.8
24 hrs.	1	256	10.4 ± 0.6
4 days	1	256	14.9 ± 0.8
7 days	1	273	15.6 ± 0.9*
	2	210	42.2 ± 1.6*
14 days	1	329	23.9 ± 1.3*
	2	229	40.5 ± 1.7*
	3	133	50.2 ± 2.1*
21 days	1	244	25.4 ± 1.6*
	2	182	34.4 ± 2.0*
	3	68	45.1 ± 3.5*

* indicates means that are significantly ($P < 0.05$) different from the other means within the same time period (Kruskal-Wallis one-way ANOVA or Student's t-test where applicable).

To determine the percentage of osteoblast-like cells in each cell layer that were well oriented with the grooves, cells were categorized according to their angle of orientation. The categories were based on 10-degree increments. Using Clark et al's criteria (1990) well-aligned cells fall into category 1 (0^{o}-9.9^{o} *i.e.* $< 10^{o}$). The other categories were 10^{o}-19.9^{o} (increment 2), 20^{o}-29.9^{o} (increment 3), 30^{o}-39.9^{o} (increment 4), and so on. It was found out that the 3μm-deep grooves oriented cells as early as 8 hours after plating. After 8 hours the majority of the osteoblast-like cells were in increment 1. After 7 days when the culture consisted of two cell layers or more, the osteoblast-like cells in subsequent cell layers had no apparent preferred orientation and the grooves did not appear to dictate the orientation of the cells. As a result, when the cells in cell layers 2 and 3 were categorized with respect to their angle of orientation, no particular category or increment was dominant over the others. This effect is reflected in the overall orientation angle of the cell layers as given in Table 6. With every subsequent cell layer the average angle of orientation increased, indicating the weakening orienting effect of the grooves. It was also observed that some osteoblast-like cells in layer 3 of the 14-day and 21-day cultures were oriented almost at right angles to the direction of the grooves, as the number of these cells in higher increments (6, 7, 8, and 9) was slightly higher than the number of the cells in the same increments in cell layers 1 and 2. Figure 9 shows the distribution of osteoblast-like cells according to their angle of orientation on 3μm-deep grooves.

Cell layers at a given location on the substratum had different numbers of osteoblast-like cells associated with them. For the 3μm-deep grooves, cell layer 1 had the most cells associated with it followed by cell layer 2 and cell layer 3. Figure 10 indicates cellular distribution in all cell layers at different culture times.

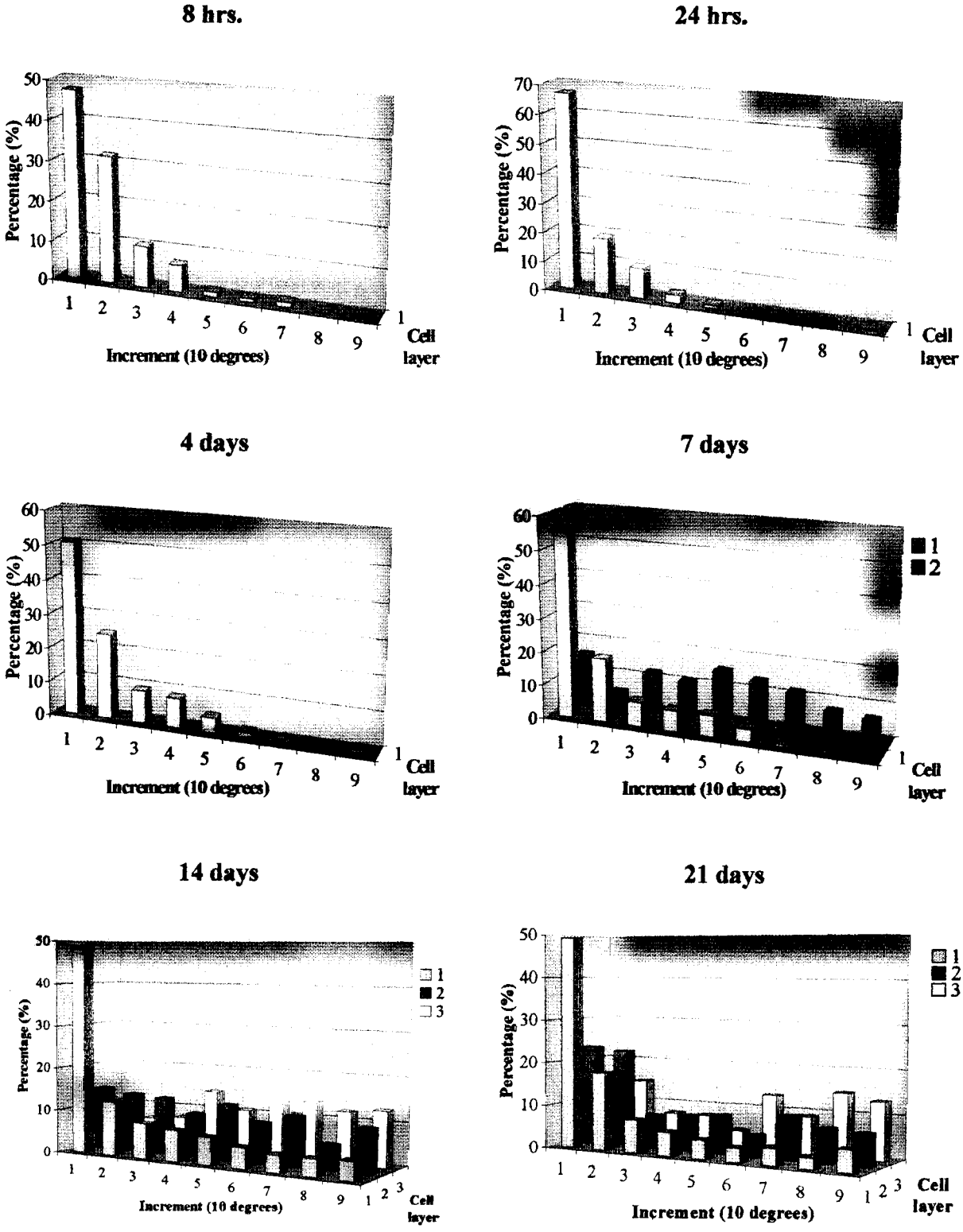

Figure 9: Distribution of osteoblast-like cells according to their angle of orientation on 3μm-deep grooves.

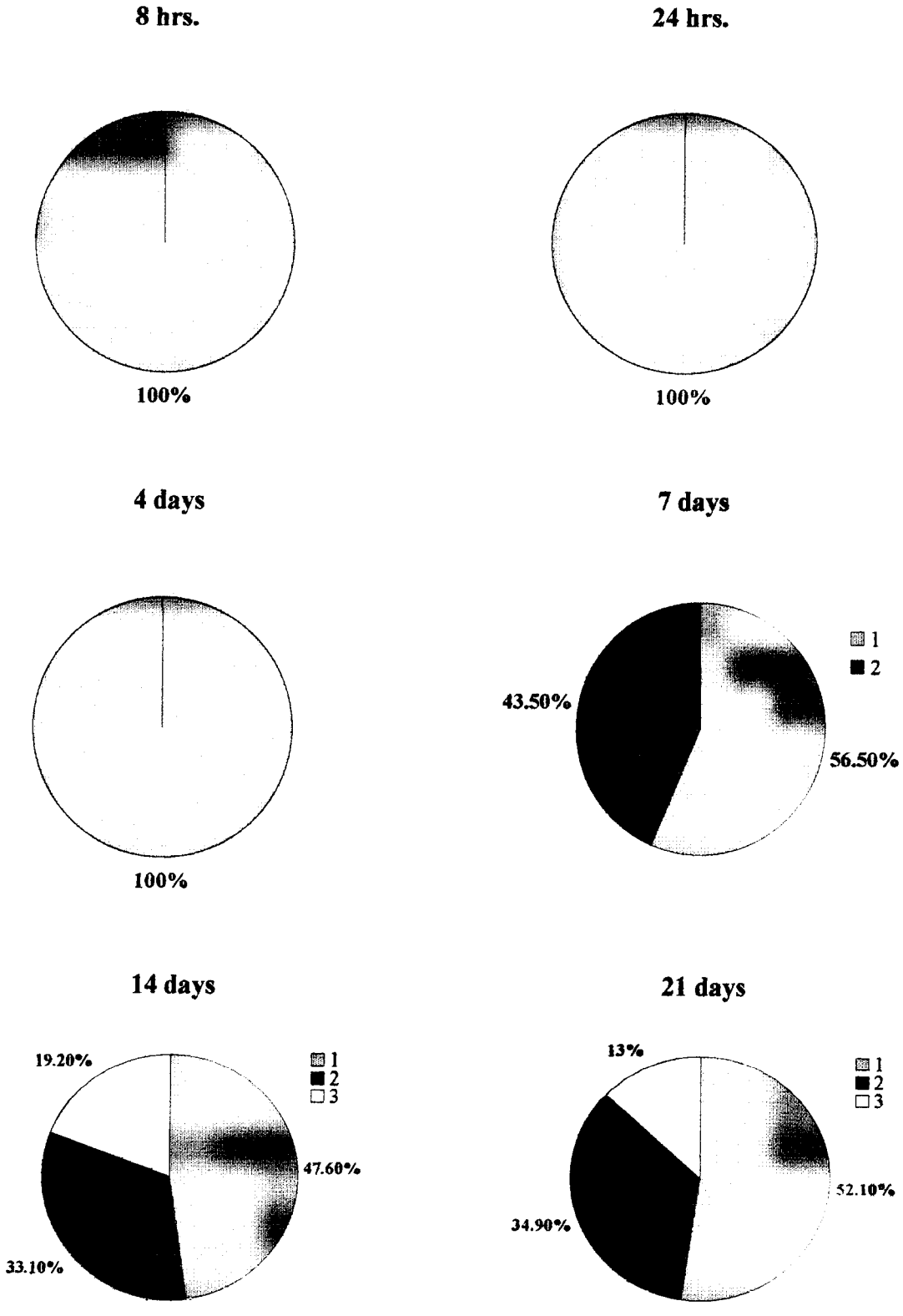

Figure 10: Percentages of total cell population associated with cell layers on 3μm-deep grooves.

2. Cell orientation on 10μm-deep grooves

Very much like the cultures on the 3μm-deep grooves, the cells plated on the 10μm-deep grooves formed monolayers of osteoblast-like cells until the 4th day. Until day 4 all cells were in contact with titanium at the bottom of the grooves. On the 7th day a second cell layer could be found on most cultures. After 14 days of incubation the cultures were three cell layers thick. On the 21st day in some places a fourth cell layer could be seen in the cultures, but there were so few cells in the fourth layer that they were not analyzed further. The mean OA's for all these cell layers were calculated by measuring the OA of individual osteoblast-like cells in every cell layer. The mean OA's of cell layers were compared and it was found that the means were statistically different ($P < 0.05$) with single exception of cell layers 1 and 2 on the 14th day where the two cell layers had similar OA's. Cell orientation with the grooves followed the order cell layer 1 > cell layer 2 > cell layer 3. Cell layer 1 when examined over time, was found to vary in the mean angle of orientation in that it went from being little oriented with the grooves at 8 hours to very oriented up to the 7th day and to less oriented after the 14th day. Cell layers 2 and 3 were found to become less oriented with the grooves, as their mean OA increased with time, but were always significantly different in orientation from cell layer 1 at all times. Table 7 summarizes the orientation of cell layers at different times.

Table 7: Orientation angles of cell layers over time for 10μm-deep grooves

Time	Cell Layer	n (No. of cells)	Mean Angle of Orientation (°) ± SE
8 hrs.	1	151	29.8 ± 2.1
24 hrs.	1	160	13.1 ± 1.0
4 days	1	255	10.0 ± 0.5
7 days	1	321	10.6 ± 0.5*
	2	138	13.1 ± 0.9*
14 days	1	186	19.2 ± 1.7
	2	170	21.9 ± 1.7
	3	60	29.7 ± 3.0
21 days	1	272	22.8 ± 1.6*
	2	177	32.2 ± 2.1*
	3	82	37.7 ± 3.2*

* indicates means that are significantly ($P < 0.05$) different from other means within the same time period (Kruskal-Wallis one-way ANOVA or Student's t-test where applicable).

When osteoblast-like cells were categorized according to their angles of orientation, it was found that after 8 hours of incubation over 25% of the cells were aligned (i.e. OA < 10^{o}) with the direction of the grooves. The number of aligned cells in increment 1 increased to over 50% and 60% after 24 hours and 4 days of incubation respectively. At any given time after 24 hours of incubation more than 50% of the osteoblast-like cells were oriented with the grooves. For the second cell layer, which was first detected after 7 days, the percentage of oriented cells decreased with time (i.e. over 50% on day 7, over 40% on day 14, and just over 30% on day 21). In cell layer 3 over 30% of the cells were oriented with the grooves on days 14 and 21. Briefly, cell layer 1 had more oriented cells than either of the cell layers 2 and 3 at any time. Figure 11 presents the distribution of osteoblast-like cells according to their angles of orientation. The 10-degree increment classification system is the same as the one used for the 3μm-deep grooves.

When more than one cell layer was present, different numbers of osteoblast-like cells were associated with each cell layer. At all times, cell layer 1 was the most populated cell layer, accommodating a minimum of 44% of the total cell population for any microscopic field examined. Cell layer 1 was followed by cell layer 2 and 3 in decreasing order of total osteoblast-like cells in them. Figure 12 shows the cell distribution among all cell layers.

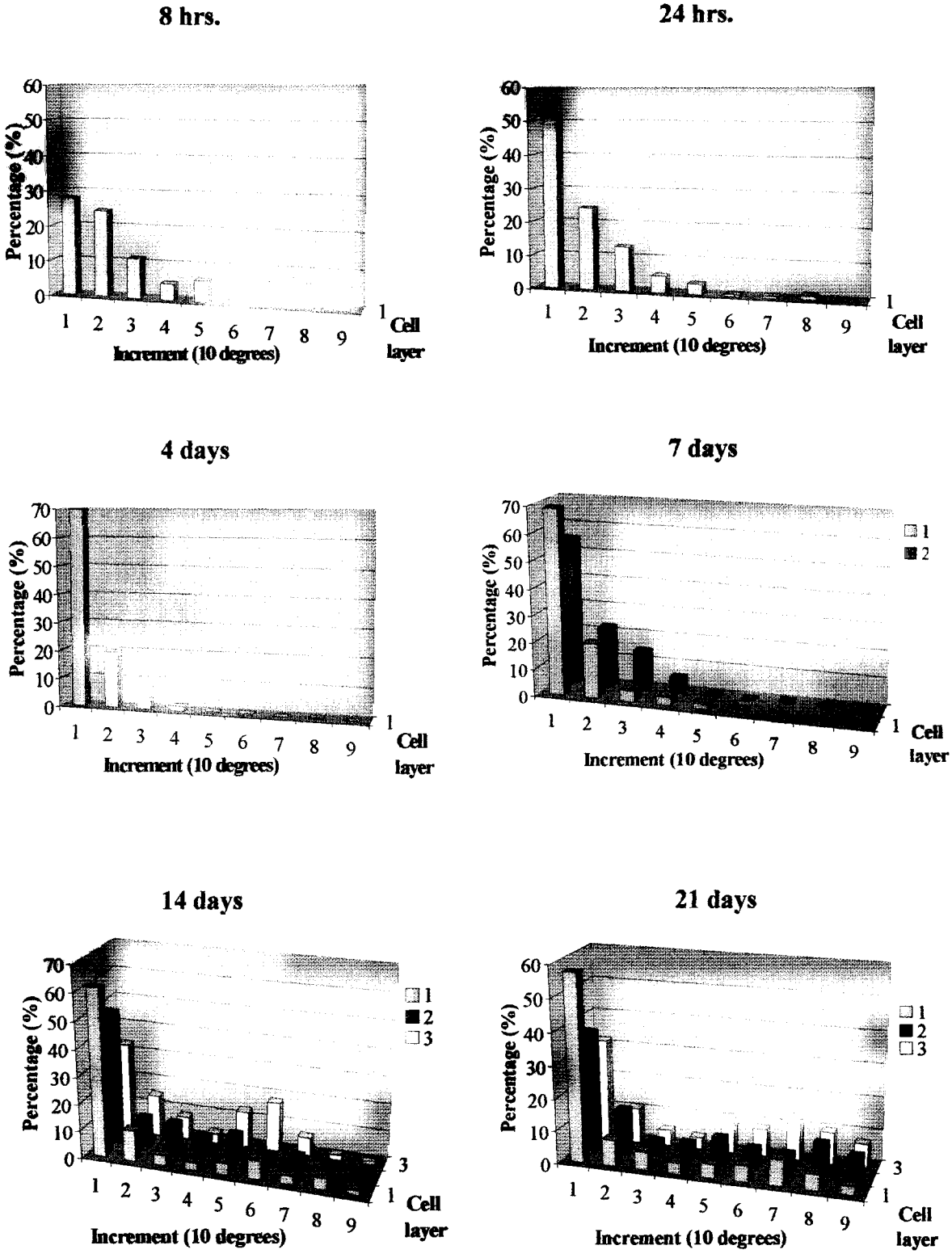

Figure 11: Distribution of osteoblast-like cells according to their angle of orientation on 10μm-deep grooves.

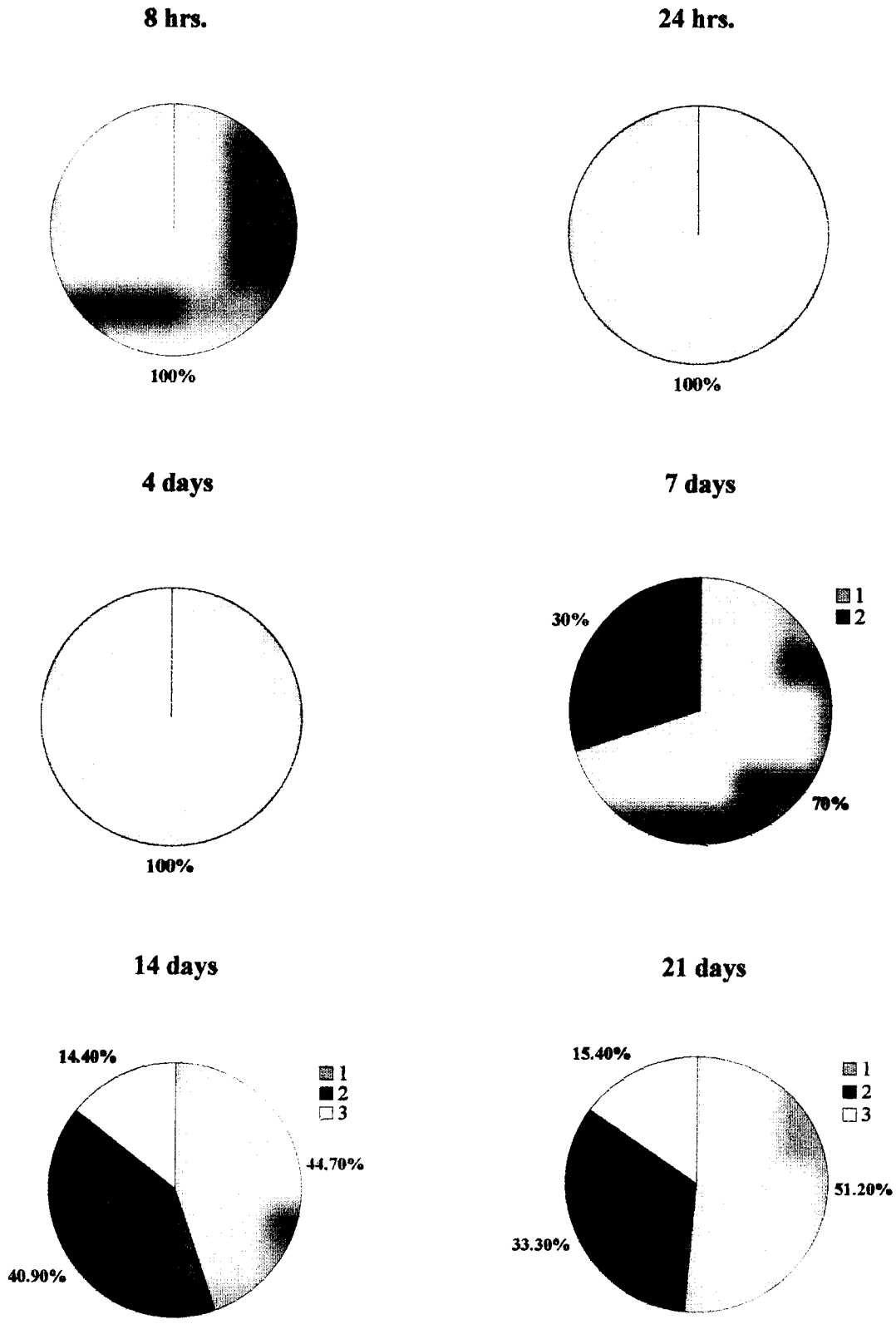

Figure 12: Percentages of total cell population associated with cell layers on 10μm-deep grooves.

3. Cell orientation on 30μm-deep grooves

As identified by optical sectioning, cell layers 1, 2, and 3 were most often within the grooves whereas cell layers 4 and 5 were above the ridge level. It should be noted once again that the concept of cell layers and their distance from the titanium surface is less well defined in deep grooves and cannot be compared directly with the cell layers on smooth or shallow-grooved substrata. On smooth surfaces the cells in layer 2 would not be in contact with the titanium for there is an underlying cell layer (1) between the layer 2 cells and the titanium. On 30μm-deep grooves, however, some of the layer 2 cells will be on the groove walls and thus in contact with the titanium while others will be in the trough of the groove with cell layer 1 cells separating them from the titanium. Figure 13A and 13B show examples of the osteoblast-like cells on the groove walls.

Cultures on the 30μm-deep grooves, similar to the cultures on the 3μm- and 10μm-deep grooves, consisted of a non-confluent monolayer of osteoblast-like cells up to and including the 4th day of incubation. The monolayer comprised cells that, optically, were at the same level and within the trough of the grooves with no cells above or beneath them. After 7 days of incubation, one could easily note three and sometimes even four cell layers. By the 21st day the number of cell layers had increased to five. The OA of cell layers 1 through 4 were not statistically different until the 21st day of incubation. During the first 14 days of incubation all cell layers were well aligned with the direction of the grooves. In the 21-day culture cell layer 4 was less oriented with the grooves and cell layer 5 was even less oriented than cell layer 4. However, cell layers 1 through 3 were well aligned with the grooves. The mean OA's for cell layers 4 and 5 were statistically ($P < 0.05$) different from the mean OA's of cell layers 1 through 3. Figure 14, a cross-section of the 30μm-deep grooves, shows that

the majority of the cells in layers 1, 2, and 3 (asterisks) were aligned with the grooves whereas the cells in the higher cell layers (arrowheads) were at an angle to the direction of the grooves. Table 8 is a summary of the measurements of the angle of orientation for cell layers on the 30μm-deep grooves.

The OA's for individual cell layers were compared over time. Cell layer 1 was found to be aligned with the grooves at all times except for the first 8 hours after plating. The results for cell layer 2 also indicated orientation with the grooves at all times, although slightly less well oriented than cell layer 1 after the 14^{th} day ($P < 0.05$). Cell layer 3 did not change much over time and most cells were aligned with the grooves. The orientation results for cell layer 4, however, indicate that the cell layer underwent an orientational change between days 14 and 21 of the incubation period. The mean angle of orientation for the 21-day culture was statistically ($P < 0.05$) higher than those of the 7- and 14-day cultures. However, the change in orientation was not sudden, as the mean OA of the cell layer for the 14-day culture was slightly higher (i.e. less aligned) than that of the 7-day culture. Cell layer 5, which was first observed on day 21, was not aligned with the direction of the grooves. Generally, cell layers 1, 2, and 3 appeared to be within the grooves whereas cell layers 4 and 5 appeared at or above the ridge level. The rows of Table 8 are shaded so that cell layers have the same gray level to facilitate comparison over time.

Table 8: Orientation angles of cell layers over time for 30μm-deep grooves

Time	Cell Layer	n (No. of cells)	Mean Angle of Orientation (°) ± SE
8 hrs.	1	194	13.9 ± 1.0
24 hrs.	1	255	9.4 ± 0.6
4 days	1	242	10.7 ± 0.8
7 days	1	98	7.4 ± 0.9
	2	105	6.9 ± 0.5
	3	106	9.0 ± 0.8
	4	72	7.8 ± 0.6
14 days	1	103	10.5 ± 1.3
	2	177	12.5 ± 1.2
	3	178	11.5 ± 1.0
	4	97	12.4 ± 1.3
21 days	1	59	6.6 ± 0.6
	2	134	8.6 ± 0.8
	3	129	11.1 ± 1.3
	4	295	19.1 ± 1.2*
	[illegible]	[illegible]	[illegible]3*

* indicates means that are significantly ($P < 0.05$) different (Kruskal-Wallis one-way ANOVA).

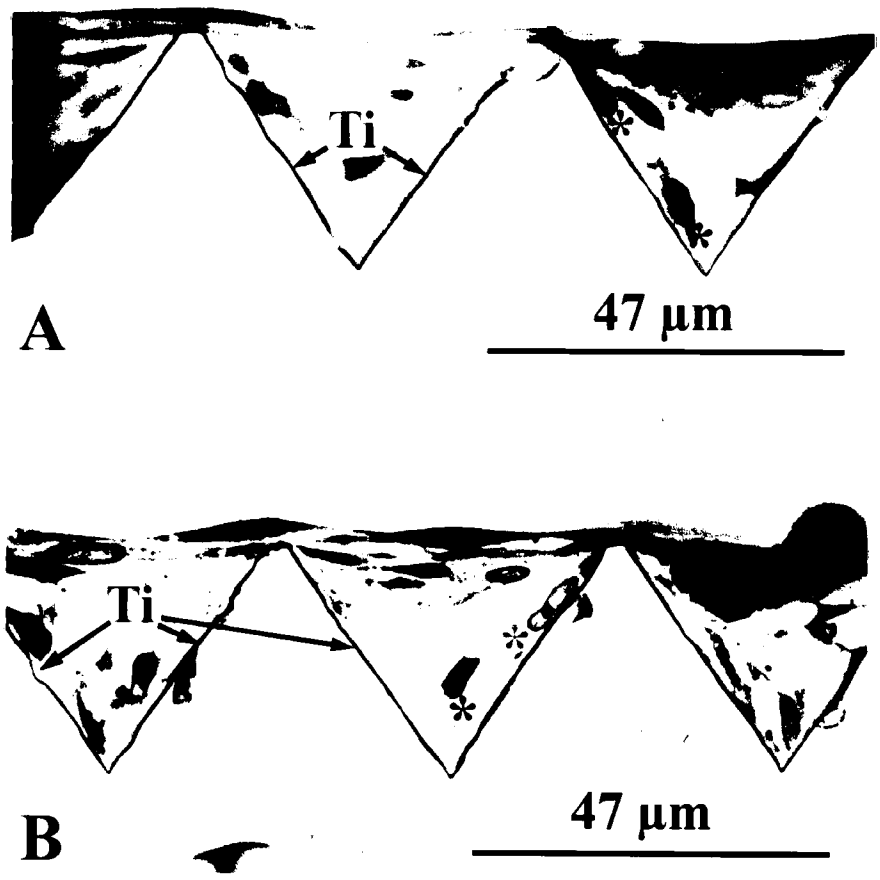

Figure 13: Toluidine blue section of 30µm-deep grooves at week 4. A and B are two instances of osteoblast-like cells (asterisks) occupying the groove walls at different depths and would be counted as being in different cell layers. Ti = titanium coating on the groove walls.

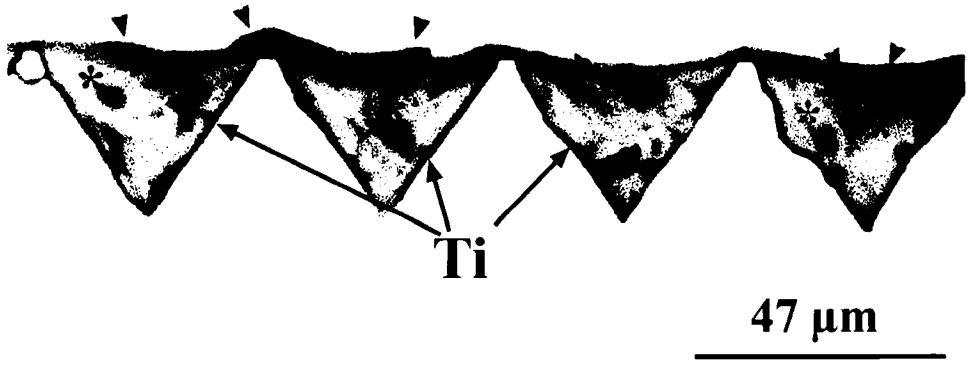

Figure 14: Methylene blue section of 30µm-deep grooves at week 4. Cells within the grooves (asterisks) appear to be in alignment with the grooves whereas the cells in higher cell layers (arrowheads) are at an angle to the direction of the grooves. Ti = titanium coating on the groove walls.

Osteoblast-like cells were categorized into 10-degree increments according to their angle of orientation. Eight hours after cells were plated on the 30μm-deep grooves, over 50% of the cells were already aligned with the grooves. After 24 hours more than 70% of cells in layer 1 were oriented with the grooves. On day 7 there were three cell layers and over 70% of cells in all three cell layers were aligned with the grooves. On day 14 four cell layers were present. In layer 1 over 70% of the cells were oriented compared to over 60% of the cells in layers 2 through 4. After 21 days when five cell layers were observed, layers 4 and 5 had fewer cells aligned compared to cell layers 1 through 3. It is worth mentioning that cell layers 4 and 5 were mostly located outside the grooves and above the ridge level. Bar graphs in Figure 15 show the distribution of osteoblast-like cells according to their angles of orientation.

The fraction of total cells associated with every cell layer was found to vary over time. An unexpected observation was that the number of cells in cell layer 1 (closest to the bottom of the grooves) decreased over time from 100% (8 hours, 24 hours, and 4 days) to just over 8% on day 21. As the cell density in higher layers increased, fewer cells were found in the layer 1. It appeared that as the culture formed multilayers of cells, fewer cells were found at the level closest to the groove bottom where 100% of the cells resided between 8 hours and 4 days. This finding is illustrated in Figures 13 and 14 where few cells can be seen at the bottom and most cells are near the top of the grooves. On days 7 and 14 cell layers 2 and 3 had the most number of osteoblast-like cells in them. On day 21 a mere 8.2% of the total cells were found in cell layer 1. Cell layers 2 and 3 had 33.4% of the total cells and cell layer 4 was the largest with over 41% of the total cells. The pie graphs in Figure 16 present the proportion of cells in different layers with respect to one another over time.

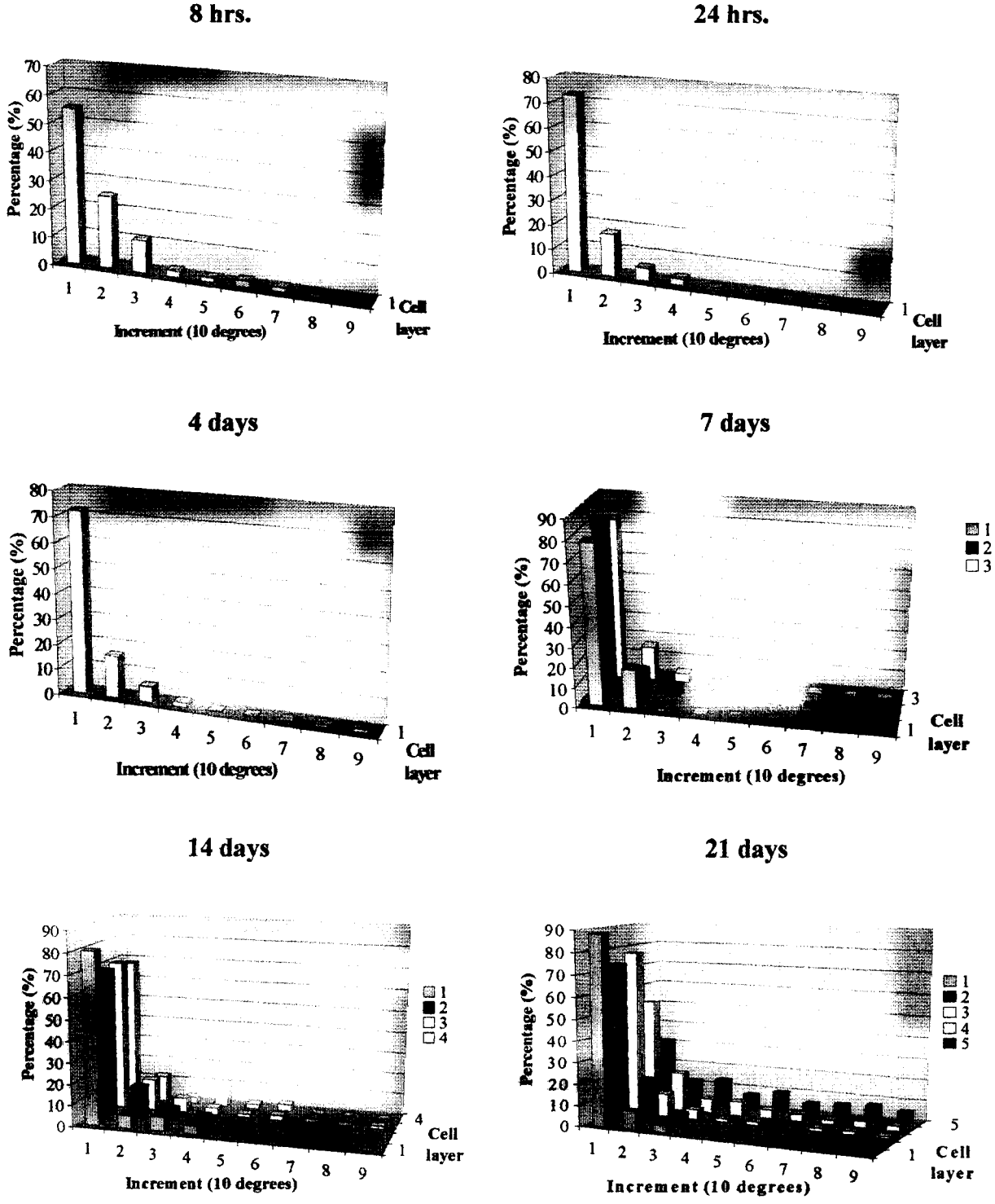

Figure 15: Distribution of osteoblast-like cells according to their angle of orientation on 30μm-deep grooves.

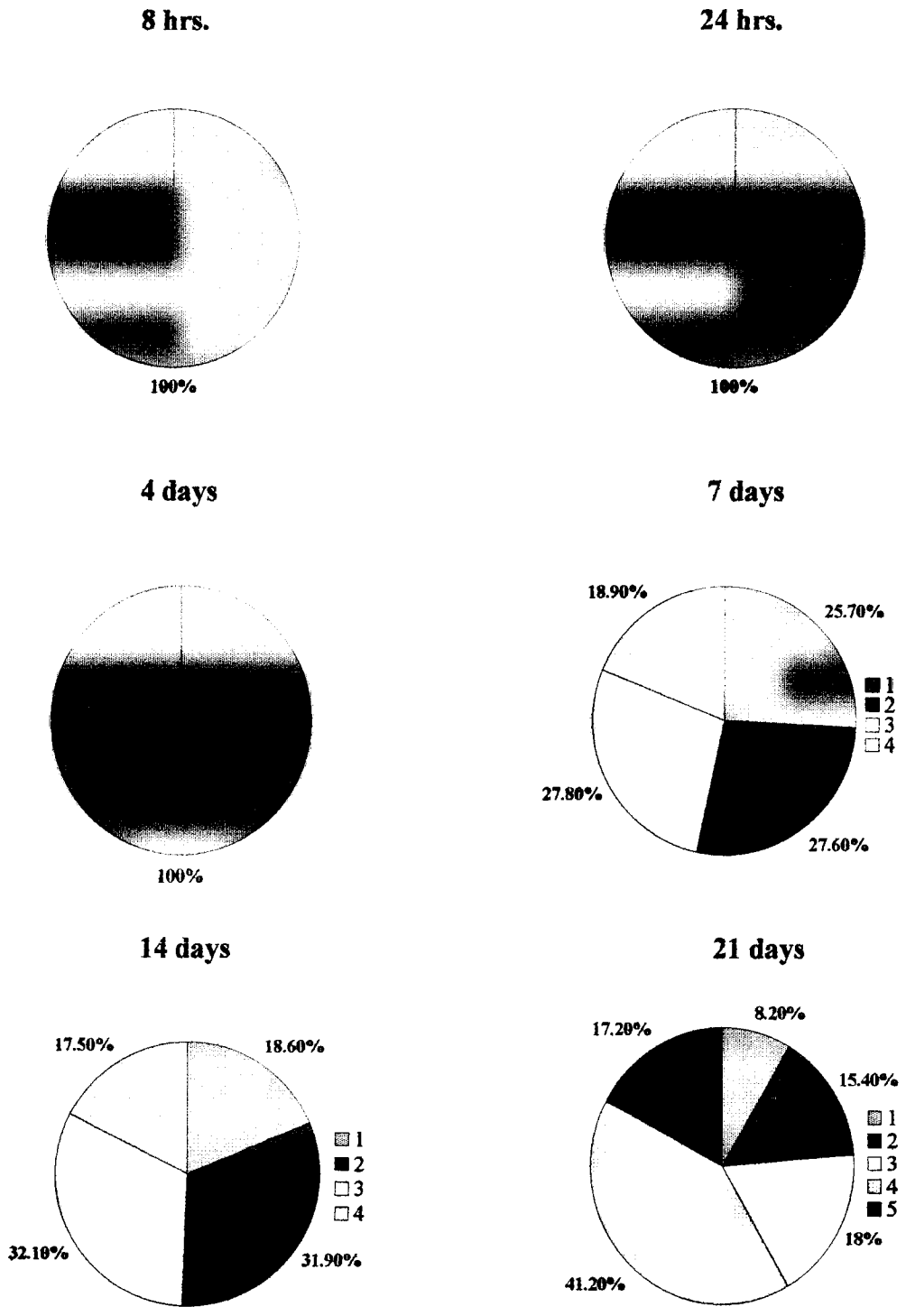

Figure 16: Percentages of total cell population associated with cell layers on 30μm-deep grooves.

4. Cell orientation on smooth gaps

The mean angle of orientation of cells was measured with respect to the direction of the flanking grooves. Similar to the grooved micromachined substrata, it was found that cultures that were younger than seven days comprised a single cell layer. Eight hours after plating the cells were still randomly oriented. At 24 hours, the orientation of cells on all the smooth gaps, with the exception of the 100μm-wide gaps, was random and very similar to the results of the 8-hour culture. On the 100μm-wide gaps, the cells were more oriented with a mean angle of orientation of about 30°. After 4 days of incubation, the orientation of osteoblast-like cells on the smooth gaps dramatically changed, as the cells became oriented with the flanking grooves. Table 9 is a summary of the orientation of the osteoblast-like cells in cultures with a monolayer of cells.

At 7 days, there were two cell layers on all the smooth gaps. It was found that the cells in cell layer 1 were slightly more oriented with the flanking grooves as the gap width increased. The mean orientation angle of cell layer 2 was significantly ($P < 0.05$) different from that of cell layer 1 only on the smooth gaps with the widths of 150 μm and 200μm (Table 10).

At 14 days, four distinct cell layers were present on all the smooth gaps compared to only three on the smooth surfaces at the same time. Osteoblast-like cells in cell layer 1, regardless of gap width, were better oriented with the flanking grooves than the cells in the other three layers. Orientation with respect to the neighbouring grooves decreased with cell layer, layer 1 being the most oriented and layer 4 the least oriented. The mean angles of orientation for cell layer 4 on 50μm- and 150μm-wide gaps were significantly ($P < 0.05$) higher than cell layer 4 of either 100μm- and 200μm-wide gaps. The mean angles of orientation of cell layers 2 and 3 were similar (no statistical difference) on all but the 200μm-wide gaps.

Table 9: Orientation angles of monolayers of osteoblast-like cells on smooth gaps on surfaces with 10μm-deep grooves

Time	Gap Width (μm)	Cell Layer	n (No. of cells)	Mean Angle of Orientation (°) ± SE
8 hrs.	50	1	85	44.5 ± 2.6
	100	1	73	39.3 ± 3.0
	150	1	113	40.0 ± 2.3
	200	1	143	39.5 ± 2.2
24 hrs.	50	1	86	40.0 ± 3.0
	100	1	91	30.5 ± 2.4
	150	1	81	36.5 ± 3.0
	200	1	89	38.3 ± 2.8
4 days	50	1	83	23.4 ± 2.6
	100	1	138	23.7 ± 2.0
	150	1	127	24.7 ± 2.1
	200	1	96	22.7 ± 2.3

At 21 days, four distinct cell layers could be found on all the smooth gaps. As with the 14-day old cultures, it was found that cell layer 1 on all smooth gaps was better oriented with the direction of the flanking grooves than the other three cell layers. The degree of orientation with the grooves decreased with cell layers (*i.e.* cell layer 1 being the most oriented and cell layer 4 being the least oriented). The difference was not always statistically significant. It was also noted that cell layers 2 and 3 had similar (no statistical difference) mean angles of orientation on all but the 150μm-wide gaps where cell layer 3 was less oriented with the flanking grooves than cell layer 2 (Table 10).

Overall, it can be generalized that the orientation with respect to the grooves of cell layers in gaps decreased going from the lower cell layers to the higher ones (Table 10). The data gathered on the orientation of osteoblast-like cells suggest that cell layers generally become less oriented with the grooves as the cell layers get farther from the surface, similar to the results of the grooved areas. The histological cross sections in Figure 17 illustrate the above arrangement of cell layers on smooth gaps.

Table 10: Orientation angles of cell layers on gaps with two or more cell layers

Time	Gap Width (μm)	Cell Layer	n (No. of cells)	Mean Angle of Orientation (°) ± SE
7 days	50	1	61	27.0 ± 3.7
		2	49	27.0 ± 2.6
	100	1	69	27.4 ± 3.5
		2	65	28.2 ± 2.7
	150	1	135	21.4 ± 2.1 *
		2	94	30.0 ± 1.8 *
	200	1	140	20.2 ± 2.0 *
		2	100	24.0 ± 2.0 *
14 days	50	1	64	20.7 ± 2.1 *
		2	47	28.7 ± 2.5
		3	41	32.6 ± 3.4
		4	32	52.2 ± 3.3 *
	100	1	48	16.6 ± 2.8 *
		2	80	30.6 ± 2.6
		3	58	30.4 ± 2.7
		4	70	38.5 ± 2.2 *
	150	1	86	24.2 ± 2.2 *
		2	89	31.2 ± 2.4
		3	72	32.7 ± 2.6
		4	65	50.1 ± 2.2 *
	200	1	122	19.7 ± 1.7 *
		2	93	26.0 ± 2.0 *
		3	78	35.0 ± 2.6
		4	65	35.2 ± 1.7
21 days	50	1	74	23.9 ± 2.4 *
		2	51	35.9 ± 3.0
		3	42	38.9 ± 2.9
		4	39	42.7 ± 3.4 *
	100	1	119	27.7 ± 2.0 *
		2	70	41.2 ± 2.9
		3	68	39.6 ± 2.7
		4	44	48.5 ± 3.3 *
	150	1	150	32.3 ± 2.2 **
		2	105	28.8 ± 2.0 **
		3	61	36.4 ± 2.9 **
		4	42	52.8 ± 3.5 **
	200	1	199	24.2 ± 1.5 *
		2	151	34.2 ± 1.9
		3	82	34.7 ± 2.8
		4	47	53.8 ± 3.0 *

* indicates mean OA's of cell layers in the same gap size that are significantly ($P < 0.05$) different from one another (one-way ANOVA and Tukey's HSD tests).

** indicates that the mean OA of all four cell layers are significantly ($P < 0.05$) different.

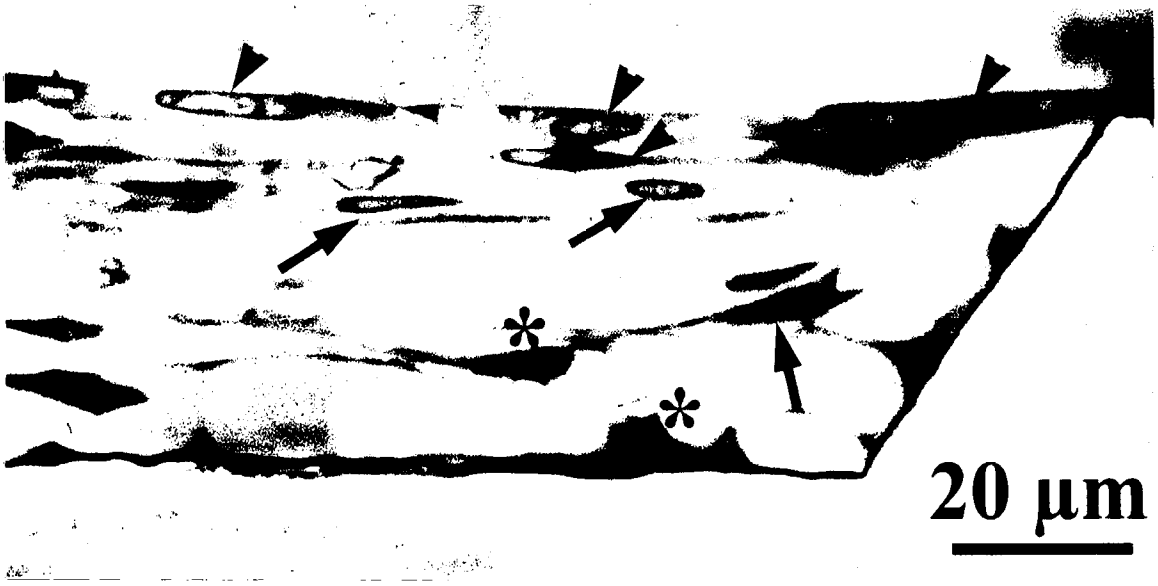

Figure 17: Toluidine blue section of a 50µm-wide gap in 30µm deep grooves with multilayers of osteoblast-like cells. The direction of the flanking grooves is coming out from the plane of the section. Cells in the lower cell layers (asterisks) are aligned with the grooves. Cells in the second and third cell layers (arrows) are at an angle with the flanking grooves. Cells in the higher layers (arrowheads) are at even higher angles to the direction of the adjacent grooves compared to the cells in the second and third layers.

Osteoblast-like cells were categorized into 10-degree increments (1-9) according to their angle of orientation with respect to the flanking grooves. Figures 18 through 21 provide an orientation profile of cells in each cell layer. No preferred orientation was observed after 8 hours, but after 24 hours some orientation with respect to the flanking grooves took place as the number of cells in increment 1 (0^{o}-9.9^{o}) increased. By the fourth day more cells were found in increment 1 than in any other category. At times when the cultures consisted of multilayers of osteoblast-like cells, the second and third layers had fewer cells aligned with the neighbouring grooves (*i.e.* in increment 1) than layer 1 and had more cells in the increments 2, 3, 4, and 5 (*i.e.* orientation angles 10^{o}-49.9^{o}). This overlap between the second and third cell layers is also apparent in the mean angles of orientation (Table 10) for both cell layers where little differences existed between the two cell layers.

The distribution of osteoblast-like cells according to their angle of orientation in cell layer 4 was different in that it had more cells in increments 6 to 8 (50^{o}-79.9^{o}) than other cell layers. Therefore, going from cell layer 1 to cell layer 4, one finds that cells become less oriented with respect to the direction of the flanking grooves.

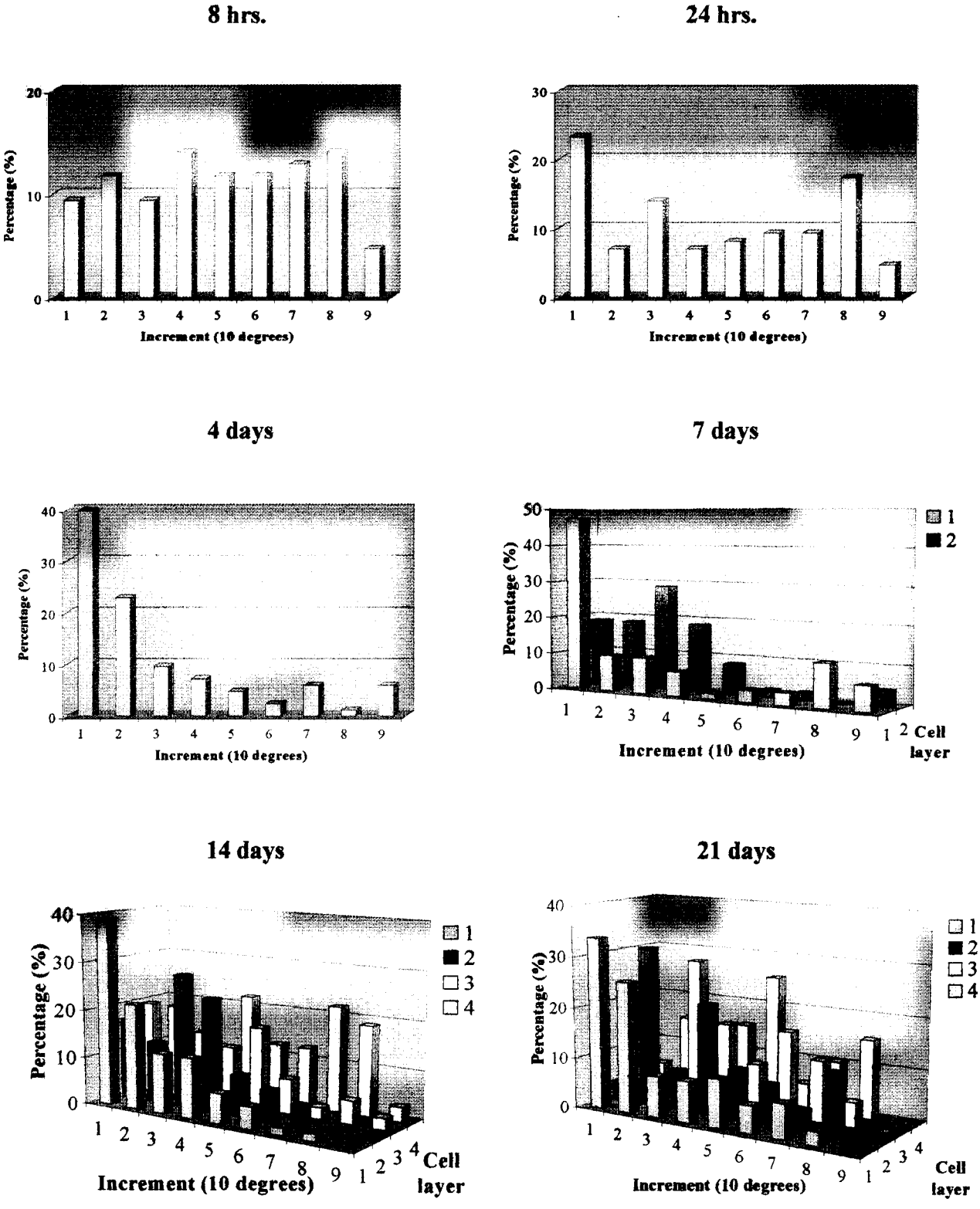

Figure 18: Distribution of osteoblast-like cells according to their angle of orientation on 50μm-wide gaps of substrata with 10μm-deep grooves.

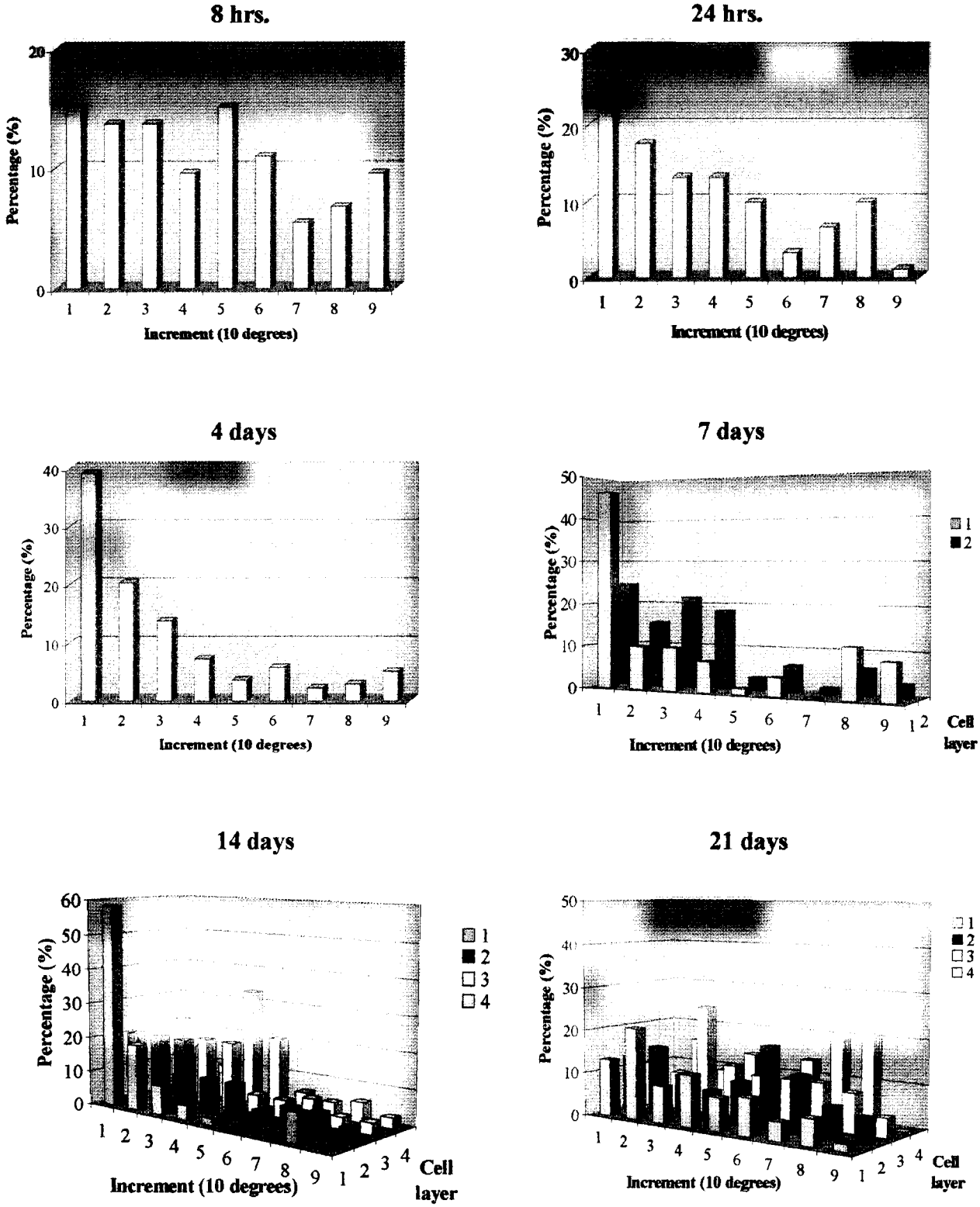

Figure 19: Distribution of osteoblast-like cells according to their angle of orientation on 100μm-wide gaps of substrata with 10μm-deep grooves.

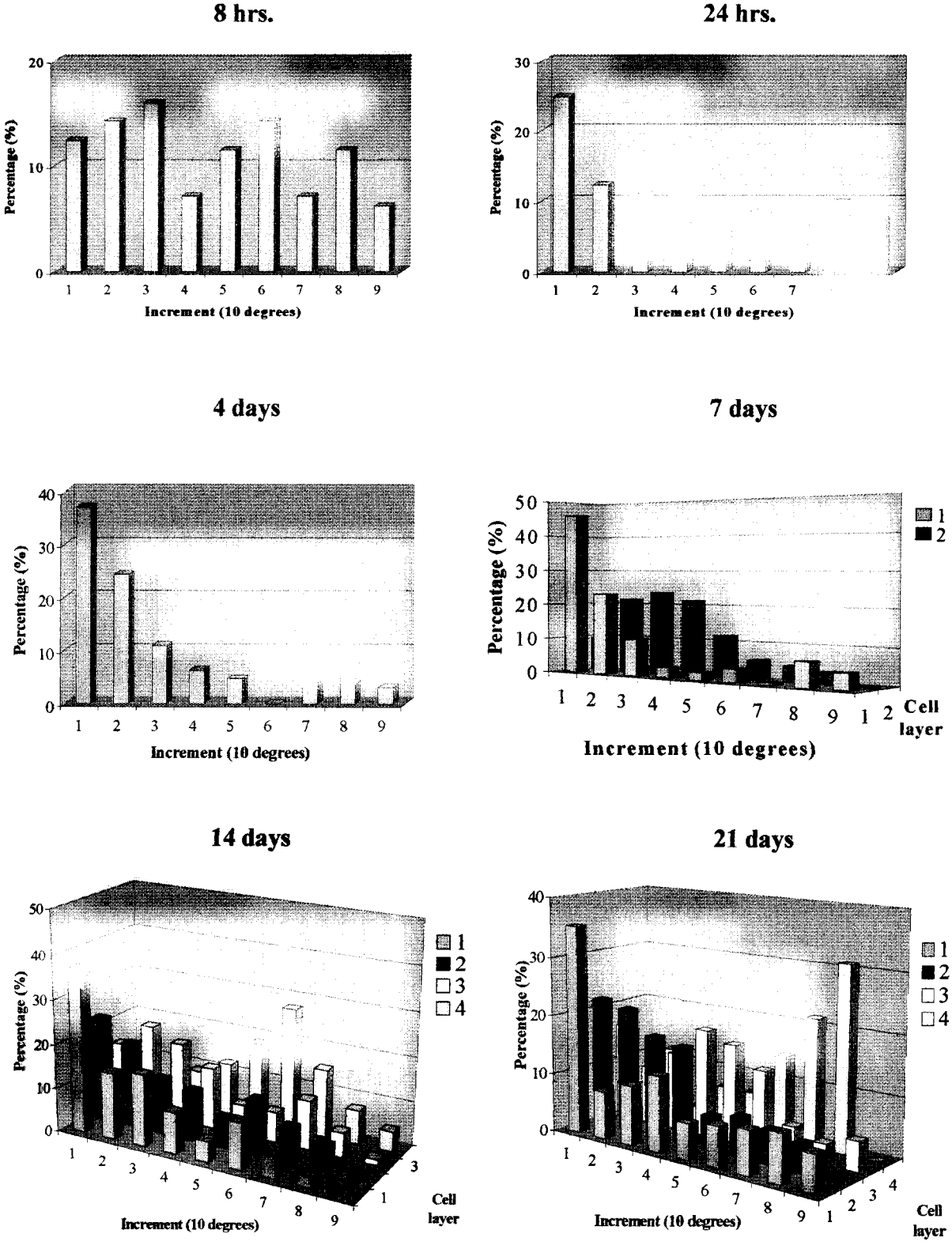

Figure 20: Distribution of osteoblast-like cells according to their angle of orientation on 150μm-wide gaps of substrata with 10μm-deep grooves.

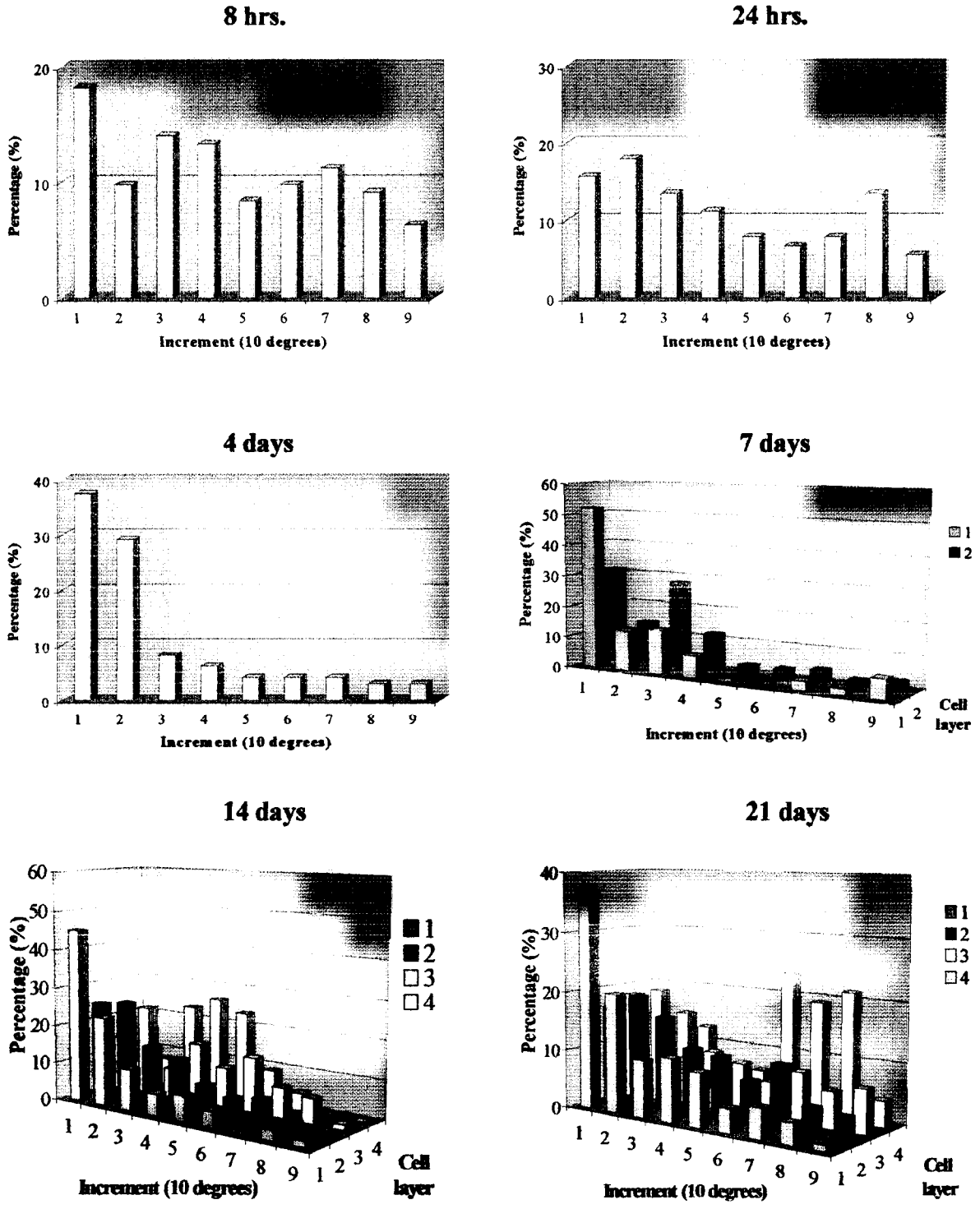

Figure 21: Distribution of osteoblast-like cells according to their angle of orientation on 200μm-wide gaps of substrata with 10μm-deep grooves.

The percentages of osteoblast-like cells associated with cell layers in the smooth gaps were calculated (Figures 22-25). The results indicated that cultures were made up of one cell layer on day 4. On the 7th day, two distinct cell layers were observed, with the cell layer closest to the titanium having the most cells. On the 14th day four cell layers could be distinguished. Except for the cultures on the 100μm and 150μm gaps, cell layer 1 had the most cells. Cell layer 1 on the 100μm gaps on day 14 had the fewest proportion of cells and on the 150μm gaps had equal proportions with cell layer 2 (Figures 23 and 24). At the same time, cell layer 3 had more cells than cell layer 4 on all gap sizes except for the 100μm gap. After 21days, there were still four distinguishable cell layers. However, the proportion of cells within cell layer 1 rebounded to have more cells than all other cell layers. The order of cell layers for the number of osteoblast-like cells associated with them was found to be cell layer 1 > cell layer 2 > cell layer 3 > cell layer 4. This order held true regardless of the number of cell layers, except for the 14th day when the proportion of cells in cell layers 1 and 2 decreased from the 7th day. This decrease in cell distribution of cell layers 1 and 2 (*i.e.* day 14) was noticed for all gap sizes. The percentages of cells associated with cell layers 1 and 2 increased on day 21, but the values were still lower than those of day 7. The actual number of cells in cell layers varied over time so that no pattern could be established, but the total number of cells (sum of the cells in all cell layers) increased as a whole (Table 10).

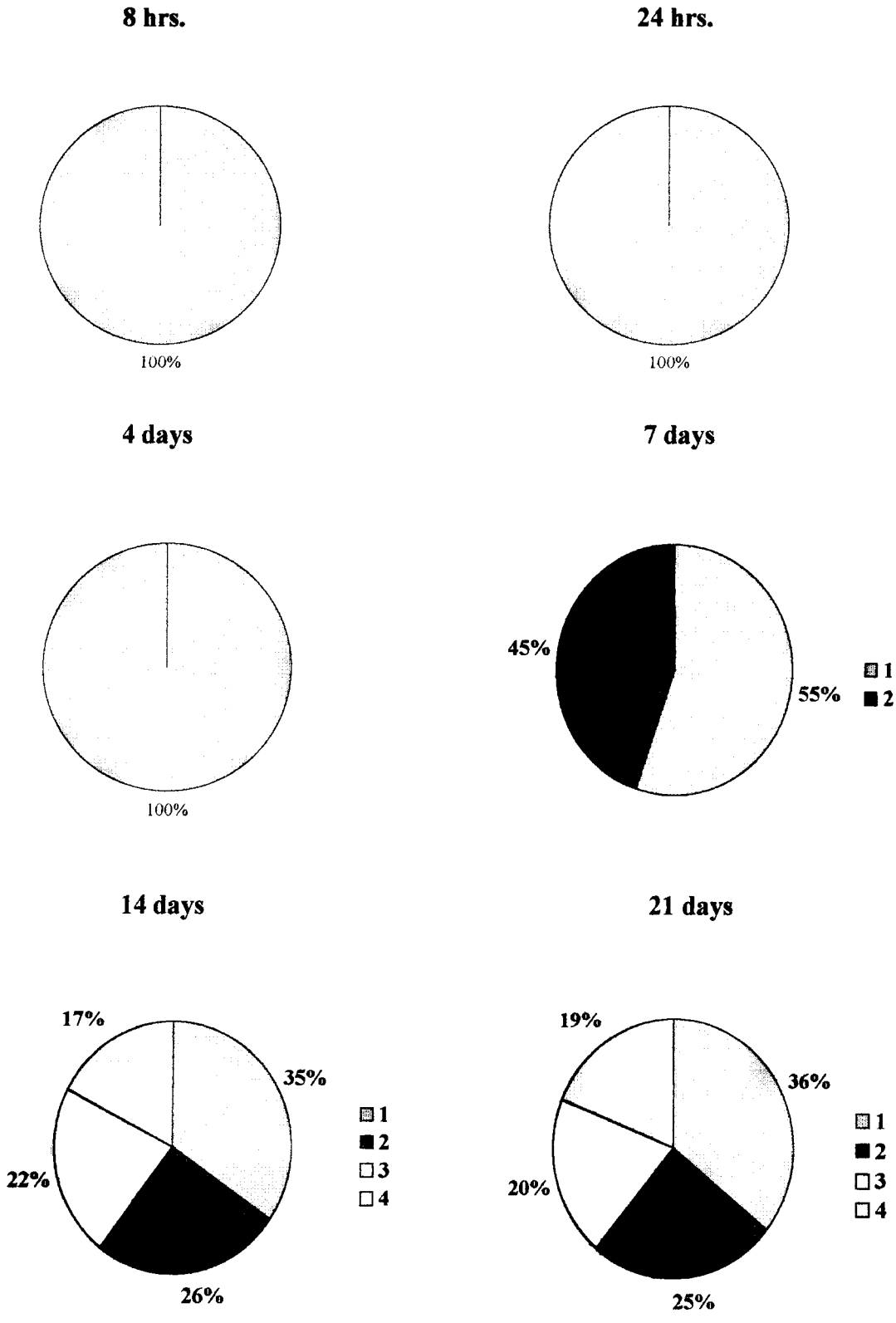

Figure 22: Percentages of total cell population associated with cell layers in 50μm gaps of substrata with 10μm-deep grooves.

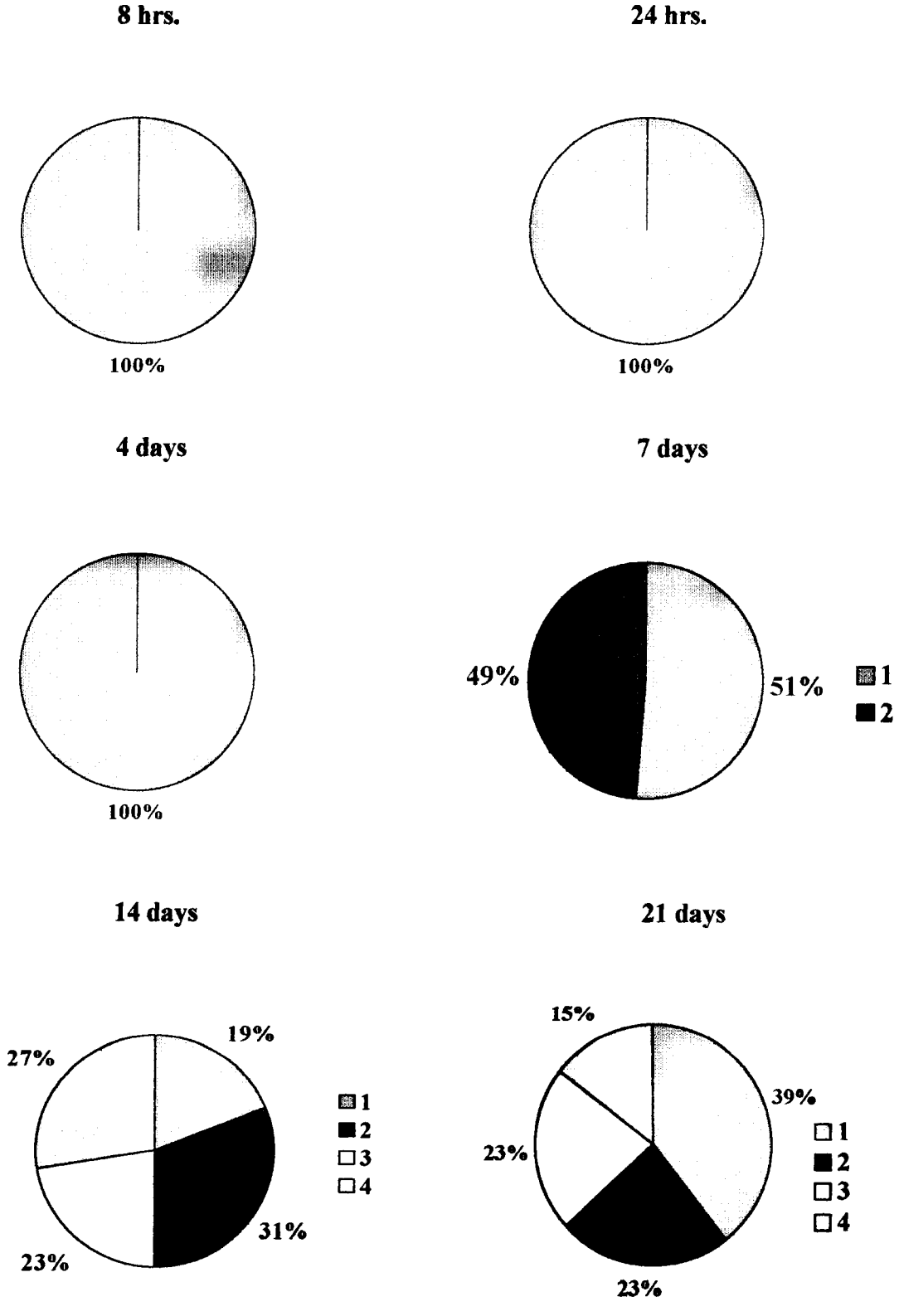

Figure 23: Percentages of cell population associated with cell layers in 100μm gaps of substrata with 10μm-deep grooves.

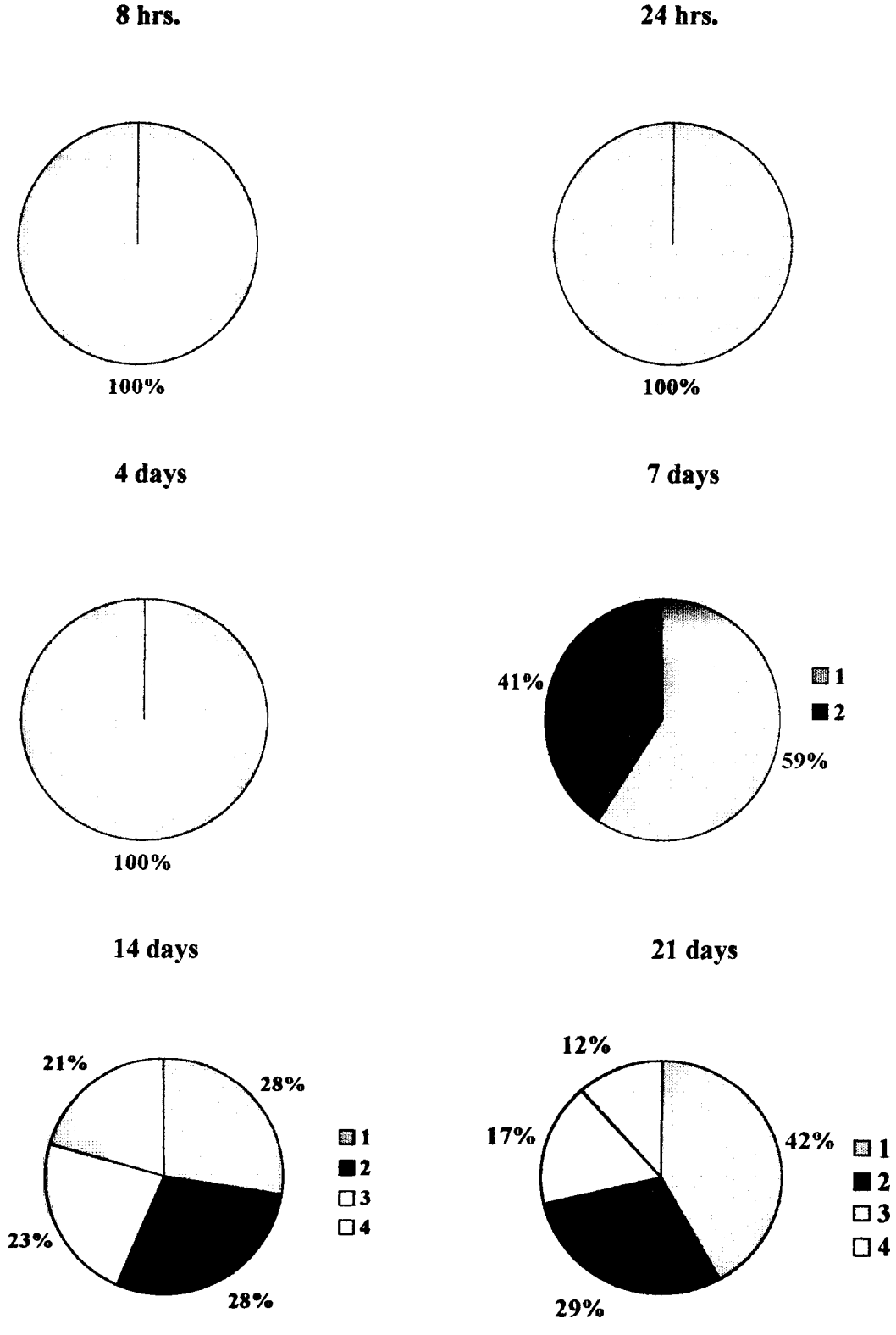

Figure 24: Percentages of cell population associated with cell layers in 150μm gaps of substrata with 10μm-deep grooves.

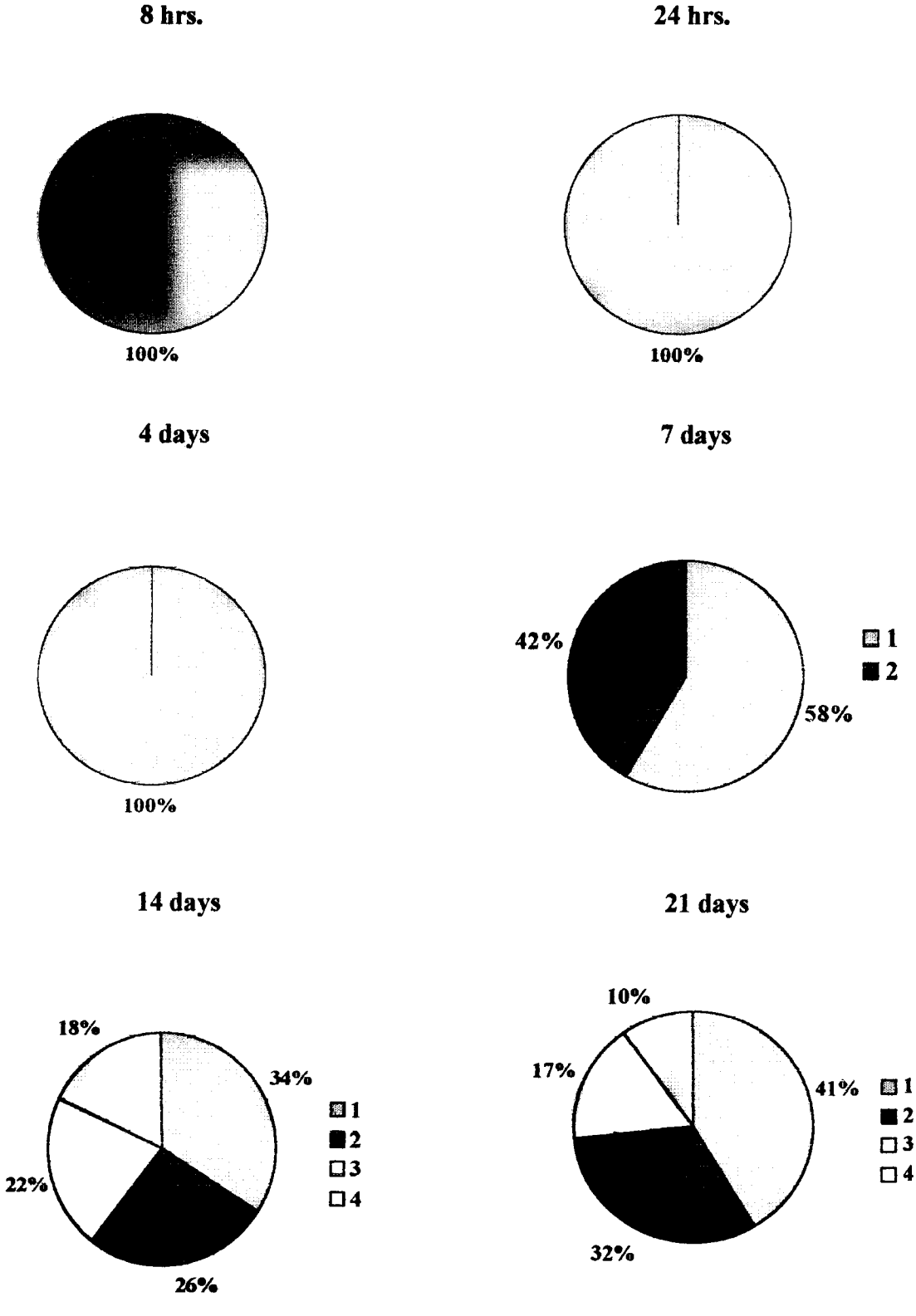

Figure 25: Percentages of cell population associated with cell layers in 200μm gaps of substrata with 10μm-deep grooves.

5. Cell orientation on smooth surfaces

The angles of orientation for osteoblast-like cells on smooth surfaces were measured with respect to the horizontal axis of every field. It was found that cells on the smooth surfaces showed no preferred orientation (*i.e.* mean OA close to 45° as expected if no orienting influences were present) and no statistical differences were found either with time or cell layer.

Table 11: Orientation angles of cell layers on smooth surfaces

Time	Cell Layer	n (No. of cells)	Mean Angle of Orientation (°) ± SE
8 hrs.	1	256	42.8 ± 1.5
24 hrs.	1	256	40.8 ± 1.5
4 days	1	256	45.4 ± 1.6
7 days	1	267	40.8 ± 1.4
	2	92	45.2 ± 2.7
14 days	1	321	41.9 ± 1.4
	2	203	43.6 ± 1.7
	3	102	48.1 ± 2.5
21 days	1	342	41.6 ± 1.3
	2	165	41.7 ± 1.8
	3	63	44.0 ± 1.4

The cultures on the smooth surfaces consisted of a monolayer of osteoblast-like cells before the 7th day, when two cell layers were distinguished. On the 7th day cell layer closest to titanium (cell layer 1) had more cells than cell layer above it (Figure 26). On the 14th day, three cell layers were found in all cultures. At this time, cell layer 1 had a smaller proportion of the total cell population than the 7th day. However, the proportion of cells in cell layer 2 increased from day 7. After 21 days, there were still three cell layers. The percentage of cells in cell layer 1 increased, but it was still lower than the figure on the 7th day. This pattern is similar to the pattern observed for the smooth gaps. Cell layer 3's proportion of cell population decreased between days 14 and 21.

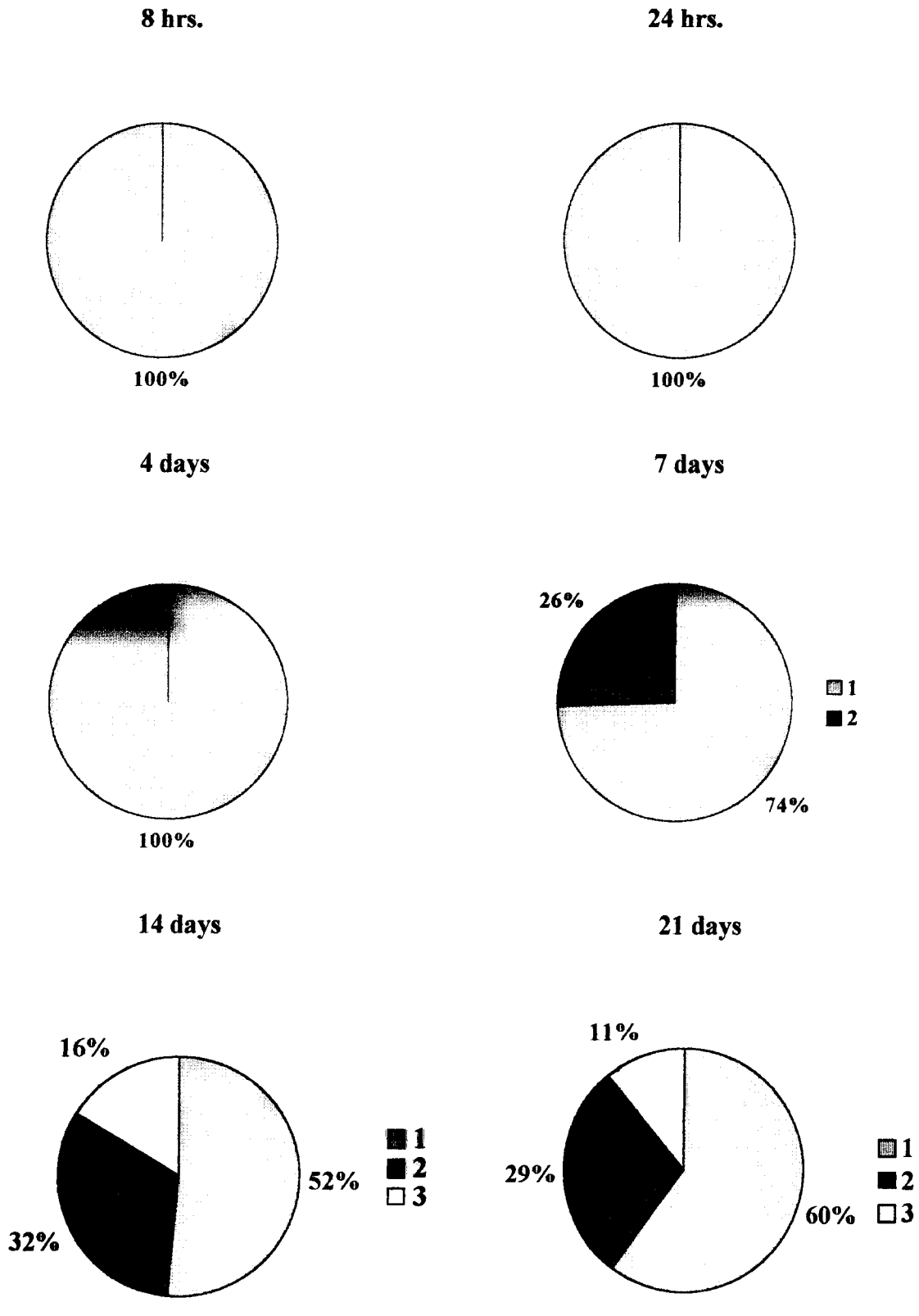

Figure 26: Percentages of cell population associated with cell layers on smooth surfaces.

6. Scanning electron microscopy (SEM)

Another approach to studying the orientation of osteoblast-like cells on the microfabricated substrata is scanning electron microscopy (SEM). However, using SEM as the sole technique for determining cell orientation is limited since, typically, it allows for examining only the cells on the surface layer at any time.

Osteoblast-like cultures were prepared for SEM studies after 14 and 21 days of incubation. At 14 days most of the osteoblast-like cells were either below or at the ridge level and were mostly oriented with the direction of the grooves. Rarely would cells be found above the ridge level. The number of cell layers could not be discerned by looking at the SEM micrographs, as the top layers obscured the lower ones. Figure 27A shows osteoblast-like cells on day 14. At 21 days, it was noticed that the cells that were situated above the ridges had their long axis at an angle to the direction of the grooves (Figure 27B). This type of cell arrangement with cells lacking conformity to the underlying grooves was frequent in the 21-day old culture whereas in the 14-day old culture it was only rarely observed. The cells that were below or at the ridge level were mostly aligned with the grooves, as found with the 14-day old culture.

On the smooth gaps the cells that were situated at the top were mostly at an angle with the direction of the flanking grooves. This lack of orientation was apparent in both the 14- and 21-day old cultures. The cells below or the number of cell layers could not be determined by looking at the micrographs. Figure 28 shows osteoblast-like cells on a 100-μm wide gap after 14 days of incubation.

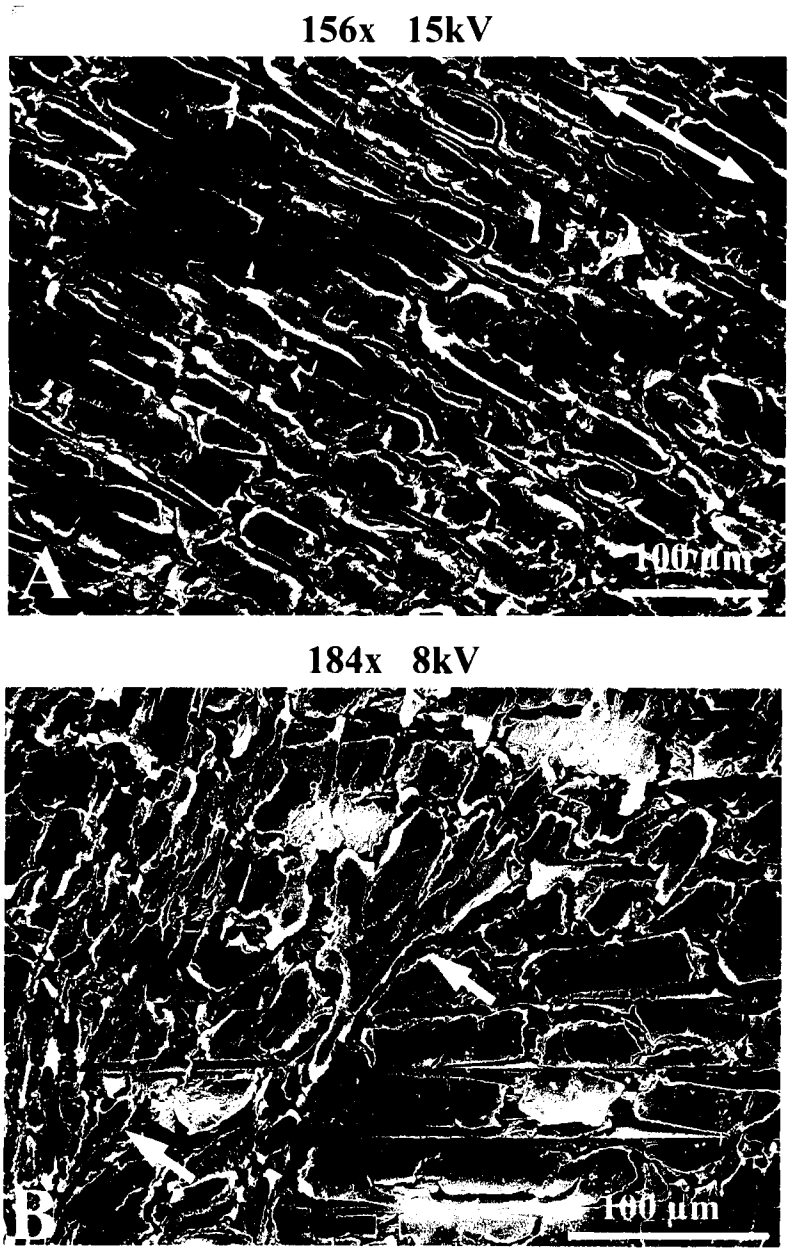

Figure 27: A. Osteoblast-like cells on 10µm-deep grooves after 14 days. Note that the majority of the cells are aligned with the direction of the grooves (double-headed arrow). B. Osteoblast-like cells on 10µm-deep grooves after 21 days. Cells above the ridge level (arrows) did not align with the grooves, but the cells below them were mostly aligned with the grooves.

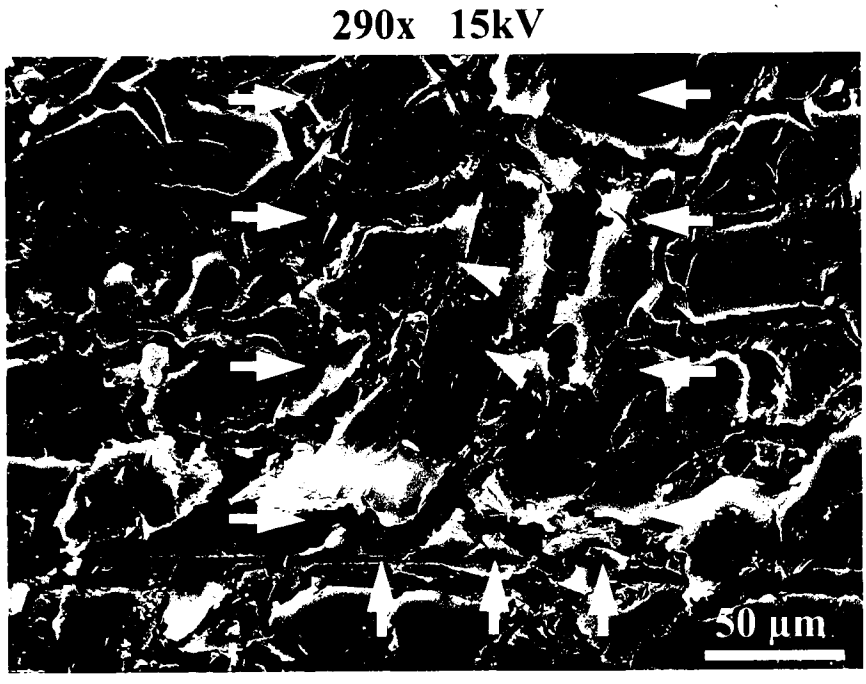

Figure 28: Osteoblast-like cells on a 100µm-wide gap (area marked by arrows) flanked by 10µm-deep grooves. Note that the cells on top (arrowheads) are not oriented with the flanking grooves. Cracks in the culture are artifacts of normal shrinkage during critical point drying.

D. Collagen orientation and distribution in cultures stained with Picro-sirius Red

Collagen orientation and distribution over a span of six weeks were also examined for osteoblast-like cell cultures. Pictures taken from Picro-sirius Red stained cultures indicated that the amount of collagen increased over time. The control surface, which was incubated with medium and no cells, showed no birefringence (data not shown). For the grooved surfaces, collagen fibers were generally oriented with the grooves. Figure 29 shows collagen orientation on the grooved substrata after five weeks of incubation. Groove walls in 29A appear red due to reflected light.

On the smooth gaps collagen fibers were oriented somewhat differently. One group of collagen fibers was oriented with the flanking grooves and appeared as if they were bridging the gap. Another set of collagen fibers was oriented at right angles to the direction of the grooves. Finally, when the microscope stage was rotated 45°, a third set of birefringent collagen fibers were observed that were oriented diagonally with the direction of the flanking grooves. These diagonally oriented collagen fibers were the most frequent. Figure 30 shows the three different orientations of collagen fibers on the smooth gaps.

Collagen fibers on the smooth surface were found not to have any preferred orientation (Figure 31). At higher magnification the collagen fibers appeared to be parallel, but on a closer examination one could see shadows (*i.e.* dark lines) created by another set of collagen fibers at nearly right angles to the predominant ones. These fibers (shadows) seem to interdigitate with the visible fibers. A stage rotation of 45° revealed a third set of collagen fibers that are at an angle (almost 45°) to the first set.

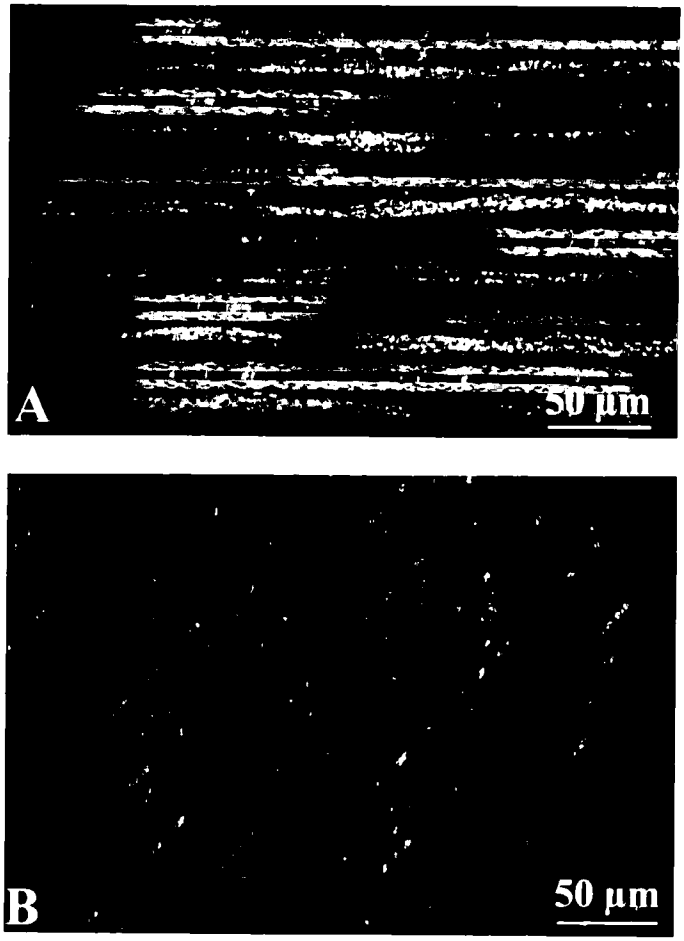

Figure 29: Picro-sirius Red staining of collagen fibers on 10µm-deep grooves from a five-week-old culture of osteoblast-like cells. A. Grooves at 0°. B. Grooves at 45°.

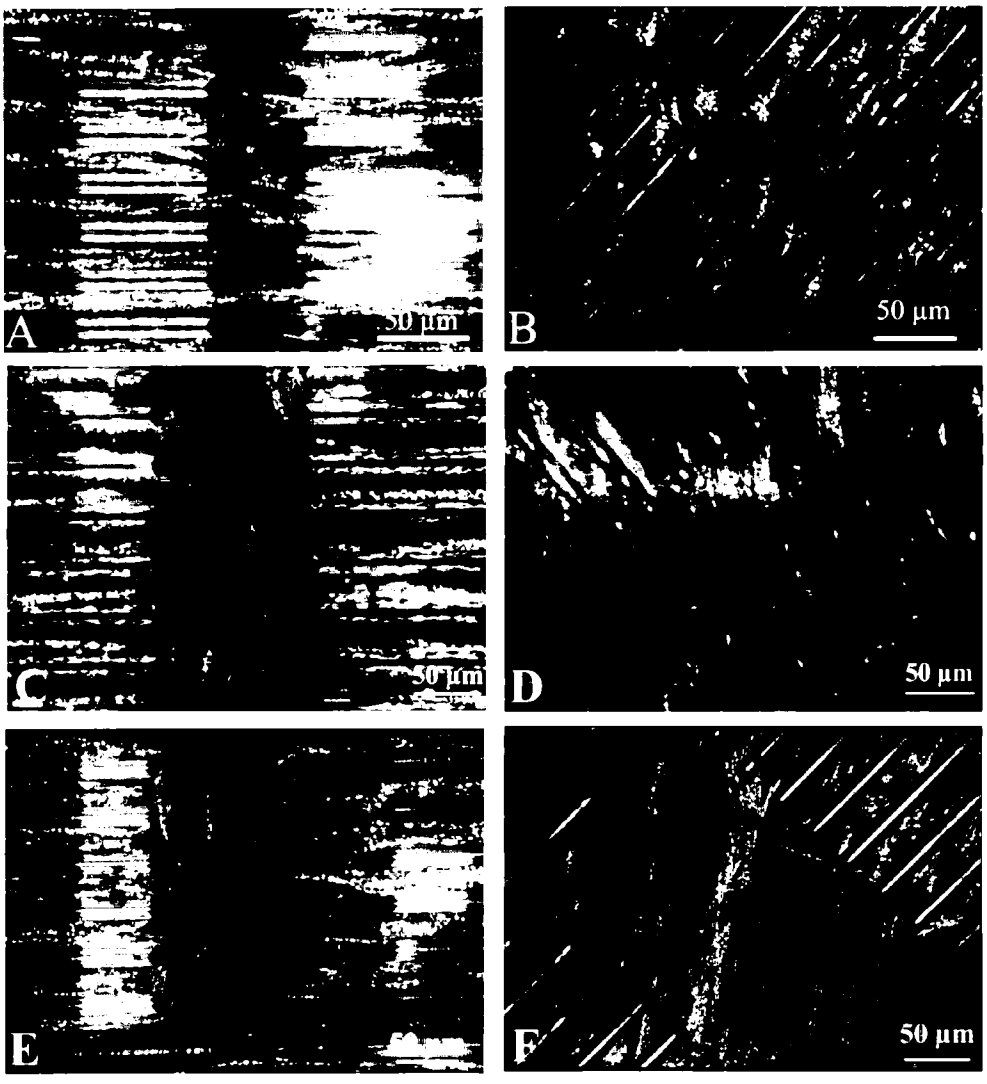

Figure 30: Picro-sirius Red staining of collagen fibers on smooth gaps. A & B show collagen on a 50µm-wide gap from a six-week old culture at 0^{o} and 45^{o} respectively. Note collagen fibers almost bridging the gap in A. C & D show collagen on a 100µm-wide gap from a six-week old culture at 0^{o} and 45^{o} respectively. In C collagen fibers are almost at the right angle with the flanking grooves. E & F show collagen fibers on a 200µm-wide gap from a five-week-old culture at angles of 0^{o} and 45^{o} respectively. In E two orientations of collagen fibers can be seen; fibers that are aligned with the grooves and fibers that are perpendicular with the grooves. B, D, and F show collagen fibers that form an angle with the direction of the grooves.

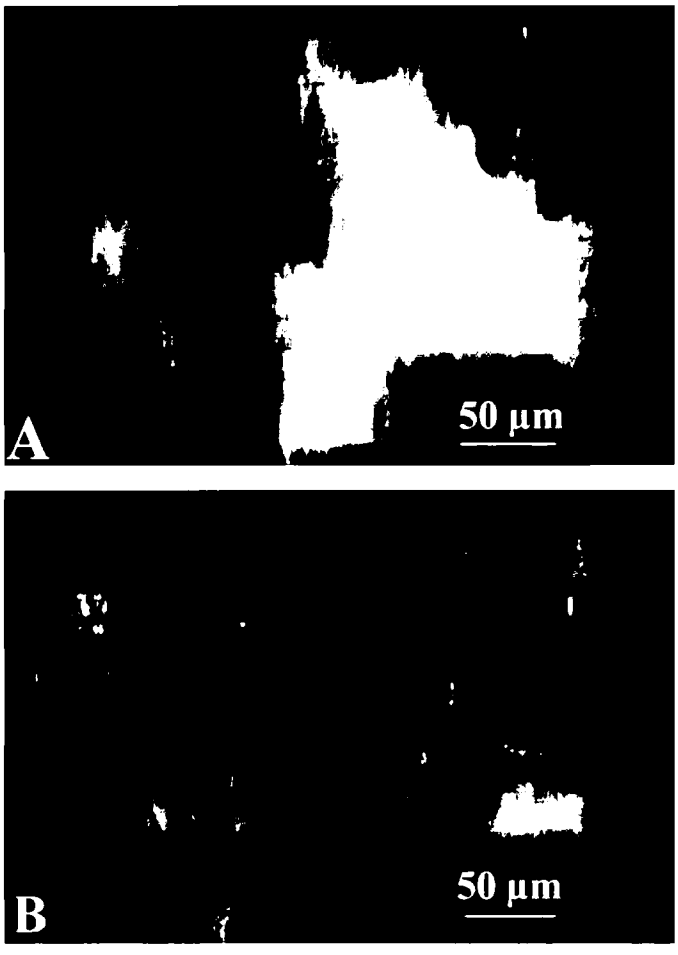

Figure 31: Picro-sirius Red staining of collagen fibers on smooth surface. A demonstrates collagen fibers at 0^{o}. B shows the field in A at 45^{o}. Note the shadows (crossing dark lines) created by other collagen fibers in both A and B. The shadows are almost at right angle to the birefringent fibers.

E. Observations from time-lapse video microscopy (TLVM)

1. Osteogenic cell migration and behaviour on grooves and smooth gaps

The movies are provided in QuickTime format in the CD ROM attached to the thesis. Osteoblast-like cells became oriented with the 10μm-deep grooves almost instantaneously and only moved within the walls of the grooves. Shortly after spreading, cells formed lamellipodia. Lamellipodia are thin forward protrusions that are filled with a meshwork of actin fibers, and mechanically are stiff enough to resist bending by a glass microneedle (Harris, 1998). In some instances, it was noticed that the spreading cells on the smooth gaps became oriented with the grooves upon touching another cell that was already oriented (Movie 1). Inside the grooves, cells would rarely hinder each other's movements, as they would often slide by one another before confluency (Movies 2-5). Cells that spread on the smooth gaps mostly moved along the length of the gap and some moved into the grooves (Movies 1 and 2). Cells that spread in the grooves would generally move across the gap and would rarely stay in the gap (Movies1, 2, and 3). Movement of cells across a smooth gap was bidirectional, as cells moved out of the grooves and crossed the gap from both sides of the gap (Movies 1, 2, and 3).

Once cells spread on the smooth gaps they moved apparently randomly unless influenced by groove walls or other cells (Movies 2-5). By the fourth or the fifth day the culture was almost confluent and most cells were either oriented with the neighbouring grooves or were moving up and down the smooth gap, treating the gap as if it was another wide groove at a right angle to the flanking grooves. The cells on the smooth gaps appeared more spread than in the grooves. Very often cells coming out of one groove onto the smooth gap would cross

the gap and enter a groove on the other side that was not necessarily the groove directly opposite from where the cell entered the gap (Movies 2-5). It was also noticed that cells would move under one another on the smooth gap. This behaviour was rarely noticed on the grooved areas where cells would slide by each other. It was also noticed that cells on the smooth gaps moved faster than the cells in the grooves.

Cell movement was visibly much slower as the culture neared confluency (Movie 5). At or near confluency, when there was only a monolayer of cells, most cells were aligned with the flanking grooves when trafficking across the gap (Movie 5). In the smooth gaps, when the culture consisted of multilayers of cells, the top layer was at an angle with respect to the flanking grooves (Movie 6). Mitotic activity was visible even after confluency (Movie 6). Once cells divided, they would often move in opposite directions. After 14 days (Movie 6) cell movement was slow and almost non-existent within the gaps and the grooves. However, cells exhibited oscillating motions, as they moved back and forth along their long axis. Cells within the topmost layer had very limited movement (Movies 6 and 7). Very rarely a few cells would break free from the topmost layer and would move about above the topmost layer (Movies 6 and 7).

Cell movement over the ridges was only noticed at or near nodules (Movies 6, 7, and 8). After 21 days, there was more cell movement on the ridges than inside the grooves (Movie 8). Close examination of the cells on or above the ridges, revealed that most of these cells were moving at an angle to the direction of the grooves (Movie 8). Cells in the grooves were either static or moving towards the nodule (Movie 8).

2. Characteristics of calcified nodules

Nodules on both the grooves and the smooth gaps were mostly round in shape (Movies 6,7, and 10), but some nodules on the grooves were aligned with the direction of the grooves (Movies 8 and 9). Most nodules appeared mound-like (Movies 6, 7, and 10) and had a cobble stone appearance (Movie 7 and 8). The edges of all nodules were rough and cellular. The overall size of the nodules did not appear to change markedly over time (5-7 days), but the edges were constantly changing in shape.

Some oriented nodules on the 10μm-deep grooves oscillated in the direction of the groove axis (Movies 7 and 9), but no net movement of the nodules was observed. Nodules on both 10μm- and 3μm-deep grooves were higher than the ridges of the grooves and appeared more cellular than the rest of the substrata (Movies 6 and 7). Another observation was that in some instances osteoblast-like cells would leave the 3μm-deep grooves and would move towards the nodules. This behaviour of the osteoblast-like cells was best demonstrated by Movie 10 in which cells travelled over the ridges of several grooves to reach the nodules.

3. Movie legends

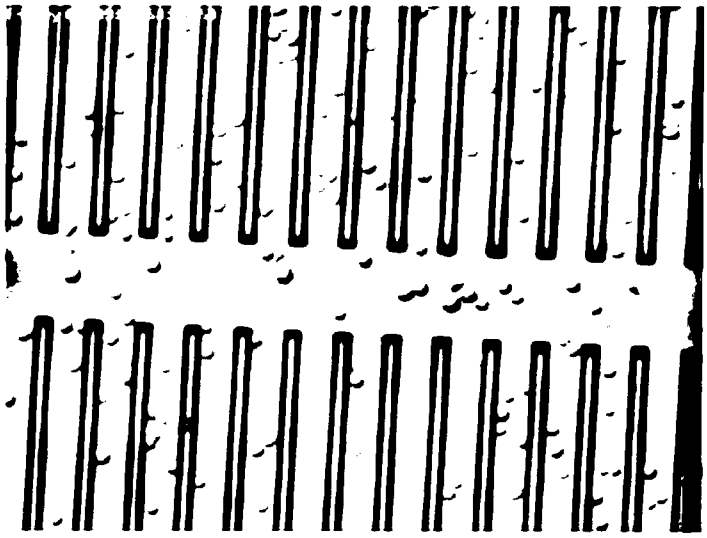

Movie 1: Frame 1: Osteoblast-like cells spreading on a 50μm-wide gap of a surface with 10μm-deep grooves. Time: after plating. 8x objective. Pitch = 47μm. Length of the movie: 20 seconds.

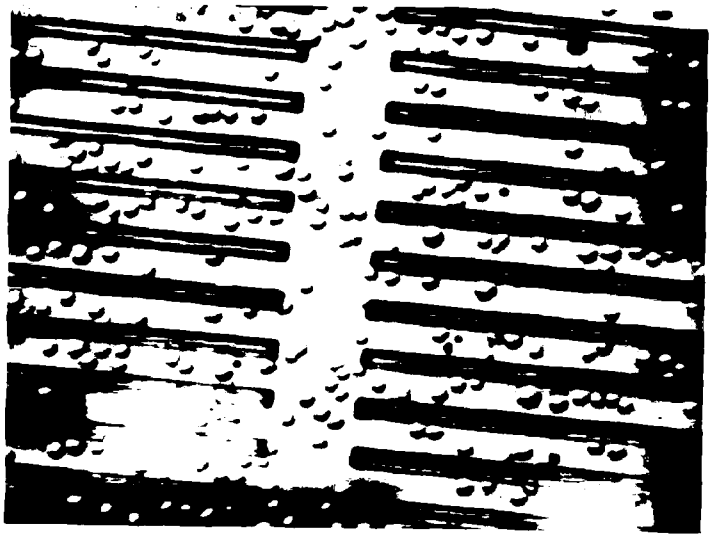

Movie 2: Frame 1: Osteoblast-like cells spreading on a 50μm-wide gap of a surface with 10μm-deep grooves. Time: after plating. 8x objective. Pitch = 47μm. Length of movie: 12 seconds.

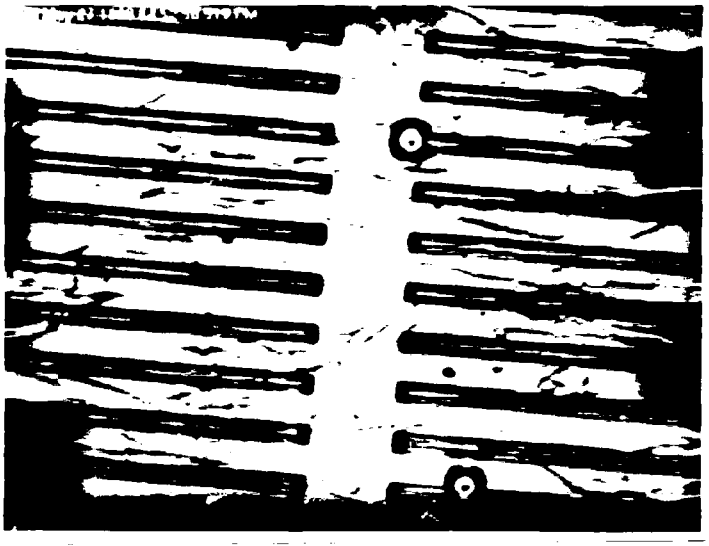

Movie 3: Frame 1: Osteogenic cells shortly after spreading on a 50μm-wide gap of a surface with 10μm-deep grooves (8 hours). 8x objective. Pitch = 47μm. Length of movie: 12 seconds.

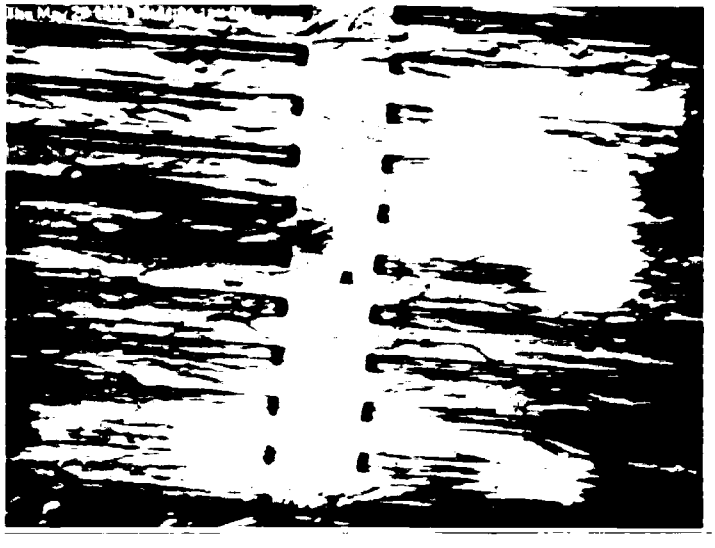

Movie 4: Frame 1: Osteogenic cells on a 50μm-wide gap of a surface with 10μm-deep grooves on day 3. 8x objective. Pitch = 47μm. Length of movie: 21 seconds.

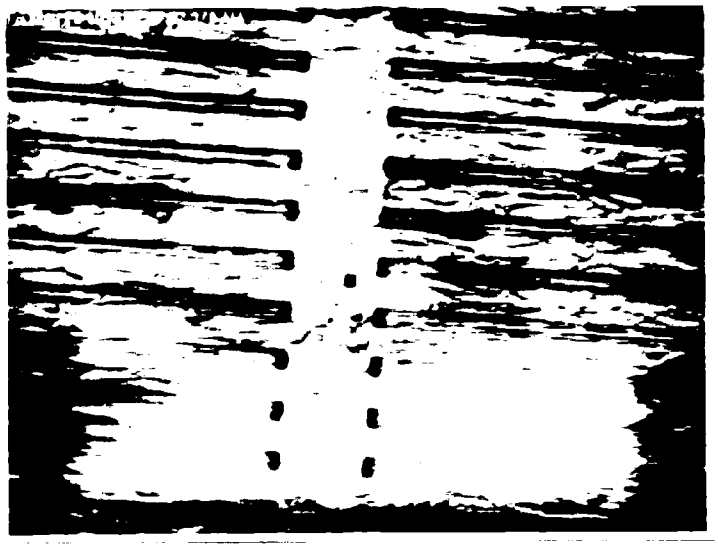

Movie 5: Frame 1: Osteogenic cells on a 50μm-wide gap of a surface with 10μm-deep grooves on day 4. 8x objective. Pitch = 47μm. Length of movie: 8 seconds.

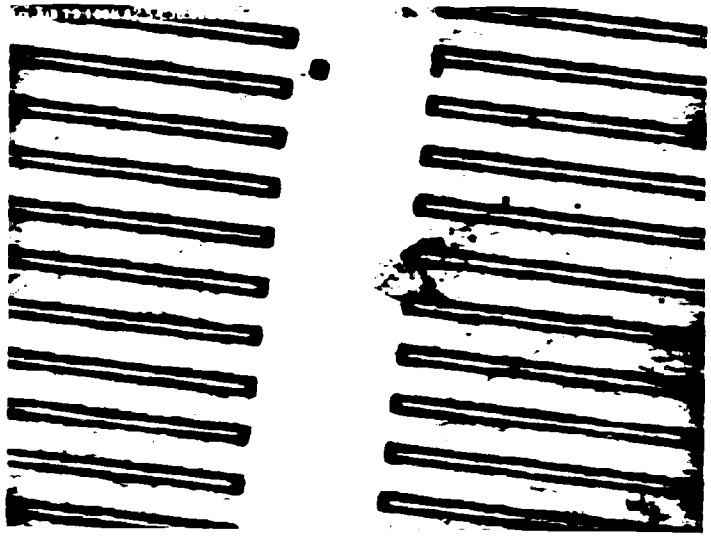

Movie 6: Frame 1: A calcifying nodule situated on the border of a 100μm-wide gap and 10μm-deep grooves on day 14. 8x objective. Pitch = 47μm. Length of movie: 18 seconds.

Movie 7: Frame 1: Possible developing nodule on 10μm-deep grooves next to a 50μm-wide gap on day 16. 8x objective. Note: Cells move onto the ridge near the nodule site. Pitch = 47μm. Length of movie: 18 seconds.

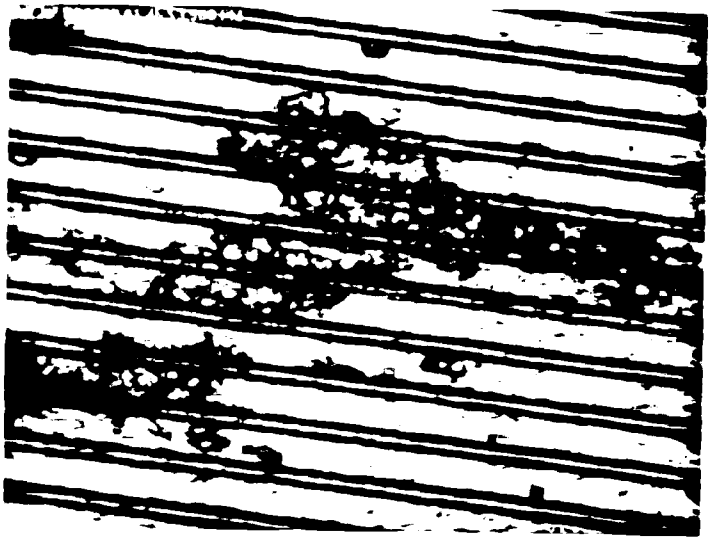

Movie 8: Frame 1: An oriented nodule on 10μm-deep grooves on day 21. 8x objective. Pitch = 47μm. Length of movie: 21 seconds.

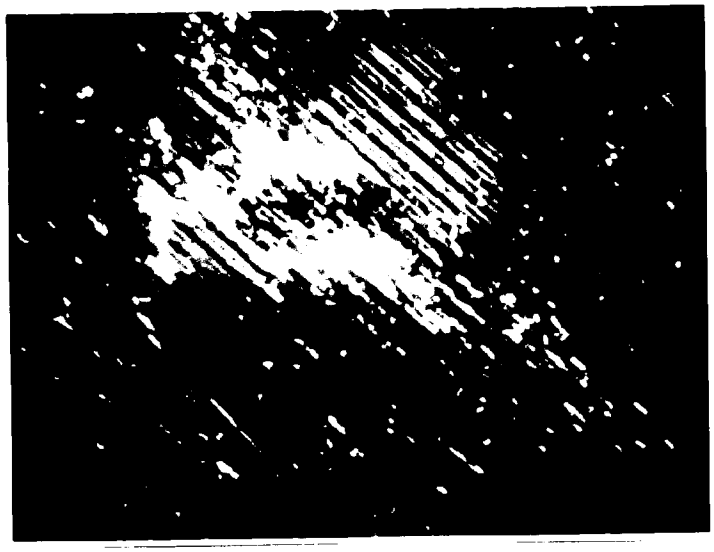

Movie 9: Frame 1: An oriented nodule on 10μm-deep grooves on day 21. Inverted background (NIH) used for better contrast. Nodule oscillates. 8x objective. Pitch = 47μm. Length of movie: 16 seconds.

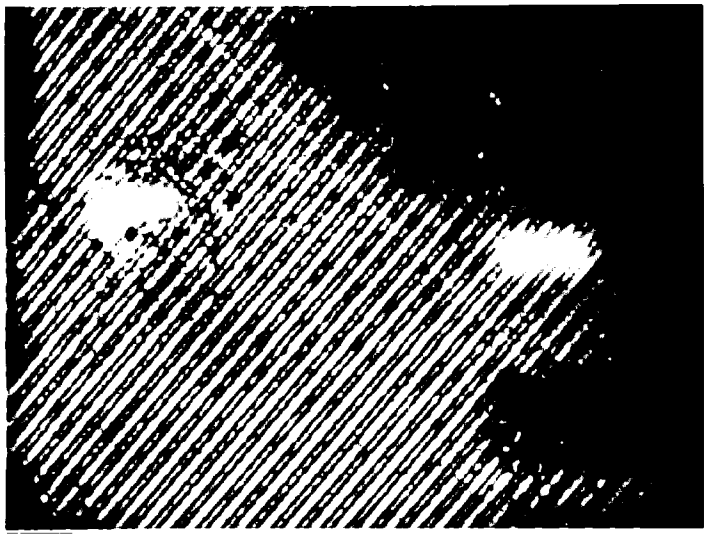

Movie 10: Frame 1: Two round nodules on 3μm-deep grooves on day 44. Cells attracted by nodules. 8x objective. Pitch = 47μm. Length of movie: 16 seconds.

IV. Discussion

To better understand the formation of bone-like nodules *in vitro*, several parameters including cell orientation, collagen organization and distribution, and surface characteristics were examined as a function of time in culture. The effect of feature depth on cell orientation and nodule formation was studied in the range of 3-30μm while the pitch was kept constant. Another surface feature introduced into the experimental design was smooth gaps of different widths in the grooved regions of substrata, an attempt to separate the effect on osteogenesis of cell orientation from that of the microenvironment that was thought to be produced by the restriction of diffusion by the groove walls. The following are the findings of this thesis:

1. The number of bone-like nodules was found to be in the order: smooth gaps > 3μm-deep grooves > 10μm-deep grooves > 30μm-deep grooves > smooth surfaces.
2. The average diameter of nodules was in the order: 30μm-deep grooves > 10μm-deep grooves > 3μm-deep grooves > smooth surfaces > smooth gaps.
3. Osteoblast-like cells in the grooves formed multilayers that aligned with the grooves when inside the trough of the grooves, but were diagonal to the grooves when above the ridge of the grooves. Generally, the cell layer closest to the titanium was the best aligned cell layer with respect to the direction of the flanking grooves and this alignment decreased progressively with subsequent layers above. Cell layers on the smooth surfaces showed no preferred orientation.
4. Collagen fibers in the grooves were generally oriented with the grooves whereas collagen fibers in the smooth gaps had several distinguishable orientations including fibers oriented with the flanking grooves, fibers diagonal with the flanking grooves, and fibers at right angles with them. Collagen on the smooth surfaces was organized in arrays of

parallel fibers, in a criss-cross pattern.

A. Introduction to nodule formation

1. Culture conditions

Nodule formation or osteogenesis *in vitro* involves differentiation of mesenchymal cells to osteoblasts through a series of commitment steps. Through these steps, osteoblasts acquire the ability to synthesize the extracellular matrix of bone and regulate its mineralization (Liu *et al*, 1997). Immunohistochemical markers have provided a better understanding of differentiation steps (Aubin and Turksen, 1996) which seem to follow a temporal sequence of events including elevation in alkaline phosphatase activity, increase in collagen type I synthesis, expression of bone matrix proteins (i.e. osteopontin, bone sialoprotein, and osteocalcin), and deposition and mineralization of the extracellular matrix to produce bone (Liu *et al*, 1997).

Differentiation of mesenchymal cells into osteoblasts, alone, is not sufficient for bone formation *in vitro*. Organic phosphate is the substrate for the enzyme alkaline phosphatase, without which mineralization cannot take place (Tenenbaum, 1981; Nijweide *et al*, 1982; Nefussi *et al*, 1985; Bellows *et al*, 1986). Another requirement for nodule formation *in vitro* is ascorbic acid, which is required for collagen synthesis (Barnes, 1975; Kivirikko and Myllyla, 1984; Schwartz *et al*, 1987).

Bellows *et al* (1986) have also suggested that nodule formation increases as a function of cell density, as they reported a positive correlation between the two, a finding that parallels

the results of a preliminary study to determine the optimal cell population density for my experiments (Appendix A).

Bellows *et al* (1986) also observed that three-dimensional nodules (approx. 75μm thick) covered by polygonal osteoblast-like cells only formed where cells were able to multilayer. In Bellows *et al*'s experiments they studied nodule formation on 35mm culture dishes and reported a mean of 14.2 ± 0.9 nodules/cm^2.

One study of interest that made use of micromachined surfaces was that of Chehroudi *et al* (1992). Chehroudi *et al* (1992) investigated the effect of grooved substrata on osteogenesis both *in vivo* and *in vitro*. They used grooved substrata with 19μm and 30μm-deep grooves and smooth surfaces as controls. Their results, both *in vivo* and *in vitro*, suggested that the 30μm-deep grooves were better in promoting osteogenesis, as their *in vitro* experiment resulted in more nodules with the 30μm-deep grooves and their *in vivo* implants with the deeper grooves resulted in more bone production. Chehroudi *et al* (1997) reinvestigated the micromachined grooved substrata *in vivo*, but this time with the grooves of higher depths (> 30μm deep). They reported that bone formation next to their subcutaneous implants, which were implanted above the calvaria of rats, decreased as the groove depth increased.

Another study of interest is that of Perizzolo (2000, in an M.Sc. just completed in this laboratory). Perizzolo utilized the surfaces designed for this study but with somewhat different culture conditions. Perizzolo observed that the shallower grooves (3μm deep) produced the least number of bone-like nodules followed by 10μm- and 30μm-deep grooves. Perizzolo reported, as found in my work, both the grooved areas and the smooth gaps produced more nodules than the smooth controls.

2. Underlying mechanisms leading to nodule formation

Apart from the above conditions and requirements, it has been suggested that certain mechanisms, such as cell orientation and collagen organization, may play a role in promoting nodule formation. In lamellar bone, collagen fibers are orthogonally arranged in longitudinal and transverse arrays (Gebhardt, 1905, cited in Boyde and Riggs, 1990; Boyde *et al*, 1984; Ascenzi and Benvenuti, 1986; Weiner *et al*, 1997) and this arrangement serves a functional purpose (Schenk and Buser, 1998). Using structural models, Gebhardt demonstrated that longitudinal fibers might be expected to endow tensile strength whereas transverse fibers would endow compressive strength (Boyde and Riggs, 1990). Gerstenfeld (1988) observed that embryonic chicken calvariae osteoblast cultures, when three to four layers thick formed a matrix and each layer was associated with a layer of collagen fibers orthogonally arranged with respect to neighbouring layers. It has been suggested that through this orthogonal arrangement the extracellular matrix can make cells more responsive to soluble signals by allowing them to assume a particular spatial arrangement (Watt, 1991).

The relationship between cell shape and orientation and cell metabolism is well documented (Emerman and Pitelka, 1977; Emerman *et al*, 1977; Brunette, 1984; Hasegawa *et al*, 1985; Watt, 1986). As osteogenic cells *in vivo* polarize to differentiate into osteoblasts, bone production could be enhanced *in vitro* by, perhaps, producing a cell orientation that is instrumental in the development of a functional cell polarity (Chehroudi *et al*, 1992). Micromachined grooved surfaces, through orienting osteoblast-like cells, seem to achieve such functional polarity, as the grooved areas in my studies produced more bone-like nodules than the smooth controls.

B. Number of nodules

The data collected from the mineralization experiments showed that the micromachined grooved surfaces produced significantly ($P < 0.05$) more nodules than the smooth surfaces. An interesting finding was that as the groove depth increased the number of nodules formed decreased. On first examination this decrease in the number of nodules suggests that the groove walls may have a negative effect on mineralization *in vitro*. It was, however, discovered that the diameter of the nodules generally increased with groove depth; the order being 30μm-deep grooves > 10μm-deep grooves > 3μm-deep grooves > smooth surfaces > smooth gaps. Thus, the number of nodules is not necessarily a sound indication of the amount of mineralization since the grooved surfaces that produced the fewest number of nodules had the largest nodules.

In comparing my results to those of other studies, it is apparent that culture conditions are very important in determining the number of nodules formed. In the study done by Bellows *et al* (1986) the number of nodules reported (14.2 ± 0.9 nodules/cm^2) were somewhat low. It is worth noting that Bellows *et al* used a much lower cell population density (about 100x lower). In the study of Chehroudi *et al* (1992) where they used 19μm- and 30μm-deep grooves and smooth surfaces for controls, their results, both *in vivo* and *in vitro*, suggested that the 30μm-deep grooves were better in promoting osteogenesis. The cell density used in their *in vitro* experiments was lower (2×10^3 cells/cm^2) than the one used in my experiment. In Perizzolo's study (2000), a cell density of 1×10^5 cells/cm^2, half the cell density in my study, was used. However, Perizzolo observed more nodules on his surfaces (2181 ± 98 for 30μm-deep grooves, 1917 ± 59 for 10μm-deep grooves, 1611 ± 39 for 3μm-deep grooves, and 938 ± 10 for smooth controls). The comparison between my results and those of

Perizzolo's suggests that cell population density does not, by itself, seem to explain the differences.

Another difference between my culture conditions and those of Perizzolo's was that he used a derivative of vitamin C, L-ascorbate-2-phosphate, which is more stable than the underivitized vitamin C used in my study. The more stable L-ascorbate-2-phosphate allowed Perizzolo to reduce the number of medium changes to two times per week compared to three times per week used in my experiments. As vitamin C is required for collagen synthesis (Barnes, 1975), it is quite possible that the more stable L-ascorbate-2-phosphate supplement enhanced collagen synthesis relative to the standard vitamin C. However, the amount of collagen fibers did not appear to differ in the two studies, as assessed by a qualitative method (Picro-sirius Red staining).

In addition, Perizzolo added tetracycline that was incorporated into the newly formed apatite. The addition of tetracycline was meant to facilitate the localization of newly formed nodules with little background, since the incorporated tetracycline fluoresces under blue light. However, tetracycline not only acts as an antibacterial agent, but also inhibits collagenase, a metalloproteinase (Golub *et al*, 1999), and serves as a bone formation enhancer (Park *et al*, 2000). Park *et al* (2000) implanted tetracycline-loaded membranes on rat calvariae and observed increased new bone formation in calvarial defects after two weeks of implantation.

Another source of differences between my results and those of Perizzolo's is that the medium was changed twice weekly in his study as opposed to the three times weekly in this study. It is possible that changing the medium less frequently allowed for the development of a microenvironment that promoted nodule formation.

Finally, in comparing Perizzolo's study and mine, it should be noted that the use of tetracycline seems to be a more precise and reliable method for investigating mineralization *in vitro*, particularly in deeper grooves. A problem with the use of von Kossa staining method is that some calcified nodules could be undetected as part of the background in deeper grooves (10μm- and 30μm-deep grooves) whereas the fluorescing tetracycline-labelled hydroxyapatite is more easily detected.

Despite the experimental differences, the above studies share a common finding that the micromachined grooved substrata and the smooth gaps within them produced more bone-like nodules than the smooth controls. As the different features of the grooved surfaces can be controlled through the science of microfabrication, more work will be needed to better understand the role of a variety of groove features, such as pitch and ridge width.

C. Nodule characteristics

1. Nodule size and surface topography

Different surface topographies produced nodules of somewhat different sizes, as determined from the diameters of the nodules. The order of nodules sizes on different surfaces was: 30μm-deep grooves > 10μm-deep grooves > 3μm-deep grooves > smooth controls > smooth gaps. However, the sizes of the nodules were not significantly different from one another at all times. For example, although the size of the nodules on the 3μm-deep grooves was slightly larger than the nodules on the smooth controls, but the difference was not significant. The same can be said about the difference between the size of the nodules on 30μm- and 10μm-deep grooves.

Generally, the 30μm-deep grooves produced the largest nodules and the smooth gaps produced the smallest nodules. This finding would raise the question as to which surface better promoted osteogenesis *in vitro*. The present data cannot determine from the nodule numbers (in the previous section) the microfabricated surface the most effective in enhancing mineralization, since the grooved surface that produced the least number of nodules had the largest nodules. To better compare the microfabricated surfaces, the development of a method to assess the total mineralized volume on each surface may be required.

2. Nodule orientation and surface topography

Nodule orientation was measured as the angle between the longest axis of a nodule and the direction of the grooves. For the smooth surfaces, the angle between the longest axis of the nodule and an arbitrary horizontal axis in the field was measured. It was found that the grooves flanking the smooth gaps had no orienting effect on the nodules on the smooth gaps, as those nodules showed no preferred orientation with their OA close to what would be expected for random orientation (45^{o}). Also, it was found that the widths of the smooth gaps had no orienting effect on the nodules. However, on the grooves, nodules became more oriented with the direction of the grooves as the grooves became deeper. The difference between the OA's of nodules of 10μm- and 30-μm deep grooves was not significant. It is worth noting that the 3μm-deep grooves produced nodules with OA's that were not significantly different from those of the smooth gaps and the smooth controls. Hence, it can be concluded that groove depth is a determining factor in the orientation of the mineralized tissue.

D. Role of cell orientation in nodule formation

Grooved surfaces are effective in orienting fibroblasts and epithelial cells (Brunette, 1983, 1986a,b) as well as osteoblasts (Qu *et al*, 1996; Movies in this study). Grooved surfaces are also known to promote osteoblast-like cell attachment (Qu *et al*, 1996) as well as increase mineralization *in vitro* and *in vivo* (Chehroudi *et al*, 1992; Qu *et al*, 1996). Based on the reports that cell shape and metabolism are related (Emerman *et al*, 1977; Brunette, 1984; Hasegawa *et al*, 1985; Watt, 1986), it is likely that the micromachined grooved surfaces change the shape of osteoblast-like cells, which may affect their gene expression of extracellular matrix proteins, such as metalloproteinase-2 (Chou *et al*, 1998). Similarly, it is possible that the increased nodule formation on the grooved surfaces is a result of the orientation and polarity of the osteoblast-like cells effected by the grooves themselves.

The reason why the smooth gaps produced more bone-like nodules is not clear, but there are several possibilities. The cell layers on the smooth surfaces showed no preferred orientation when averaged over large fields, but there were small patches of osteoblast-like cells in parallel arrays, similar to the observations of Elsdale and Foley (1969) and Elsdale and Bard (1972) on human fetal lung fibroblasts. However, in any given low power microscopic field there were many such patchworks oriented randomly. Because all the patchworks were taken into consideration when calculating the orientation for the cell layer, the average orientation of the cell layer was close to the angle of 45° expected when there are no orienting influences. The criss-cross arrangement of the cell layers on the smooth surface was confirmed by the orientation of collagen fibers, as cell orientation governs collagen orientation (Trelstad, 1973; Jones *et al*, 1975; Jones and Boyde, 1976).

On the smooth gaps, at day 21, there were four distinct cell layers, compared to only three on the smooth surfaces. The cell layers on the smooth gaps did not comprise patchworks of cells like the cell layers on the smooth surfaces. Moreover, the orientation of the cell layers, with respect to the flanking grooves and each other, was not random at all. The bottommost cell layer was generally oriented with the direction of the flanking grooves and as one moved to the topmost layer, cell layers became progressively less oriented with respect to the grooves and adjacent cell layers were positioned at an angle with respect to one another, but not necessarily at a 90° angle to each other (Figure 32). The collagen fiber organization on the smooth gaps mirrored the cell layer orientation. Some collagen fibers were parallel with the direction of the flanking grooves, some were at an angle to the grooves, and some almost at right angles to the grooves.

In the light of the comparison between the smooth gaps and the smooth surfaces it is noted that the cell layers on the smooth gaps were different in that their mean OA progressively increased as the distance between the cell layers and the titanium surface increased and they did not exist as randomly oriented patchworks of cells that occurred on the smooth surfaces. Moreover, the histological sections from the grooved surfaces indicated that in most instances mineralization took place above the ridge of the grooves where cell layers were progressively at higher angles relative to the oriented cell layers in the grooves beneath them, an arrangement similar to the cell layers in the smooth gaps. The data from this thesis, thus suggest that there seems to be a relationship between the orientation of large, relative to smooth surfaces, areas of cell layers at an angle to one another (approx. 9°-27°) and nodule formation because mineralization predominantly occurred in areas (i.e. gaps and area above the ridges) where adjacent cell layers were at an angle relative to each other.

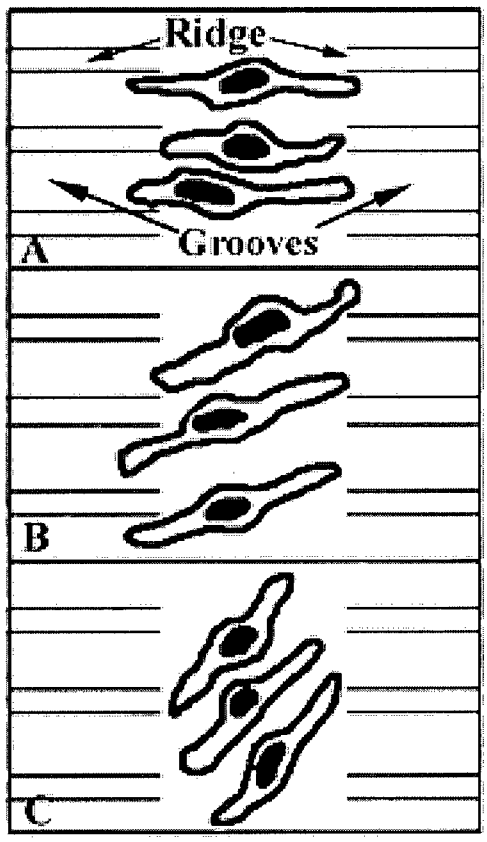

Figure 32: A drawing showing the orientation of three cell layers on a smooth gap relative to one another and the flanking grooves. A. Cell layer 1. B. Cell layer 2. C. Cell layer 3. Note that cell layers 1 through 3 become progressively less oriented relative to the grooves. Cell layer 1 is the closest of the three cell layers to the titanium surface.

E. Role of number of layers of osteoblast-like cells in nodule formation

It has been reported that multilayeredness is one of the requirements for mineralization *in vitro* (Bellows *et al*, 1986). Supporting evidence for the importance of multilayer formation comes from the work of Casser-Bette *et al* (1990) who cultured osteogenic cell line MC3T3-E1 onto a three-dimensional matrix of denatured collagen type I. After culturing for eight weeks they discovered mineralization in the upper surface of a newly synthesized collagen type I matrix which resembled osteoid. Casser-Bette *et al* (1990) used fibroblasts as control and found that fibroblasts passed through the network of denatured collagen and formed a monolayer at the bottom. Moreover, Gerstenfeld *et al* (1988) noted that mineralization in the cultures of chicken calvaria osteoblasts only took place in the deepest parts of the culture and when the culture cell layers were three to four cells thick.

One noticeable difference between the smooth surfaces and the smooth gaps was that the cultures on the smooth gaps formed multilayers faster than the smooth surfaces. By the 14th day the smooth gaps had four distinct cell layers (Table 10) whereas the smooth surfaces had only three (Table 11). The groove walls guide cells from the grooves into the gaps at high levels (Movies 4 and 5). The cells in the smooth gaps also divided and the net result was multilayers made up of cell layers whose mean OA with respect to the flanking grooves progressively increased with the distance from the titanium surface. Mitotic divisions in the smooth gap areas are best observed in Movie 6.

Further support for the importance of multilayer formation in mineralized nodule production comes from the observations on cell cultures on the 30μm-deep grooves. From the histological sections of the grooves it is apparent that most of the mineralization took place above the ridge level, where cell layers are more in contact with each other than the cell

layers inside the trough of the grooves. Inside the grooves, cell layers are not continuous as the groove walls interrupt them and as a result each cell layer is only 1-3 cells wide.

From the results of this thesis it is apparent that nodule formation or mineralization *in vitro* seemed to depend on the formation of multilayers of osteoblast-like cells where the layers, without any interruptions, were in contact with one another and their orientation with respect to each other changed from layer to layer.

F. Role of collagen organization in nodule formation

Picro-sirius Red staining of collagen indicated that collagen fiber organization on the grooves, smooth gaps, and smooth controls differed. Collagen fibers on the grooved surfaces were better oriented than those on the smooth controls. On the smooth surfaces, collagen fibers were in arrays of parallel fibers. These arrays were arranged in a criss-cross fashion and sometimes interdigitated each another (Figure 31). Overall, the organization of collagen on the smooth controls had no preferred orientation. On the smooth gaps, however, collagen fibers were organized in several distinguishable orientations that included collagen fibers that were parallel with the flanking grooves, fibers that were perpendicular to the flanking grooves, and fibers that were at an angle to the flanking grooves.

It has long been known that collagen fibers in adjacent lamellae of human osteons are organized in an orthogonal arrangement (Ascenzi and Bonucci, 1967 and 1968). Subsequent studies (Frasca *et al*, 1977; Ascenzi and Benvenuti, 1986) reported that there was another orientation of collagen fibers that included fibers that were at an angle close to 45^{o} to the direction of the fibers in two adjacent lamellae and this orientation only happened in the area between two adjacent lamellae. Cells in culture or in situ may use collagen orientation to

communicate with each other without being in direct contact. Tension created by cells can lead to collagen fiber orientation, which in turn, determines the orientation and morphology of other cells (Klebe *et al*, 1989). Moreover collagen orientation plays a role in the mechanical responses of bone, as fibers oriented longitudinally are expected to provide tensile strength (Ascenzi and Bonucci, 1967) and those oriented transversely are expected to provide compressive strength (Ascenzi and Bonucci, 1968).

Based on the examination of the collagen fibers on the smooth gaps, it appears as though the collagen orientation resembles that *in vivo*, but in the present study it is hard to tell the order (with depth) in which the collagen fibers of different orientation exist relative to one another. However, if cell orientation is any indication (Trelstad *et al*, 1973; Jones *et al*, 1975; Jones and Boyde, 1976), the fibers that are aligned with the flanking grooves should be the ones in the bottom, the fibers that are at an angle should be the middle ones, and the fibers that are at a right angle to the grooves should be on the top. The collagen orientation of the fibers within the trough of the grooves was in the direction of the grooves. However, I could not clearly determine the orientation of the fibers above ridge level. As it is generally believed that cell orientation is an indication of collagen orientation, the fibers above the ridge should be at an angle to the grooves, in which case, they would also resemble the collagen orientation *in vivo*. On the smooth controls, where the least number of nodules were produced, collagen fibers had no preferred orientation and were arranged in a criss-cross pattern.

Therefore, based on the results of my experiments it appears that there is a relationship between collagen orientation and nodule formation *in vitro*. It appears likely that surfaces that orient collagen fibers in an orderly fashion that resembles collagen orientation *in vivo*

(smooth gaps and grooves) produce the most nodules and the surfaces on which collagen fibers has no preferred orientation (i.e. smooth controls) produce the lowest number of nodules.

From the comparisons drawn among the three different surfaces (*i.e.* smooth, smooth gaps, and grooves) it is clear that both cell orientation and collagen orientation on the grooves and the smooth gaps are more orderly than those on the smooth surfaces. Moreover, it is clear that nodule formation appear to be related to the ability of the surfaces to promote multilayer formation. In the light of the observations made in this thesis it appears that nodule formation *in vitro* does not depend on one single aspect of cell and matrix geometry, but on the interplay of several factors including cell orientation, number of cell layers, and collagen organization.

V. Future work

This thesis provides further evidence that micromachined grooved substrata promote bone-like nodule formation *in vitro*. It was learned that nodule formation is associated with an interplay of several factors including cell orientation, number of cell layers, and collagen fiber organization. The conditions of the *in vitro* experiments may not mimic exactly those *in vivo* due to the complexity of the physiological conditions and many biological factors involved, such as hormones and cytokines, but under the controlled conditions of cell culture these surfaces can be studied thoroughly and consequently potentially improved surfaces identified for future *in vivo* applications. Although few studies have been done to test the effectiveness of implants with a grooved microtopography, those surfaces that have been tested have shown good promise (Chehroudi *et al*, 1992 and 1997). However, there is still room for improving the surface through variations (*e.g.* groove depth and pitch) and other modifications (*e.g.* addition of smooth gaps of different sizes and depths).

A. Smooth gap variation and modification

The additions of the smooth gaps into the grooved surfaces was an attempt to separate the effect of cell orientation from that of the microenvironment postulated to exist as a result of the groove walls, but unexpectedly the smooth gaps produced an increased number of nodules compared to the smooth surface controls. However, because of the difficulties of nodule quantification with the von Kossa technique on deep (30μm) grooves, the effect of the smooth gaps cannot be accurately compared with that of the deep grooves. One possible way to study the smooth gaps would be through varying their size, frequency, and depth. As it was desired to get cell orientation in the absence of groove walls, the current sizes for the smooth gaps were designed on the basis of an estimate of the ability of an osteoblast-like cell

to stretch across the gap. According to my results, the current gap sizes did not produce significantly different results from each other in terms of bone-like nodule formation. A greater variation in size (*e.g.* gaps with width differences of 100μm and more) should be tested. By testing different sizes of the smooth gaps their role in enhancing the mineralizing ability of the grooved surfaces can be studied and their effects can be maximized. Another approach to using the gaps would be to make them deeper than the flanking grooves (Figure 33). It would be expected that osteoblast-like cells would treat the deeper gap, which is actually the floor of a groove, as a groove and would align themselves with the direction of the gap. Cells coming out of the flanking grooves (above the cells already in the gap) would be mostly aligned with the direction of the flanking grooves. The result would be cell layers that are at a right angle to one another. These deeper gaps would be made by prolonging the etching time in the microfabrication process. This process, however, would require two photomasks, one to produce the flanking grooves and the second one to protect the grooves while the gaps were etched. The result would be grooves and gaps that are different in depth. Similar approaches could be used to align cells at desired angles and the effects of relative orientation of cell layers could be studied.

B. Cell shape and mineralization

Another issue that still needs to be addressed is the relationship between cell shape and bone-like tissue formation. It is hypothesized that the grooves change the shape of the osteoblast-like cells and by analogy to other systems, change their pattern of gene expression. Future studies are needed to compare the shape of the cells, through measurements, on the smooth surfaces, the smooth gaps, and the grooves and correlate them

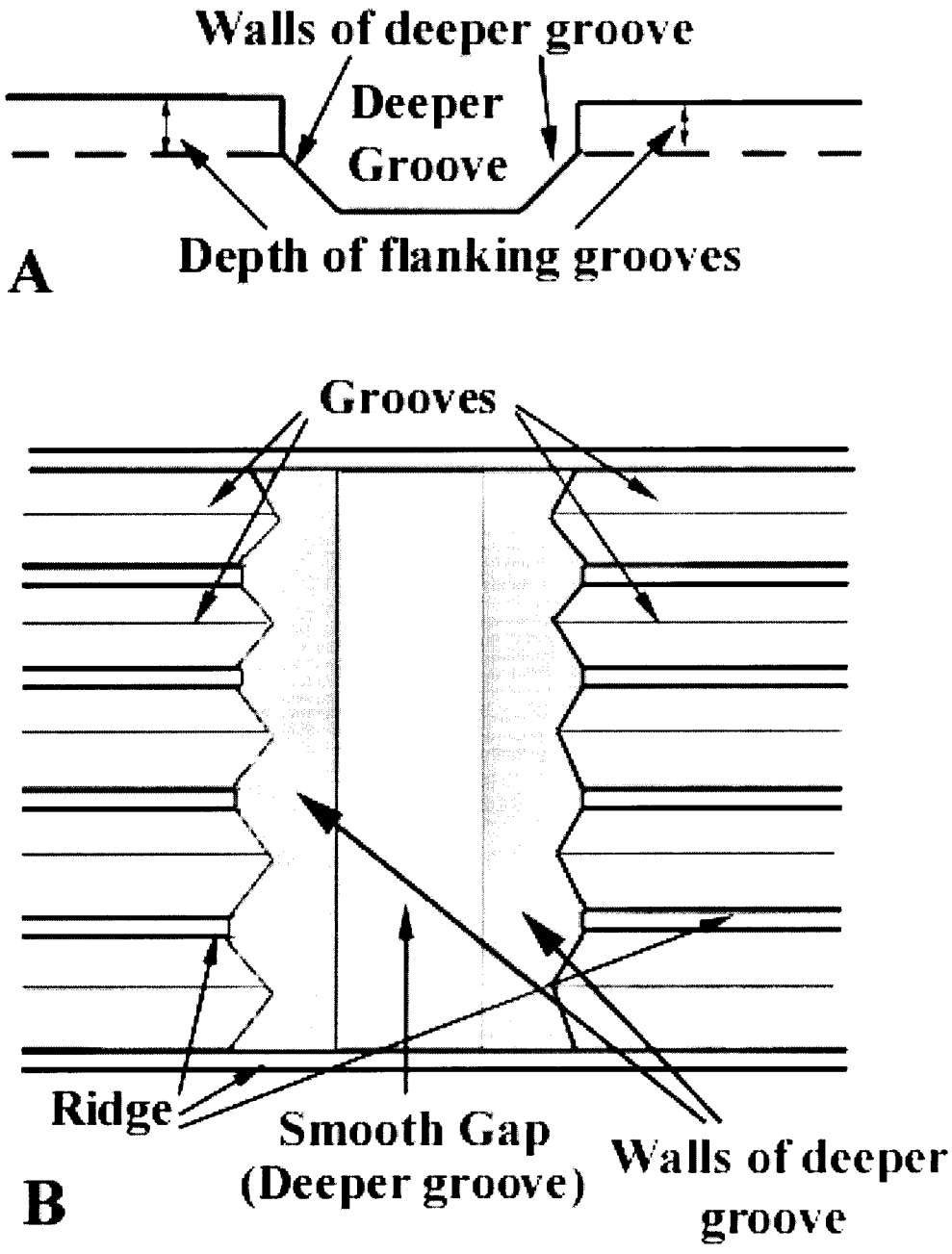

Figure 33: A diagram of a grooved substratum with a smooth gap (i.e. floor of a groove) deeper than the grooves. A. A cross-sectional diagram of the smooth gap. B. Top view of the substratum.

with nodule formation. Such studies would determine the extent to which cell shape could promote mineralization *in vitro*. Cell shape on grooved surface has been quantified by two form factors, FORM ELL and FORM PE (Brunette, 1986a). FORM ELL is the ratio of the major axis of the cell to its minor axis and considers the cell as an ellipse. A perfectly spherical cell would yield a FORM ELL value of 1.0 and an elliptical or spindle-shaped cell gives a value greater than 1.0. FORM PE is calculated using the area to the perimeter ratio of the cell. The formula for FORM PE is: 4π area/(perimeter)^2 (Brunette, 1986a). Another aspect of cell shape is cell thickness, which can be measured and studied by CLSM. The surfaces and culture conditions in this study can be used to establish a relationship between the effect of cell shape, measured by the above methods, and mineralization *in vitro*. It can also be determined whether different gap sizes (50-200μm) and different groove depths (3μm, 10μm, and 30μm) alter cell shape differently.

C. Phenotypic expression of cells on different surface topographies

Another study of interest would be to examine the phenotypic expressions of osteoblast-like cells on different topographies. This study would determine if cells on different surfaces differed in the timing or pattern of differentiation. Monoclonal antibodies along with Aubin's model of osteoblast differentiation (1996) can be used to find out whether surface topographies (*e.g.* smooth gaps, grooves, *etc.*) have any influence on the differentiation of osteogenic cells.

In such an experiment, osteogenic cells from rat calvariae would be grown on the surfaces as in the current study. At different times, monoclonal antibodies against certain phenotypic markers, such as osteopontin, osteocalcin, alkaline phosphatase, and bone

sialoprotein can be used to determine the proportion of cells exhibiting these markers on different topographies. According to Aubin and Turksen (1996) these markers are differentially expressed by cells at different stages of differentiation. The level of expression of each marker could be compared with Aubin's model of osteoblast differentiation (1996) and it could be determined whether different topographies altered differentiation of the osteogenic cells. For example, if micromachined grooved substrata altered differentiation by increasing the proportion of cells entering the osteoblastic pathway, one might expect to see an early burst of osteopontin-positive cells, but progression at the usual rate after that stage.

D. *In vivo* trials of the surfaces with smooth gaps

Pending better characterization of the smooth gaps through *in vitro* studies and based on the interesting results from the current study, it is of interest to examine their effectiveness *in vivo*. If the smooth gaps of different depths are able to produce different cell layer orientations, it is possible that they will also affect mineralization.

Surfaces in this study and others with gaps that have different depths from their flanking grooves could be duplicated in epoxy and coated with titanium. These surfaces, then, could be implanted subcutaneously on the calvariae of Sprague-Dawley rats using the methods of Chehroudi *et al* (1992). At different times rats would be sacrificed and the implants would be processed for light and transmission electron microscopy (TEM) to determine the level of mineralization in association with different surface features. This experiment would yield valuable information on the possible clinical usefulness of the surfaces that an *in vitro* study could not provide. The *in vivo* study with the help of TEM could also provide information

about the orientation of collagen fibers on these surfaces that would help determine whether the effects on orientation of extracellular matrix found in this study also occurred *in vivo*. Therefore, a more detailed relationship between collagen orientation and osteogenesis could be established.

VI. Bibliography

Abe K, Kanno T, Schneider GB; Surface structures and osteoclasts of mouse parietal bones: a light and scanning electron microscopic study; *Archivum Histologicum Japonicum*; 46(5):663-676; 1983.

Aebi U, Pollard TD; A glow discharge unit to render electron microscope grids and other surfaces hydrophilic; *Journal of Electron Microscopy Technique*; 7:29-33; 1987.

Albrektsson T, Branemark P.-I, Hansson H.-A, Lindstrom J; Osseointegrated titanium implants; *Acta orthop. scand.*; 52:155-170; 1981.

Albrektsson T, Branemark P.-I, Hansson H.-A, Kasemo B, Larsson K, Lundstrom I, McQueen DH, Skalak R; The interface zone of inorganic implants *in vivo*: Titanium implants in bone; *Annual Biomedical Engineering*; 11:1-27; 1983.

Ascenzi A, Bonucci E; The tensile properties of single osteon; *The Anatomical Records*; 158:375-386; 1967.

Ascenzi A, Bonnuci E; The compressive properties of single osteon; *The Anatomical Records*; 161:377-392; 1968.

Ascenzi A, Benvenuti A; Orientation of collagen fibers at the boundary between two successive osteonic lamellae and its mechanical interpretation; *Journal of Biomechanics*; 19(6):455-463; 1986.

Aubin JE, Heersche JN, Merrilees MJ, Sodek J; Isolation of bone cell clones with differences in growth, hormone responses, and extracellular matrix production; *Journal of Cell Biology*; 92(2):452-461; 1982.

Aubin JE, Turksen K; Monoclonal antibodies as tools for studying the osteoblast lineage; *Microscopy Research and Technique*; 33:128-140; 1996.

Aubin JE; Advances in the osteoblast lineage; *Biochemistry and Cell Biology*; 76:899-910; 1998.

Baier RE, Meyer AE, Akers CK, Natiella JR, Meenaghan M, Carter JM; Degradative effects of conventional steam sterilization on biomaterial surfaces; *Biomaterials*; 3:241-245; 1982.

Baier RE, Meyer AE, Natiella JR, Natiella RR, Carter JM; Surface properties determine bioadhesive outcomes: Methods and results; *Journal of Biomedical Materials Research*; 18:337-355; 1984.

Baier RE, Meyer AE; Implant surface preparation; *The International Journal of Oral & Maxillofacial Implants*; 3:9-20; 1988.

Barnes MJ; Function of ascorbic acid in collagen metabolism; *Ann. NY Acad. Sci.*; 258:264-277; 1975.

Basset CAL; Current Concepts of Bone Formation; *The Journal of Bone and Joint Surgery*; 44A(6):1217-1242; 1962.

Bellows CG, Aubin JE, Heersche JNM; Physiological Concentrations of Glucocorticoids Stimulate Formation of Bone Nodules from Isolated Rat Calvaria Cells *in Vitro*; *Endocrinology*; 121(6):1985-1992; 1985.

Bellows CG, Aubin JE, Heersche JNM, Antosz ME; Mineralized Bone Nodules Formed *In Vitro* from Enzymatically Released Rat Calvaria Cell Populations; *Calcified Tissue International*; 38:143-154; 1986.

Benecke BJ, Ben-Ze'ev A, Penman S; The control of mRNA production, translation and turnover in suspended and reattached anchorage-dependent fibroblasts; *Cell*; 14(4):931-939; 1978.

Ben-Ze'ev A; Animal cell shape changes and gene expression; *BioEssays*; 13(5):207-212; 1991.

Birk DE, Silver FH, Trelstad RL; Matrix Assembly; in Hay ED ed.; *Cell Biology of Extracellular Matrix*; Plenum Press, New York; 2nd edition:221-254; 1991.

Bonewald LF, Mundy GR; Role of transforming growth factor-beta in bone remodelling; *Clin. Orthop. Rel. Res.*; 250:261-276; 1990.

Bowers KT, Keller JC, Randolph BA, Wick DC, Michaels CM; Optimization of surface micromorphology for enhanced osteoblast responses *in vitro*; *International Journal of Oral & Maxillofacial Implants*; 7:302-310; 1992.

Boyan BD, Schwartz Z, Hambleton JC; Response of bone and cartilage cells to biomaterials *in vivo* and *in vitro*; *Journal of Oral Implant*; 19:116-122; 1993.

Boyde A, Bianco P, Portigliatti Barbos M, Ascenzi A; Collagen orientation in compact bone: I. A new method for the determination of the proportion of collagen parallel to the plane of compact bone sections; *Metab. Bone Dis. Relat. Res.*; 5(6):299-307; 1984.

Boyde A, Riggs CM; The Quantitative Study of the Orientation of Collagen in Compact Bone Slices; *Bone*; 11:35-39; 1990.

Branemark P.-I, Breine U, Adell R, Hansson B.-O, Lindstrom J, Ohlsson A; Intraosseous anchorage of dental prostheses: Experimental studies; *Scandinavian Journal of Plastic Reconstructional Surgery*; 3:81-100; 1969.

Branemark P.-I, Hansson B.-O, Adell R, Breine U, Lindstrom J, Hallen O, Ohaman A; Osseointegrated implants in the treatment of edentulous jaw; *Scandinavian Journal of Plastic Reconstructional Surgery*; 11:suppl. 16; 1977.

Brunette DM, Kenner GS, Gould TRL; Grooved titanium surfaces orient growth and migration of cells from human gingival explants; *Journal of Dental Research*; 62:1045-1048; 1983.

Brunette DM; Mechanical stretching increases the number of epithelial cells synthesizing DNA in culture; *Journal of Cell Science*; 69:35-45; 1984.

Brunette DM; Fibroblasts on Micromachined Substrata Orient Hierarchically to Grooves of Different Dimensions; *Experimental Cell Research*; 164:11-26; 1986a.

Brunette DM; Spreading and Orientation of Epithelial Cells on Grooved Substrata; *Experimental Cell Research*; 167:204-217; 1986b.

Brunette DM; The effect of surface topography on cell migration and adhesion; in Ratner BD ed., *Surface Characterization of Biomaterials*; Elsevier Science Publishers, Amsterdam, Netherlands; 203-217; 1988a.

Brunette DM; The effects of implant surface topography on the behaviour of cells; *The International Journal of Oral & Maxillofacial Implants*; 3:231-246; 1988b.

Brunette DM, Ratkay J, Chehroudi B; The behaviour of osteoblasts on micromachined surfaces; in *Bone-Biomaterial Interface*, JE Davies (ed.), University of Toronto Press, Toronto; 179-180; 1991.

Buser D, Schenk RK, Steinemann S, Fiorellini JP, Fox CH, Stich H; Influence of surface characteristics on bone integration of titanium implants. A histomorphometric study in miniature pigs; *Journal of Biomedical Materials Research*; 25(7):889-902; 1991a.

Camporese DS, Lester TP, Pulfrey DL; Development of fine line silicon shadow masks for the deposition of solar cell grids; *Proceedings of the fifteenth IEEE photovoltaic specialists conference*; IEEE, New York; 527-529; 1981.

Carlsson LV, Berman C; Bone Response to Plasma-Cleaned Titanium Implants; *The International Journal of Oral & Maxillofacial Implants*; 4(3):199-204; 1989.

Casser-Bette M, Murray AB, Closs EI, Erfle V, Schmidt J; Bone formation by osteoblast-like cells in a three-dimensional cell culture; *Calcified Tissue International*; 46:46-56; 1990.

Chehroudi B, Gould TRL, Brunette DM; Effects of grooved epoxy substratum on epithelial cell behaviour *in vitro* and *in vivo*; *Journal of Biomedical Materials Research*; 22:459-473; 1988.

Chehroudi B, Gould TRL, Brunette DM; Effects of grooved titanium-coated implant surface on epithelial cell behaviour *in vitro* and *in vivo*; *Journal of Biomedical Materials Research*; 23:1067-1085; 1989.

Chehroudi B, Gould TRL, Brunette DM; Titanium-coated micromachined grooves of different dimensions affect epithelial and connective-tissue cells differently *in vivo*; *Journal of Biomedical Materials Research*; 24:1203-1219; 1990.

Chehroudi B, Ratkay J, Brunette DM; The role of implant surface geometry on mineralization *in vivo* and *in vitro*: A transmission and scanning electron microscopic study; *Cells and Materials*; 2(2):89-104; 1992.

Chehroudi B, Brunette DM; Effect of Surface Topography on Cell Behaviour; *Encyclopedic Handbook of Biomaterials and Bioengineering*; A(1):813-842; 1995.

Chehroudi B, McDonnell D, Brunette DM; The effects of micromachined surfaces on formation of bonelike tissue on subcutaneous implants as assessed by radiography and computer image processing; *Journal of Biomedical Materials Research*; 34:279-290; 1997.

Chou L, Firth JD, Uitto VJ, Brunette DM; Effects of titanium substratum and grooved surface topography on metalloproteinase-2 expression in human fibroblasts; *Journal of Biomedical Materials Research*; 39(3):437-445; 1998.

Clark P, Connolly P, Curtis ASG, Dow JAT, Wilkinson CDW; Topographical control of cell behaviour. I. Simple step cues; *Development*; 99:439-448; 1987.

Clark P, Connolly P, Curtis ASG, Dow JAT, Wilkinson CDW; Topographical control of cell behaviour. II. Multiple grooved substrata; *Development*; 108:635-644; 1990.

Clokie CM, Warshawsky H; Morphologic and radioautographic studies of bone formation in relation to titanium implants using the rat tibia as a model; *TheInternational Journal of Oral & Maxillofacial Implants*; 10(2):155-165; 1995.

Collins DH; Tissue changes in human femurs containing plastic appliances; *Journal of Bone Joint Surgery*; 36B:458-67; 1954.

Constantine VS, Mowry RW; The selective staining of human dermal collagen. II. The use of Picrosirius Red F3BA with polarization microscopy; *Journal of Investigative Dermatology*; 50:419-423; 1968.

Critchlow MA, Bland YS, Ashhurst DE; The effects of age on the response of rabbit periosteal osteoprogenitor cells to exogenous transforming growth factor-β2; *Journal of Cell Science*; 107:499-516; 1994.

Curtis ASG, Varde M; Control of cell behaviour: Topological factors; *Journal of National Cancer Institute*; 33:15-26; 1964.

Davies JE, Matsuda T; Extracellular Matrix Production by Osteoblasts on Bioactive Substrata; *Scanning Microscopy*; 2(3):1445-1450; 1988.

Davies JE, Chernecky R, Lowenberg B, Shiga A; Deposition and resorption of calcified matrix *in vitro* by rat marrow cells; *Cells & Materials*; 1(1):3-16; 1991a.

Davies JE; In Vitro Modeling of the Bone/Implant Interface; *The Anatomical Records*; 245:426-45; 1996.

Davies JE, Baldan N; Scanning electron microscopy of the bone-bioactive implant interface; *Journal of Biomedical Material Research*; 36(4):429-40; 1997.

Davies JE; Mechanisms of Endosseous Integration; *The International Journal of Prosthodontics*; 11(5):391-401; 1998.

Dayan D, Hiss Y, Hirshberg A, Bubis JJ, Wolman M; Are the polarization colors of picrosirius red-stained collagen determined by the diameter of the fibers?; *Histochemistry*; 93(1):27-29; 1989.

den Braber ET, Ruijter JE, Ginsel LA, von Recum AF, Jansen JA; Quantitative analysis of fibroblast morphology on microgrooved surfaces with various groove and ridge dimensions; *Biomaterials*; 17:2037-2044; 1996.

den Braber ET, Ruijter JE, Ginsel LA, von Recum AF, Jansen JA; Orientation of ECM protein deposition, fibroblast cytoskeleton, and attachment complex components on silicone microgrooved surfaces; *Journal of Biomedical Materials Research*; 40(2):291-300; 1998.

Doillon CJ, Silver FH, Berg RA; Fibroblast growth on a porous collagen sponge containing hyaluronic acid and fibronectin; *Biomaterials*; 8:195-200; 1987.

Doundoulakis JH; Surface analysis of titanium after sterilization: Role in implant-tissue interface and bioadhesion; *The Journal of Prosthetic Dentistry*; 58(4):471-478; 1987.

Duyck J, Naert IE; Biomechanics of oral implants: a review of the literature; *Technology and Health Care*; 5:253-273; 1997.

Dunn GA, Heath JP; A new hypothesis of contact guidance in tissue cells; *Experimental Cell Research*; 101:1-14; 1976.

Dunn GA; Contact guidance of cultured tissue cells: a survey of potentially relevant properties of the substratum; in Bellairs R et al ed.; *Cell Behaviour*; Cambridge University Press, London; 247-280; 1982.

Dunn GA, Brown AF; Alignment of fibroblasts on grooved surfaces described by a simple geometric transformation; *Journal of Cell Science*; 83:313-340; 1986.

Dunn GA; How do cells respond to ultrafine surface contours?; *Bioessays*; 13:541-543; 1991.

Dziedzic-Goclawska A, Rozycka M, Czyba JC, Moutier R, Lenczowski S, Ostrowski K; Polarizing microscopy of Picrosirius stained bone sections as a method for analysis of spatial distribution of collagen fibers by optical diffractometry; *Basic Appl. Histochemistry*; 26(4):227-239; 1982.

Ecarot-Charrier B, Glorieux FH, van der Rest M, Pereira G; Osteoblasts isolated from mouse calvaria initiate matrix mineralization in culture; *Journal of Cell Biology*; 96(3):639-643; 1983.

Ecarot-Charrier B, Shepard N, Charette G, Grynpas M, Glorieux FH; Mineralization in Osteoblast Cultures: A Light and Electron Microscopic Study; *Bone*; 9:147-154; 1988.

Elsdale TR, Foley R; Morphogenetic aspects of multilayering in petri dish cultures of human fetal lung fibroblasts; *Journal of Cell Biology*; 41:298-311; 1969.

Elsdale TR, Bard JBL; Collagen substrata for studies on cell behaviour; *Journal of Cell Biology*; 54:626-637; 1972.

Emerman JT, Pitelka DR; Maintenance and induction of morphological differentiation in dissociated mammary epithelium on floating collagen membranes; *In Vitro*; 13(5):316-328; 1977.

Emerman JT, Enami J, Pitelka DR, Nandi S; Hormonal effects on intracellular and secreted casein in cultures of mouse mammary epithelial cells on floating collagen membranes; *Proc. Natl. Acad. Sci. U.S.A.*; 74(10):4466-4470; 1977.

Evans GS, Potten CS; Stem cells and the elixir of life; *Bioessays*; 13(3):135-138; 1991.

Fisher LW, Termine JD; Noncollagenous proteins influencing the local mechanisms of calcification; *Clin. Orthop. Rel. Research*; 200:362-385; 1985

Frasca P, Harper RA, Katz JL; Collagen fiber orientations in human secondary osteons; *Acta Anat.*; 98:1-13; 1977.

Furlong RJ, Osborn JF; Fixation of hip prostheses by hydroxyapatite ceramic coatings; *Journal of Bone and Joint Surgery, British Volume*; 73(5):741-745; 1991.

Gerstenfeld LC, Chipman SD, Kelly CM, Hodgens KJ, Lee DD, Landis W; Collagen expression, ultrastructural assembly and mineralization in cultures of chicken embryo osteoblasts; *Journal of Cell Biology*; 106:979-989; 1988.

Glimcher MJ; Mechanism of calcification in bone: role of collagen fibrils and collagen-phosphoprotein complexes *in vitro* and *in vivo*; *The Anatomical Records*; 224:139-153; 1989.

Golub LM, Ramamurthy NS, Llavaneras A, Ryan ME, Lee HM, Liu Y, Bain S, Sorsa T; A chemically modified nonantimicrobial tetracycline (CMT-8) inhibits gingival matrix metalloproteinases, periodontal breakdown, and extra-oral bone loss in ovariectomized rats; *Ann. N.Y. Acad Sci.*; 30(878):290-310; 1999.

Groessner-Schreiber B, Tuan RS; Enhanced extracellular matrix production and mineralization by osteoblasts cultured on titanium surfaces *in vitro*; *Journal of Cell Science*; 101:209-217; 1992.

Gruber HE; *In vitro* tetracycline labelling and bone cell survival in human trabecular bone explants; *Bone*; 14(3):531-535; 1993.

Gundberg CM, Hauschka PV, Lian JB, Gallop PM; Osteocalcin: isolation, characterization and detection; *Meth. Enzym.*; 107:516-544; 1984.

Hambleton JC, Schwartz Z, Windeler SW; Culture surfaces coated with various implant materials affect chondrocyte growth and differentiation; *Journal of Orthopaedic Research*; 12:542-552; 1994.

Hardingham TE, Fosang AJ; Proteoglycans: many forms and many functions; *FASEB J.*; 6:861-870; 1992.

Harris AK; Polarity and polarization of fibroblasts in culture; *Advances in Molecular and Cell Biology*; 26:201-252; 1998.

Hartman LC, Meenaghan MA, Schaaf NG, Hawker PB; Effects of pretreatment sterilization and cleaning methods on materials properties and osseoinductivity of a threaded implant; *The International Journal of Oral & Maxillofacial Implants*; 4:11-18; 1989.

Hasegawa S, Sato S, Saito S, Suzuki Y, Brunette DM; Mechanical Stretching Increases the Number of Cultured Bone Cells Synthesizing DNA and Alters Their Pattern of Protein Synthesis; *Calcified Tissue International*; 37:431-436; 1985.

Hench LL, Ethridge EC; *Biomaterials: An Interfacial Approach*; Academic Press, New York; 1982.

Hill PA; Bone Remodelling; *British Journal of Orthodontics*; 25:101-107; 1998.

Holtrop ME; Light and electron microscopic structure of bone-forming cells; in Hall BK ed; *Bone Volume 1: The osteoblast and osteocyte*; The Telford Press, New Jersey; 1-39; 1990.

Hong HL, Brunette DM; Effect of cell shape on proteinase secretion by epithelial cells; *Journal of Cell Science*; 87:259-267; 1987.

Hudson B, Upholt WB, Devinny J, Vinograd J; The use of an ethidium analogue in the dye-buoyant density procedure for the isolation of closed circular DNA: the variation of the superhelix density of mitochondrial DNA; *Proc. Natl. Acad. Sci. USA*; 62:813-820; 1969.

Ingber DE, Madri JA, Folkman J; Endothelial growth factors and extracellular matrix regulate DNA synthesis through modulation of cell and nuclear expansion; *In Vitro Cellular & Developmental Biology*; 23(5):387-394; 1987.

Jackson RL, Busch SJ, Cardin AD; Glycosaminoglycans: molecular properties, protein interactions and role in physiological processes; *Physiol. Rev.*; 71:481-539; 1991.

Jensen JA, van der Waerden JPCM, de Groot K; Fibroblast and epithelial cell interactions with surface-treated implant materials; *Biomaterials*; 12:25-31; 1991.

Johansson C, Lausmaa M, Ask M, Hansson H.-A, Albrektsson T; Ultrastructural differences of the interface zone between bone and Ti6Al4V or commercially pure titanium; *Journal of Biomedical Engineering*; 11:3-8; 1989.

Jones SJ, Boyde A, Pawley JB; Osteoblasts and collagen orientation; *Cell and Tissue Research*; 159:73-80; 1975.

Jones SJ, Boyde A; Is there a relationship between osteoblasts and collagen orientation in bone?; *Israel Journal of Medical Sciences*; 12(2):98-107; 1976.

Jones SJ, Boyde A; The migration of osteoblasts; *Cell Tissue Research*; 184(2):179-193; 1977.

Junqueira LCU, Bignolas G, Brentani RR; Picrosirius staining plus polarization microscopy, a specific method for collagen detection in tissue sections; *Histochemical Journal*; 11:447-455; 1979.

Junqueira LCU, Montes GS, Sanchez EM; The influence of tissue section thickness on the study of collagen by the Picrosirius-polarization method; *Histochemistry*; 74:153-156; 1982.

Karagianes MT, Westerman RE, Rasmussen JJ, Lodmell AN; Development and evaluation of porous dental implants in miniature swine; *Journal of Dental Research*; 55:85-88; 1976.

Kasemo B, Lausmaa J; Biomaterial and implant surfaces: a surface science approach; *The International Journal of Oral & Maxillofacial Implants*; 3:247-259; 1988.

Kasemo B, Lausmaa J; Biomaterial and implant surfaces: on the role of cleanliness, contamination and preparation procedures; *Journal of Biomedical Materials Research*; 22 (suppl. A2):145-158; 1988.

Kiernan JA; *Histological & histochemical methods: Theory & Practice*; Pergamon Press, New York; 1990.

Kieswetter K, Schwartz Z, Dean DD, Boyan BD; The Role of Implant Surface Characteristics in the Healing of Bone; *Critical Review of Oral Biology and Medicine*; 7(4):329-345; 1996.

Kilpadi DV, Raikar GN, Liu J, Lemons JE, Vohra Y, Gregory JC; Effects of surface treatment on unalloyed titanium implants: Spectroscopic analyses; *Journal of Biomedical Materials Research*; 40(4):646-659; 1998.

Kivirikko KI, Myllyla R; Biosynthesis of the collagens; in Piez KA et al ed.; *Extracellular Matrix Biochemistry*; Elsevier, New York; 83-118; 1984.

Klawitter JJ, Weinstein AM; The status of porous materials to obtain direct skeletal attachment by tissue ingrowth; *Acta Orthop. Belg.*; 40:755-760; 1974.

Klebe RJ, Caldwell H, Milam S; Cells transmit spatial information by orienting collagen fibers; *Matrix*; 9:451-458; 1989.

Kononen M, Hormia M, Kivilahti J, Hautaniemi J, Thesleff, Effect of surface processing on the attachment, orientation, and proliferation of human gingival fibroblasts on titanium; *Journal of Biomedical Materials Research*; 26:1325-1341; 1992.

Lazarides E, Revel JP; The molecular basis of cell movement; *Scientific American*; 240:100-113; 1979.

Lian JB, Stein GS; Concepts of osteoblast growth and differentiation: Basis for modulation of bone cell development and tissue formation; *Critical Review of Oral Biology and Medicine*; 3:269.

Lillie RD; Histochemical acylation of hydroxyl and amino groups: Effect on the periodic acid Schiff reaction, anionic and cationic dye and van Gieson collagen stains; *Journal of Histochem. Cytochem.*; 12:821-841; 1964.

Linde A; Dentin matrix proteins: composition and possible functions in calcification; *Anat. Rec.*; 224:154-166; 1989.

Linder L, Lundskog J; Incorporation of stainless steel, titanium and vitallium in bone; *Injury*; 6:277-285; 1975.

Liu F, Malaval L, Aubin JE; The mature osteoblast phenotype is characterized by extensive plasticity; *Experimental Cell Research*; 232:97-105; 1997.

Lowenberg B, Chernecky R, Shiga A, Davies JE; Mineralized matrix production by osteoblasts on solid titanium *in vitro*; *Cells & Materials*; 1(2):177-185; 1991.

Maniatopoulos C, Sodek J, Melcher AH; Bone formation in vitro by stromal cells obtained from bone marrow of young adult rats; *Cell Tissue Research*; 254(2):317-330; 1988.

Margolis LB, Samoilov VI, Vasiliev JM, Gelfand IM; Quantitative evaluation of cell orientation in culture; *Journal of Cell Science*; 17:1-10; 1975.

Martin JY, Schwartz Z, Hummert TW, Schraub DM, Simpson J, Lankford J, Dean DD, Cochran DL, Boyan BD; Effect of titanium surface roughness on proliferation, differentiation, and protein synthesis of human osteoblast-like cells (MG63); *Journal of Biomedical Materials Research*; 29:389-401; 1995.

Matsuzaki T, Suzuki T, Fujikura K, Takata K; Nuclear Staining for Laser Confocal Microscopy; *Acta Histochemica et Cytochemica*; 30(3):309-314; 1997.

McKee MD, Farach-Carson M, Butler W, Hauschka P, and Nanci A; Ultrastructural immunolocalization of non-collagenous (osteopontin and osteocalcin) plasma (albumin) proteins in rat bone; *Journal of Bone and Mineral Research*; 8:485-496; 1993.

Meenaghan MA, Natiella JR, Moresi L, Flynn HE, Wirth JE, Baier RE; Tissue Response to Surface-Treated Tantalum Implants: Preliminary Observations in Primates; *Journal of Biomedical Materials Research*; 13:631-643; 1979.

Meloan SN, Puchtler H; Chemical Mechanisms of Staining Methods: Von Kossa's Technique: What von Kossa really wrote and a modified reaction for selective demonstration of inorganic phosphates; *Journal of Histotechnology*; 8(1):11-13; 1985.

Mikuni-Takagaki Y, Kakai Y, Satoyoshi M, Kawano E, Suzuki Y, Kawase T, Saito S; Matrix mineralization and the differentiation of osteocyte-like cells in culture; *Journal of Bone and Mineral Research*; 10(2):231-242; 1995.

Mundy G, Rodan SB, Majeska RJ, DeMartino S, Trimmer C, Martin T, Rodan GA; Unidirectional migration of osteosarcoma cells with osteoblast characteristics in response to products of bone resorption; *Calcified Tissue International*; 34:542-546; 1982.

Nakahara H, Dennia JE, Bruder SP, Haynesworth SE, Lennon DP, Caplan AI; *In vitro* differentiation of bone and hypertrophic cartilage from periosteal-derived cells; *Experimental Cell Research*; 195:492-503; 1991.

Nefussi JR, Boy-Lefevre ML, Boulekbache H, Forest M; Mineralization *in vitro* of matrix formed by osteoblasts isolated by collagenase digestion; *Differentiation*; 29:160-168; 1985.

Nijweide PJ; Calcium and strontium metabolism of bone *in vitro*; *Proc. Kon. Ned. Akad. Wet.*; C78:416-417; 1975.

Nijweide PJ, van Iperen-van Gent AS, Kawilarang-de Haas EWM, van der Plas A, Wassenaar AM; Bone formation and calcification by isolated osteoblast-like cells; *Journal of Cell Biology*; 93:318-323; 1982.

Oakley C, Brunette DM; The sequence of alignment of microtubules, focal contacts and actin filaments in fibroblasts spreading on smooth and grooved titanium substrata; *Journal of Cell Science*; 106:343-354; 1993.

Oakley C; Role of cytoskeleton and substratum in cell topographic guidance; PhD Thesis; 1995.

Oakley C, Jaegar NAF, Brunette DM; Sensitivity of Fibroblasts and Their Cytoskeletons to Substratum Topographies: Topographic Guidance and Topographic Compensation by Micromachined Grooves of Different Dimensions; *Experimental Cell Research*; 234:413-424; 1997.

Ohara PT, Buck RC; Contact guidance *in vitro*. A light, transmission and scanning electron microscopy study; *Experimental Cell Research*; 121:235-249; 1979.

Orsulic S, Peifer M; A method to stain nuclei of Drosophila for confocal microscopy; *Biotechniques*; 16(3):441-447; 1994.

Park YJ, Lee YM, Park SN, Lee JY, Ku Y, Chung CP, Lee SJ; Enhanced guided bone regeneration by controlled tetracycline release from poly(L-lactide) barrier membranes; *Journal of Biomedical Materials Research*; 51(3):391-397; 2000.

Perizzolo D; Effects of hydroxyapatite-coated micromachined substrata on osteogenesis; Master Thesis; 2000.

Peterson WJ, Yamaguchi DT; Cell density downregulates DNA synthesis and proliferation during osteogenesis *in vitro*; *Cell Prolif.*; 29:665-677; 1996.

Pfeilschifter J, Bonewald L, and Mundy GR; Characterization of latent transforming beta complex in bone; *Journal of Bone and Mineral Research*; 5:49-58; 1990a.

Pfeilschifter J, Wolf O, Naumann A, Minne HW, Mundy GR, and Ziegler R; Chemotactic response of osteoblast-like cells to transforming growth factor beta; *Journal of Bone and Mineral Research*; 5:825-830; 1990b.

Pilliar RM; Implant stabilization by tissue ingrowth; in van Steenberghe D. (ed.); *Tissue Integration in Oral and Maxillofacial Reconstruction*; Excerpta Medica, Amsterdam, The Netherlands; 60-76; 1986.

Price PA, Urist MR, Otawara Y; Matrix Gla-protein: a new γ-carboxyglutamic acid-containing protein which is associated with the organic matrix of bone; *Biochem. Biophys. Res. Comm.*; 117:765-771; 1983.

Price PA, Williamson MK; Primary structure of bovine matrix Gla-protein, a new vitamin K-dependent bone protein; *Journal of Biological Chemistry*; 260:14971-14975; 1985.

Price PA; Vitamin K-dependent formation of bone Gla-protein (osteocalcin) and its function; *Vitam. Horm.*; 42:65-108; 1985.

Qu J, Chehroudi B, Brunette DM; The use of micromachined surfaces to investigate the cell behavioural factors essential to osseointegration; *Oral Diseases*; 2:102-115; 1996.

Rao LG, Ng B, Brunette DM, Heersche JNM; Parathyroid hormone- and prostaglandin E_1-response in a selected population of bone cells after repeated subculture and storage at $-80^{\circ}C$; *Endocrinology*; 100(5):1233-1241; 1977.

Ratkay J; The effect of micromachined surfaces on osteogenesis *in vitro*; Master Thesis; 1995.

Ratner BD, McElroy BJ; Electron spectroscopy for chemical analysis: applications in the biomedical sciences, in RN Gendreau (ed.); *Spectroscopy in the Biomedical Sciences*; CRC Press, Boca Raton; 107-140; 1986.

Ratner BD; Biomaterial surfaces; *Journal of Biomedical Materials Research*; 21:59-90; 1987.

Ratner BD; New ideas in biomaterials science-a path to engineered biomaterials; *Journal of Biomedical Materials Research*; 27:837-850; 1993.

Reichardt LF, Tomaselli KJ; Extracellular matrix molecules and their receptors: functions in neural development; *Annu. Rev. Neurosci.*; 14:531-570; 1991.

Rich A, Harris AK; Anomalous preferences of cultured macrophages for hydrophobic and roughened substrata; *Journal of Cell Science*; 50:1-7; 1981.

Rovensky YA, Slavnaja IL, Vasiliev JM; Behaviour of fibroblast-like cells on grooved surfaces; *Experimental Cell Research*; 65(1):193-201; 1971.

Sammon PJ, Thomas MV; Mineralized Tissue; in Roth GI and Calmes R Ed.; *Oral Biology*; The CV Mosby Co.; 1981.

Schenk RK, Buser D; Osseointegration: a reality; *Periodontology 2000*; 17:25-35; 1998.

Schwartz RI, Kleinman P, Owens N; Ascorbate can act as an inducer of the collagen pathway because most steps are tightly coupled; *Ann. New York Acad. Sci.*; 498:172-185; 1987.

Schwartz Z, Boyan BD; Underlying Mechanisms at the Bone-Biomaterial Interface; *Journal of Cellular Biochemistry*; 56:340-347; 1994.

Schwartz Z, Kieswetter K, Dean DD, and Boyan BD; Underlying mechanisms at bone-surface interface during regeneration; *Journal of Periodontal Research*; 32:166-171; 1997.

Scott DM, Kent GN, Cohn DV; Collagen synthesis in cultured osteoblast-like cells; *Biochem. Biophys.*; 201:384-391; 1980.

Sodek J, Zhang Q, Goldberg HA, Domenicucci C, Kasugai S, Wrana JL, Shapiro H, Chen J; Non-collagenous bone proteins and their role in substrate-induced bioactivity; in Davies JE ed.; *The bone-biomaterial interface*; University of Toronto Press, Toronto; 97-110; 1991.

Solursh M; Extracellular matrix and cell surface as determinants of connective tissue differentiation; *American Journal of Medical Genetics*; 34:30-34; 1989.

Southam JC, Chir B, Selwyn P; Structural changes around screws used in the treatment of fractured human mandibles; *British Journal of Oral Surgery*; 8:211-221; 1970.

Spindler KP, Shapiro DB, Gross SB, Brighton CT, Clark CC; The Effect of Ascorbic Acid on the Metabolism of Rat Calvarial Bone Cells *In Vitro*; *Journal of Orthopaedic Research*; 7:696-701; 1989.

Stanford CM, Keller JC; The concept of osseointegration and bone matrix expression; *Critical Review of Oral Biology and Medicine*; 2:83-101; 1991.

Stanford CM, Keller JC, Solursh M; Bone Cell Expression on Titanium Surfaces is Altered by Sterilization Treatments; *Journal of Dental Research*; 73(5):1061-1071; 1994.

Stedman TL; *Medical Dictionary*; Williams & Wilkins, Baltimore; 26th ed.:858; 1995.

Tenenbaum HC; Role of Organic Phosphate in Mineralization *in vitro*; *Journal of Dental Research*; 60(C):1586-1589; 1981.

Tenenbaum HC, Heersche JNM; Differentiation of osteoblasts and formation of mineralized bone *in vitro*; *Calcified Tissue International*; 34:76-79; 1982.

Tenenbaum HC, McCulloch CAG, Fair C, Birek C; The regulatory effect of phosphates on bone metabolism *in vitro*; *Cell & Tissue Research*; 257:555-563; 1989.

Termine JD, Belcourt AB, Conn KM, Kleinman HK; Mineral and collagen-binding proteins of fetal calf bone; *Journal of Biological Chemistry*; 256:10403-10408; 1981a.

Termine JD, Kleinman HK, Whitson SW, Conn KM, McGarvey ML, Martin GR; Osteonectin: a bone-specific protein linking mineral to collagen; *Cell*; 26:99-105; 1981b.

Thomas KA, Cook SD; An evaluation of variables influencing implant fixation by direct bone apposition; *Journal of Biomedical Materials Research*; 19:875-901; 1985.

Trau H, Dayan D, Hirshberg A, Hiss Y, Bubis JJ, Wolman M; Connective tissue nevi collagens. Study with picrosirius red and polarizing microscopy; *American Journal of Dermatopathology*; 13(4):374-377; 1991.

Trelstad RL; The developmental biology of vertebrate collagens; *The Journal of Histochemistry and Cytochemistry*; 21(6):521-528; 1973.

Triffitt JT; The special proteins of bone tissue; *Clinical Science*; 72:399-408; 1987.

Uitto VJ, Larjava H; Extracellular matrix molecules and their receptors: an overview with special emphasis on periodontal tissues; *Critical Review of Oral Biology and Medicine*; 2(3):323-354; 1991.

Veis A; Mineral-matrix interactions in bone and dentin; *Journal of Bone and Mineral Research*; Suppl 2:493-497; 1993.

Vincentelli R, Evans FG; Relations among mechanical properties, collagen fibers, and calcification in adult human cortical bone; *Journal of Biomechanics*; 4:193-201; 1971.

Watt FM; The extracellular matrix and cell shape; *TIBS*; 11:482-485; 1986.

Watt FM; Cell culture models of differentiation; *The FASEB Journal*; 5:287-294; 1991.

Weiner S, Arad T, Sabanay I, Traub W; Rotated plywood structure of primary lamellar bone in the rat: orientations of the collagen fibril arrays; *Bone*; 20(6):509-514; 1997.

Weinreb M, Gal D, Weinreb MM, Pitaru S; Changes in the Shape and Orientation of Periodontal Ligament Fibroblasts in the Continuously Erupting Rat Incisor Following Removal of the Occlusal Load; *Journal of Dental Research*; 76(10):1660-1666; 1997.

Weiss MB; Development of an endosseous dental implant; *Quintess int.*; No. 9, 10, 11; 1977.

Weiss P; Cellular Dynamics; *Rev. Modern Phys.*; 31:11-20; 1959.

Wiestner M, Fischer S, Dessau W, Muller PK; Collagen types synthesized by isolated calvarium cells; *Experimental Cell Research*; 133:115-125; 1981.

Wolman M; On the use of polarized light in pathology; *Pathol. Annu.*; 5:381-416; 1970.

Wozney JM, Rosen V, Celeste AJ, Mitsack LM, Whitters MJ, Kriz RW, Hewick RM, Wang EA; Novel regulators of bone formation: molecular clones and activities; *Science*; 242:1528-1534; 1988.

Young MF, Bolander ME, Day AA, Ramis CI, Gehron-Robey P, Yamanda Y, Termine JD; Osteonectin mRNA: distribution in normal and transformed cells; *Nucleic Acids Research*; 14:4483-4497; 1986.

Appendix A: Preliminary study on the effect of cell population density on nodule formation *in vitro*

Cell population density (cells/cm^2)	No. (n)	Mean No. of nodules/cm^2 + SD
2×10^3	4	8.0 ± 8.5
2×10^4	4	8.0 ± 5.7
2×10^5	4	13.5 ± 3.5

$P < 0.05$